

Analysis of the AtMRS2 magnesium transporter family  
in *Arabidopsis thaliana* via gene-GFP fusions,  
heterologous complementations,  
and protein interaction studies

Dissertation

zur Erlangung des akademischen Grades Dr. rer. nat.  
der Mathematisch-Naturwissenschaftlichen Fakultät  
der Rheinischen Friedrich-Wilhelms-Universität Bonn

vorgelegt von

**Katrin Weyand**

geboren am 01.01.1977 in Aachen

Bonn, 01. November 2006

Erstgutachter: Herr Prof. Dr. Volker Knoop

Zweitgutachterin: Frau Prof. Dr. Dorothea Bartels

Tag der Prüfung: 21. Dezember 2006

Diese Dissertation ist auf dem Hochschulschriftenserver der ULB Bonn

[http://hss.ulb.uni-bonn.de/diss\\_online](http://hss.ulb.uni-bonn.de/diss_online) elektronisch publiziert.

Erscheinungsjahr: 2007

# Contents

<b>1. Introduction .....</b>	<b>1</b>
<b>1.1 Magnesium: chemical and biological properties .....</b>	<b>1</b>
<b>1.2 Prokaryotic magnesium transport systems.....</b>	<b>2</b>
1.2.1 History of magnesium transport analysis .....	2
1.2.2 The CorA transporter class.....	3
1.2.3 The MgtA/MgtB transporter class.....	5
1.2.4 The MgtE transporter class .....	6
<b>1.3 Eukaryotic magnesium transport systems.....</b>	<b>7</b>
1.3.1 Transport systems in yeast .....	7
1.3.2 Transport systems in mammals .....	8
1.3.3 Transport systems in plants .....	9
<b>2. Materials and Methods .....</b>	<b>13</b>
<b>2.1 Materials .....</b>	<b>13</b>
2.1.1 Plant material.....	13
2.1.2 Bacterial strains .....	13
2.1.3 Yeast strains .....	13
2.1.4 Vectors .....	14
2.1.5 Oligonucleotides.....	14
2.1.6 Laboratory equipment .....	14
2.1.7 Bioinformatics tools .....	15
<b>2.2 Methods.....</b>	<b>16</b>
2.2.1 Established methods in molecular biology.....	16
2.2.2 Designing plant expression constructs with the Gateway™ technology .....	17
2.2.3 Transformation of <i>Arabidopsis thaliana</i> via <i>Agrobacterium tumefaciens</i> .....	20
2.2.4 Transformation of <i>Arabidopsis</i> protoplasts.....	22
2.2.5 Tobacco leaf infiltration with <i>Agrobacterium tumefaciens</i> .....	23
2.2.6 Tobacco protoplast transformation.....	24
2.2.7 Fluorescence microscopy .....	25
2.2.8 Yeast complementation assays.....	26
2.2.9 Analysis of protein interactions via the mating-based split ubiquitin system..	30
2.2.10 Heterologous expression in <i>Xenopus</i> oocytes .....	33
2.2.11 <i>Xenopus</i> oocyte protein extraction and immunoblot.....	37

<b>3. Results</b> .....	<b>39</b>
<b>3.1 Investigating subcellular AtMRS2 protein localizations via gene-GFP fusions</b>	<b>39</b>
3.1.1 Full length gene-GFP constructs: cloning and transformation of <i>A. thaliana</i> .	40
3.1.2 Fluorescence of the full length gene-GFP fusion plants .....	42
3.1.3 Transcription and translation of the transgene .....	43
3.1.4 C-terminally shortened gene-GFP constructs .....	49
3.1.5 Transcription and translation within the AtMRS2short-GFP plant lines.....	51
3.1.6 Fluorescence of the C-terminally shortened GFP plant lines.....	55
3.1.7 A third approach: full length constructs in a new vector backbone .....	55
3.1.8 Transient transformation approaches I: tobacco leaf infiltration .....	57
3.1.9 Transient transformation approaches II: protoplast transformation.....	60
3.1.10 Summary of the results obtained with the numerous gene-GFP fusions .....	64
<b>3.2 Heterologous expression in yeast: complementation and measurement of transport capacities</b> .....	<b>67</b>
3.2.1 Selection of AtMRS2 proteins and cloning of the expression constructs .....	67
3.2.2 Complementation of the yeast $\Delta$ msr2 mutant strain .....	69
3.2.3 Measurement of transport capacities via the mag-fura 2 system .....	71
<b>3.3 Heterologous expression in <i>Xenopus</i> oocytes: electrophysiological measurements</b> .....	<b>74</b>
3.3.1 Selection of AtMRS2 proteins and cloning of the first constructs.....	74
3.3.2 DEVC measurements of the first constructs .....	75
3.3.3 V5-His6 tagged constructs: cloning, DEVC recordings, and oocyte blot.....	76
3.3.4 A week in Würzburg and numerous DEVC measurements.....	78
3.3.5 Stronger expression background: cloning into pDK148 and measurements ...	80
<b>3.4 Analysis of protein interactions via the mating-based split ubiquitin system ..</b>	<b>82</b>
3.4.1 Amplification of the AtMRS2-1 and AtMRS2-10 cDNAs.....	82
3.4.2 mbSUS: description of the procedure and first results.....	83
3.4.3 Extension of the screening system .....	86
<b>4. Discussion</b> .....	<b>91</b>
<b>4.1 The <i>Arabidopsis thaliana</i> MRS2 family of magnesium transport proteins</b> .....	<b>91</b>
<b>4.2 Subcellular localization: no convincing, positive results, but a multitude of insights</b> .....	<b>93</b>
4.2.1 Stable transformation approaches .....	93
4.2.2 Transient transformation approaches .....	96

4.2.3	Conclusions .....	98
4.2.4	Perspectives .....	103
<b>4.3</b>	<b>Studies on the functional properties of the AtMRS2 proteins via heterologous expression and characterisation.....</b>	<b>105</b>
4.3.1	Usage of the yeast $\Delta$ mrs2 system.....	105
4.3.2	Usage of the <i>Xenopus</i> oocyte expression system .....	110
4.3.3	Conclusions .....	113
<b>4.4</b>	<b>First indications of (hetero-) oligomerisation properties.....</b>	<b>115</b>
4.4.1	The mating-based split ubiquitin system for interaction studies.....	115
4.4.2	Conclusions .....	117
<b>5.</b>	<b>Outlook .....</b>	<b>119</b>
<b>6.</b>	<b>Summary .....</b>	<b>121</b>
<b>7.</b>	<b>Zusammenfassung .....</b>	<b>123</b>
<b>8.</b>	<b>Appendix .....</b>	<b>125</b>
<b>8.1</b>	<b>Oligonucleotide sequences .....</b>	<b>125</b>
8.1.1	Full length GFP constructs.....	125
8.1.2	C-terminally shortened GFP constructs .....	126
8.1.3	Yeast complementation and mbSUS constructs.....	127
8.1.4	<i>Xenopus</i> constructs and sequencing primers.....	128
<b>8.2</b>	<b>Sequences of exemplary constructs .....</b>	<b>129</b>
8.2.1	A destination clone of the full length gene-GFP constructs: AtMRS2-10c-GFP 129	
8.2.2	A destination clone of the C-terminally shortened GFP constructs: AtMRS2- 3short-GFP .....	133
<b>8.3</b>	<b>Abbreviations.....</b>	<b>136</b>
<b>8.4</b>	<b>Figure index .....</b>	<b>138</b>
<b>8.5</b>	<b>Table index.....</b>	<b>139</b>
<b>9.</b>	<b>Bibliography.....</b>	<b>141</b>
	<b>Acknowledgements .....</b>	<b>151</b>
	<b>Erklärung.....</b>	<b>153</b>



# 1. Introduction

## 1.1 Magnesium: chemical and biological properties

Magnesium is the most abundant divalent cation in living cells. In its metal form magnesium is highly reactive so that it is found either as the free cation  $\text{Mg}^{2+}$  in aqueous solutions or bound in a salt or mineral form, e.g. as  $\text{MgSO}_4$  or  $\text{MgCl}_2$ . Most of the magnesium in the earth's biosphere is found in the hydrosphere, with e.g. approximately 55 mM  $\text{Mg}^{2+}$  in the ocean (Maguire and Cowan, 2002).

The chemical properties of  $\text{Mg}^{2+}$  are unique compared to the other major biological cations like  $\text{K}^+$ ,  $\text{Na}^+$ , and  $\text{Ca}^{2+}$ . Its ionic radius is with 0,065 nm among the smallest of all cations whereas its hydrated radius with 0,476 nm is the largest of all cations. The volume change between ionic and hydrated radius thus is nearly 400-fold, as opposed to a 25-fold volume change for sodium and calcium and an only fourfold change for potassium. Magnesium is invariably hexacoordinate and comparatively rigid in its octahedral geometry, unlike e.g. calcium. It binds water molecules tighter than the other cations due to its high charge density, making the water exchange rate 3 to 4 orders of magnitude slower than that for  $\text{Na}^+$ ,  $\text{Ca}^{2+}$ , and  $\text{K}^+$ , respectively (Maguire and Cowan, 2002). This unique chemistry makes biological interactions of  $\text{Mg}^{2+}$  different from those of other cations, as most of the interactions occur with the hydrated ion, thus rather with the hydration sphere than with the cation itself. This mechanism has been termed “outer-sphere” chemistry in contrast to “inner-sphere” chemistry where the interaction occurs with the cation itself (Smith and Maguire, 1998).

The biological functions of  $\text{Mg}^{2+}$  are numerous: as  $\text{Mg} \cdot \text{ATP}$  it is the co-substrate for a large number of enzymes, e.g. for ATPases and inorganic  $\text{PP}_i$ ases, DNA and RNA polymerases, protein kinases, phosphatases, and carboxylases (Marschner, 1995; Shaul, 2002). It is necessary for the stability of plasma membranes and influences protein synthesis as it is a bridging element for the aggregation of the ribosomal subunits (Sperrazza and Spremulli, 1983).

In plants, the most prominent role of  $\text{Mg}^{2+}$  might be its function as the central atom of the chlorophyll molecule. 6 – 25 % of the total magnesium is bound to chlorophyll, depending on the nutritional state of the plant (Marschner, 1995). The insertion of the  $\text{Mg}^{2+}$  ion into the porphyrin structure during chlorophyll formation is catalyzed by a magnesium-dependent enzyme, the  $\text{Mg}^{2+}$ -chelatase; chlorophyll breakdown requires the  $\text{Mg}^{2+}$ -dechelatase (Walker and Weinstein, 1991; Papenbrock et al., 2000; Langmeier et al., 1993).  $\text{Mg}^{2+}$  and pH are

responsible for the tight regulation of key photosynthetic enzymes like e.g. fructose-1,6-bisphosphatase (Gardemann et al., 1986) and ribulose-1,5-bisphosphate carboxylase (Rubisco). Upon illumination, protons are pumped from the stroma into the intrathylakoid space, a process which is counterbalanced by transport of  $Mg^{2+}$  and  $H^+$  ions from the intrathylakoid space into the stroma. This leads to an alkalisation of the stroma towards the optimum for Rubisco, simultaneously providing the stroma with the appropriate  $Mg^{2+}$  concentration for this and further stromal enzymes (Oja et al., 1986; Heineke and Heldt, 1988; Portis, 1981; Portis, Jr. and Heldt, 1976).

An imbalance of magnesium content within the plant leads to a decrease in the rate of photosynthesis under  $Mg^{2+}$ -deficient conditions (when the proportion of cellular magnesium bound to chlorophyll exceeds 20 – 25 %; Marschner (1995)), but also under high magnesium conditions combined with drought stress: this results in increased  $Mg^{2+}$  levels within the chloroplast which can inhibit photosynthesis in several ways (Rao et al., 1987).

The nutritional value of magnesium can e.g. be estimated from the economic losses caused by hypomagnesia (the so-called grass tetany) in ruminants fed on plants with low  $Mg^{2+}$  content (Harris et al., 1983). In humans, magnesium deficiency resulting from insufficient  $Mg^{2+}$  intake with the diet is a world-wide clinical problem. Plant breeders aim at producing cultivars with elevated  $Mg^{2+}$  contents as a large proportion of  $Mg^{2+}$  is taken in from food of plant origin (Shaul, 2002).

## 1.2 Prokaryotic magnesium transport systems

Taking into account the unique chemical properties of the magnesium ion, it has been speculated that the proteins involved in transport of this cation would constitute novel types of transporters or channels. This does indeed hold true for the  $Mg^{2+}$  transporters identified so far.

### 1.2.1 History of magnesium transport analysis

Research on magnesium metabolism of prokaryotes started in the late 1960's when Webb (1966) noticed the importance of magnesium for bacterial growth. Genetic studies were performed in the 1960's and 1970's in the laboratories of Silver and Kennedy both working with *Escherichia coli*. The two groups identified the primary  $Mg^{2+}$  uptake system of prokaryotes by transport kinetic studies using the radioisotope  $^{28}Mg^{2+}$  (Silver, 1969; Silver and Clark, 1971; Lusk and Kennedy, 1969) and established the first  $Mg^{2+}$  transport mutant noticing that it showed increased resistance to the toxic effects of cobalt ions ( $Co^{2+}$ ; Nelsom and Kennedy (1971)) which are obviously co-transported with  $Mg^{2+}$  via the same system.



This mutant led to the identification of a second  $Mg^{2+}$  transport system in *E. coli* which is induced only under low  $Mg^{2+}$  conditions and functions independently of the first system (Nelson and Kennedy, 1972). Further research on prokaryotic magnesium transport systems was and still is mainly performed by the groups of Maguire and Smith mostly working with *Salmonella enterica* serovar Typhimurium (formerly termed *Salmonella typhimurium*). They also identified another transport system for  $Mg^{2+}$  so that to date three distinct systems are known, which will be described shortly in the following paragraphs.

### 1.2.2 The CorA transporter class

The CorA protein corresponds to the first magnesium transporter system identified in *Escherichia coli* (see above). The genetic locus was named after the mutant phenotype of increased resistance against usually toxic levels of  $Co^{2+}$  (Cor = Co<sup>2+</sup> resistance; Park et al. (1976)). CorA constitutes the major  $Mg^{2+}$  influx system of Bacteria and Archaea and has been studied intensively in *Salmonella enterica* serovar Typhimurium (*S. enterica*) from which it was cloned in 1986 (Hmiel et al., 1986).

CorA is a single gene locus encoding a 37 kDa protein and being constitutively expressed. Transport studies indicate that it mediates uptake of  $Mg^{2+}$ ,  $Co^{2+}$ , and  $Ni^{2+}$ , the latter two, however, being transported with  $K_m$  values well above the physiological concentrations of these cations (Hmiel et al., 1986; Hmiel et al., 1989) suggesting that transport of these cations is not the primary function of CorA. Transport of the cations depends on the membrane potential and does not appear to require ATP (Smith and Maguire, 1998).

The secondary structure of the CorA protein is highly unusual for a membrane protein in that it contains only two transmembrane (TM) helices at the very C-terminal part of the protein following a large soluble cytoplasmic domain at the N-terminus. This structure, together with the amino acid motif GMN (Gly-Met-Asn) at the end of TM helix 1, is conserved over the CorA homologues in Bacteria and Archaea which constitute a large part of the 2-TM-GxN proteins in the metal ion transporter (MIT) superfamily (Knoop et al., 2005). To constitute a functional transporter within the plasma membrane CorA needs to oligomerize. Biochemical evidence existed both for a tetrameric (in *S. enterica*; Warren et al. (2004)) and a pentameric (in the yeast homologue MRS2, see below; Kolisek et al. (2003)) version of the transporter. This question was finally answered by analysing the crystal structure of the CorA transporter from *Thermotoga maritima*, showing that it is constituted of five subunits (Lunin et al., 2006). Figure 1.2.1 depicts the structure of the  $Mg^{2+}$  channel apparently in the closed conformation (Lunin et al., 2006). The pore within the plasma membrane is formed by the first TM helices

of the five subunits; the large N-termini build a funnel-like domain in the cytoplasm. The conserved GMN motif is found at the periplasmic surface of the transporter, most probably being part of a selectivity filter. Transport through the membrane requires dehydration as indicated by the diameter of the pore (Lunin et al., 2006).

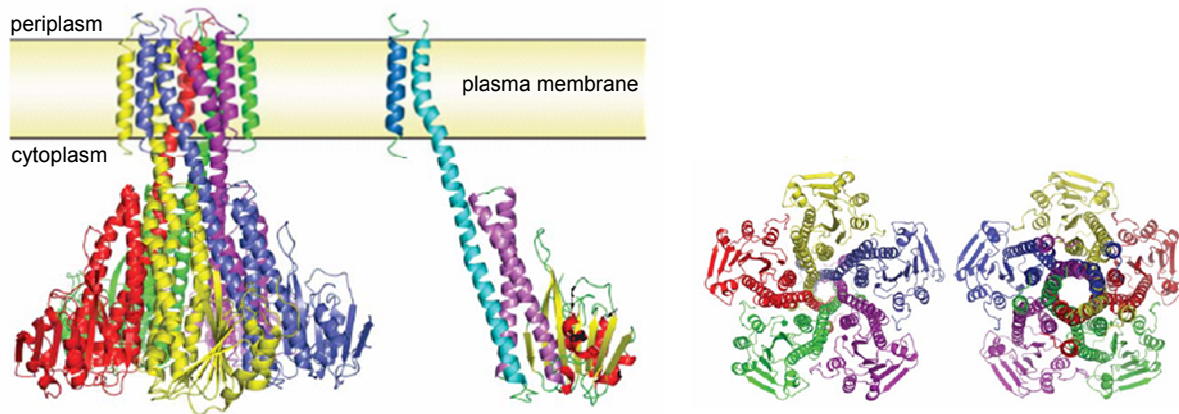


**Figure 1.2.1: The crystal structure of the CorA  $Mg^{2+}$  transporter from *Thermotoga maritima***

From left to right: ribbon diagram of the pentameric complex with each CorA protein shown in a different colour; single unit of the CorA channel with colours indicating the following structural features: inner TM1 helix and stalk helix (turquoise), outer TM2 helix (dark blue), willow helices (purple), remaining  $\alpha$ -helices (red), and  $\beta$ -sheets (yellow); view from the intracellular region, and view from the periplasm. The periplasmic loop (between amino acids 316 and 323) could not be resolved. Figure taken from Lunin et al. (2006).

Recently, a second research group published the crystal structure of the *Thermotoga maritima* CorA transporter at a higher resolution (2.9 Å versus 3.9 Å) principally reaching the same result as Lunin et al. They identified a second metal ion binding site which can be occupied both by  $Mg^{2+}$  and by  $Co^{2+}$ , confirming that magnesium is not the sole substrate of CorA (Eshaghi et al., 2006).

The crystal structure does not argue against the importance of the GMN motif and hydrophobic residues along the two TM helices for recognition and transport of  $Mg^{2+}$  as previously determined by analysis of *S. enterica* mutants (Smith et al., 1998; Szegedy and Maguire, 1999). Previous experiments by Smith et al. (1993b) gave rise to the idea of three TM helices in the *S. enterica* CorA being a rare exception within the 2-TM-GxN proteins. It should be clear now that this third TM helix preceding the two C-terminal helices is the prolonged  $\alpha$ -helical portion of the first TM domain building the side wall of the funnel-shaped cytoplasmic domain, the so-called “stalk helix” (cf. Figure 1.2.1).

Homologues of the bacterial and archaeal CorA proteins exist in every domain of life (Knoop et al., 2005); the eukaryotic members will be considered in the next chapter (see chapter 1.3).

### 1.2.3 The MgtA/MgtB transporter class

The MgtA and MgtB (Mgt =  $Mg^{2+}$  transport) proteins constitute the second magnesium influx system of *Salmonella enterica* serovar Typhimurium and differ from CorA in many aspects. They belong to the superfamily of P-type ATPases which are cation transport enzymes using phosphorylation (explaining the “P” in “P-type ATPases”) of a conserved aspartyl residue by ATP and subsequent hydrolysis of this residue for the transport cycle (Smith et al., 1993a). MgtA and MgtB are more similar to mammalian  $Ca^{2+}$ -ATPases (50 % identity) than to known prokaryotic P-type ATPases (25 % identity; Maguire et al. (1992)). The proteins of this type are more than 900 amino acids in length and generally feature ten TM helices (see Figure 1.2.2).

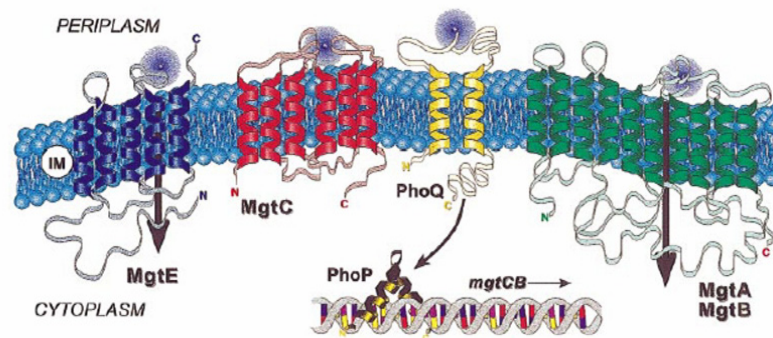


**Figure 1.2.2: The MgtA/MgtB and MgtE  $Mg^{2+}$  transporters of *Salmonella enterica* serovar Typhimurium**

Depicted are the magnesium transport systems of *S. enterica* except for CorA. Magnesium is transported into the cell via the MgtE protein (left) and via the MgtA and MgtB proteins (right). Regulation of MgtA/B expression is mediated by the two-component signal transduction system PhoQP (middle). The function of the MgtC protein (second from left) is as yet unknown. Figure taken from Moncrief and Maguire (1999).

Influx of magnesium involves phosphorylation of the conserved cytosolic aspartyl residue followed by a conformational change within the protein (Smith and Maguire, 1998). Expression of MgtA and MgtB is regulated by the two-component signal transduction system PhoQP (first identified as controlling the expression of a non-specific acid phosphatase, hence named “Pho”; Kier et al. (1979)) which itself responds to the extracellular  $Mg^{2+}$  concentration (see Figure 1.2.2):  $Mg^{2+}$  binds to the membrane-bound PhoQ receptor protein and inactivates it. If the extracellular magnesium concentration falls,  $Mg^{2+}$  dissociates from PhoQ, thus activating it to phosphorylate the transcription factor PhoP which is in turn activated and regulates transcription of at least 40 genes, two of them being MgtA and MgtB (Groisman, 1998; Vescovi et al., 1997). The PhoPQ system is an essential control element in virulence of

*S. enterica* and further bacterial species. Recent research showed that besides this regulation expression of MgtA is directly controlled by the intracellular concentration of  $Mg^{2+}$  via the gene's 5' UTR which acts as a sensor for  $Mg^{2+}$  concentration and inhibits further transcription of the coding region when sufficient amounts are present (Cromie et al., 2006).

MgtA is the endogenous P-type ATPase of *S. enterica*. MgtB is encoded in the MgtCB operon on *Salmonella* pathogenicity island 3 (SPI-3), a chromosomal insertion of 17 kb size. The function of the MgtC protein is unknown: it is not involved in  $Mg^{2+}$  transport but might have a function in virulence as *S. enterica* strains deleted for MgtC are avirulent in the mouse (BlancPotard and Groisman, 1997). Both MgtA and MgtB transport  $Ni^{2+}$  besides  $Mg^{2+}$ .

*Escherichia coli* does not possess an MgtCB operon; the MgtA protein constitutes the sole P-type ATPase within this organism (Park et al., 1976; Blattner et al., 1997). The Mgt proteins are far less widely distributed than CorA; the large majority of sequenced bacterial and archaeal genomes does not contain a homologue of MgtA or MgtB (Kehres and Maguire, 2002).

#### **1.2.4 The MgtE transporter class**

The third and least well understood magnesium transport system in prokaryotes are the MgtE proteins. These transporters, like CorA, show no homology to other known cation transporters. MgtE was cloned from the Gram-positive organism *Bacillus firmus* OF4 (Smith et al., 1995) and from the Gram-negative bacterium *Providencia stuartii* (Townsend et al., 1995). The approximately 40 kDa protein forms four or five TM helices (see Figure 1.2.2 on page 5) and mediates the influx of  $Mg^{2+}$  and  $Co^{2+}$ ;  $Ni^{2+}$  is not transported. It is not known whether MgtE is constitutively expressed or whether its expression is regulated (Kehres and Maguire, 2002).

Homologues of the MgtE protein can be found both in Bacteria and Archaea, although distribution seems not to be as widespread as that of the CorA protein (Townsend et al., 1995). Homologues can also be found within the eukaryotes, being widespread there (Kehres and Maguire (2002); see below).

### 1.3 Eukaryotic magnesium transport systems

Homologues of the three magnesium transport systems identified and characterised in prokaryotes can be found to different extents in eukaryotes. Homologues of the CorA protein are present throughout the genomes of the eukarya with the exception of non-vertebrate metazoa like *Drosophila*, *Anopheles*, and *Caenorhabditis* (Knoop et al., 2005). MgtE homologues are widespread in eukaryotes including humans, but homologous proteins are apparently not found in fungi (Kehres and Maguire (2002); Weyand and Knoop, unpublished results). The third class of prokaryotic  $Mg^{2+}$  transporters, MgtA/B, has homologous P-type ATPases in eukaryotes (cf. section 1.2.3) but so far no magnesium transporting ones have been described (Kehres and Maguire, 2002).

The non-uniform distribution of the prokaryotic  $Mg^{2+}$  transporters within the eukarya gives rise to the possibility that additional  $Mg^{2+}$  transport systems exist in this domain of life. The following paragraphs give an overview of the so far characterised magnesium transport systems in yeast, mammals, and plants.

#### 1.3.1 Transport systems in yeast

As expected, magnesium transport is studied best in the fungal model organism *Saccharomyces cerevisiae*, the baker's yeast, which will be referred to as "yeast" in the following.

Fungi, as far as it is known, seem to possess only CorA-like proteins for uptake and distribution of magnesium. The first transporters cloned were ALR1 and ALR2, homologues of CorA mediating uptake of  $Mg^{2+}$  through the plasma membrane of yeast (MacDiarmid and Gardner, 1998; Grischopf et al., 2001). They were named after their ability to confer resistance to the toxic effects of  $Al^{3+}$  when overexpressed (ALR = Al<sup>3+</sup> resistance; MacDiarmid and Gardner (1998)). Two further homologues of CorA, MRS2 and LPE10, are localized to the yeast inner mitochondrial membrane and mediate the uptake of  $Mg^{2+}$  into this organelle (Bui et al., 1999; Gregan et al., 2001a). ScMRS2 was originally identified as an important factor involved in splicing of group II introns (MRS2 = mitochondrial RNA splicing 2; Wiesenberger et al. (1992)) which was later related to its ability to confer proper  $Mg^{2+}$  concentrations essential for the splicing process *in vivo* (Gregan et al., 2001b).

Every homologue of the CorA protein found in yeast exhibits the structural features typical for the 2-TM-GxN proteins: a large cytoplasmic (in case of ALR1/2) or matrix (in case of MRS2/LPE10) N-terminal domain followed by two TM helices with the overall conserved GMN motif at the end of the first helix (Knoop et al., 2005). It is very likely that the three-

dimensional structure is very similar to that determined for *Thermotoga maritima* CorA (Lunin et al., 2006; Eshaghi et al., 2006), although ALR1 and ALR2 display an extended N-terminal region preceding the N-terminal domain homologous to CorA (Lee and Gardner, 2006).

A yeast strain deleted for the *mrs2* gene ( $\Delta$ *mrs2* strain) exhibits a *pet*<sup>-</sup> (*petit*) phenotype defective in the mitochondrial cytochrome complexes and as a result is unable to grow on non-fermentable carbon sources like glycerol (Wiesenberger et al., 1992). The growth defect cannot be suppressed by the second mitochondrial Mg<sup>2+</sup> transporter, LPE10, indicating that although the two proteins are 32 % identical they cannot functionally substitute for each other (Gregan et al., 2001a). The  $\Delta$ *mrs2* yeast strain thus provides a powerful tool for the functional analysis of other members of the 2-TM-GxN family.

### 1.3.2 Transport systems in mammals

Whereas the 2-TM-GxN family has multiple members in lower eukaryotes like fungi (see above), vertebrates clearly possess only one copy of the MRS2 protein localized to the mitochondrial membrane, as shown for the human MRS2 functionally characterised in yeast (Zsurka et al., 2001; Knoop et al., 2005). This raises the question of the identity of further Mg<sup>2+</sup> transport systems in the remaining membranes of the mammalian cell.

A human homologue of the bacterial MgtE transporters was identified in 2003 and named SLC41A1 (for solute carrier family 41 member 1). This protein has additional homologues in *Homo sapiens* and further metazoa, constituting a eukaryotic gene family (Wabakken et al., 2003). Expression and transport capacities of SLC41A1 as well as of one of the human paralogues, SLC41A2, have been studied showing that both proteins indeed mediate transport of Mg<sup>2+</sup> and further divalent cations, but so far the subcellular localization is unknown (Wabakken et al., 2003; Goytain and Quamme, 2005c; Goytain and Quamme, 2005d).

Two magnesium channels localized to the mammalian plasma membrane are found within the melastatin-related transient receptor potential (TRPM) subfamily of cation transporters belonging to the TRP superfamily of ion channels, that is TRPM6 and TRPM7. Both proteins possess six TM helices like further TRPM proteins but as a unique feature a kinase domain at the C-terminus which seems to regulate channel activity (Schmitz et al., 2003). Besides Mg<sup>2+</sup>, at least TRPM7 (formerly named LTRPC7) is also permeable to a range of divalent and, in the absence of divalent charge carriers, monovalent cations (Nadler et al., 2001; Monteilh-Zoller et al., 2002). TRPM7 appears to be ubiquitously expressed, whereas TRPM6 expression is restricted mostly to colon and kidney and co-expression of TRPM7 seems to be

needed to form functional multimeric complexes in the plasma membrane (Chubanov et al., 2004).

A fourth magnesium transport system in mammals was identified recently and designated MagT1 (for magnesium transporter 1; Goytain and Quamme (2005a)). This protein has no identity to other known transporters, once again highlighting that magnesium transporters in general constitute novel types of proteins. MagT1 possesses five TM helices, is expressed in a number of tissues, and its expression is upregulated under low magnesium conditions. Transport seems to be limited to the  $Mg^{2+}$  ion (Goytain and Quamme, 2005a).

Mammalian cells obviously possess a number of different systems mediating transport of magnesium. It cannot be ruled out that further transporters will be discovered in the future.

### 1.3.3 Transport systems in plants

In plants, to date two different systems for magnesium transport have been discovered: the vacuolar  $Mg^{2+}/H^+$  exchanger AtMHX and a gene family of 2-TM-GxN proteins homologous to the yeast MRS2 protein (Shaul et al., 1999; Schock et al., 2000). No proteins homologous to the two further prokaryotic systems, MgtE and MgtA/B, are present in plants. But, as Orit Shaul puts it in a recent review on magnesium transport in plants, only “the tip of the iceberg” is known, and further transport systems might be discovered (Shaul, 2002).

AtMHX shares limited sequence homology only with a mammalian plasma membrane  $Na^+/Ca^{2+}$  exchanger, NCX1, once again pointing out to the uniqueness of  $Mg^{2+}$  transport systems. It contains eleven TM helices, locates to the tonoplast and mediates the electrogenic exchange of protons with  $Mg^{2+}$  and  $Zn^{2+}$  ions. The protein seems to be expressed mainly in the vascular cylinder, most abundantly in the xylem parenchyma cells so that AtMHX might play a role in determining the amount of  $Mg^{2+}$  stored in the vacuole and vice versa available for loading into the xylem (Shaul et al., 1999). A recent report shows that expression of AtMHX is repressed by the 5' UTR of its gene independent of the  $Mg^{2+}$  and  $Zn^{2+}$  concentrations (David-Assael et al., 2005).

Homologues of the yeast MRS2 gene were discovered in *Arabidopsis thaliana* by our group in 2000 and designated AtMRS2-X (Schock et al., 2000). As often found in plants, a single copy gene is extended into a large gene family both in *Arabidopsis* and in rice, as can be seen in the phylogenetic tree in Figure 1.3.1. *Arabidopsis thaliana* contains 11 members in the “core” AtMRS2 family distributed over all five chromosomes, with AtMRS2-9 being a misspliced pseudogene in the ecotype used in our laboratory, Columbia (Col). A similar number of genes is found in *Oryza sativa*. Recent extended database searches revealed the

presence of further plant members of the 2-TM-GxN protein family, being only distantly related to the “core” gene family (Knoop et al. (2005); see Figure 1.3.1). These four *Arabidopsis* and three rice proteins show higher similarity to a subclade of bacterial 2-TM-GxN proteins, one of them being the ZntB protein from *Salmonella enterica* serovar Typhimurium. The ZntB protein seems not to transport  $Mg^{2+}$  but to mediate the efflux of  $Zn^{2+}$  from the bacterium; the GMN motif found in the  $Mg^{2+}$  transporting 2-TM-GxN proteins is changed into GIN (Worlock and Smith, 2002). This GIN motif is correspondingly also found in the plant homologues (Knoop et al., 2005).

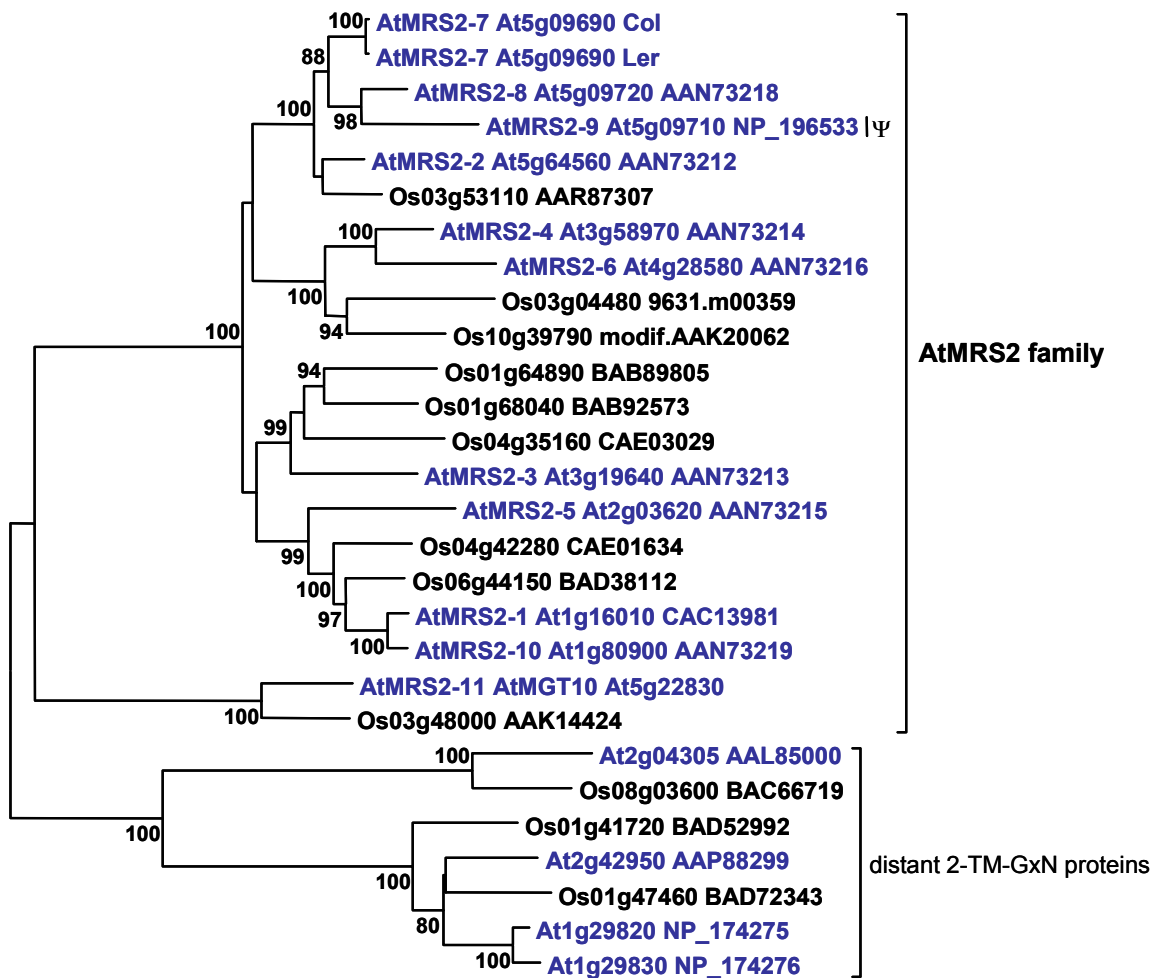


**Figure 1.3.1: Phylogeny of the plant 2-TM-GxN homologues**

Phylogenetic tree based on the protein sequences of the *Arabidopsis* and rice MRS2 homologues including the newly discovered distant members. The *Arabidopsis* sequences are derived from a complete set of Landsberg (Ler) cDNAs. For AtMRS2-7 the Columbia (Col) sequence is given as well, the divergence between the two ecotypes is highest here with six amino acid exchanges. AtMRS2-9 is a misspliced pseudogene in Col showing no transcription in Ler (R. Drummond, pers. comm.). Tree calculated with MEGA3.0 (Kumar et al., 2004): Neighbour Joining method with Poisson correction and pairwise gap deletion, 1000 bootstrap replicates.



---

Analyses on the members of the *Arabidopsis* gene family conducted both by our and by a second group show that single members can complement both prokaryotic (*S. enterica*) and eukaryotic (*S. cerevisiae*) mutants defective in magnesium transport demonstrating that the AtMRS2 proteins indeed constitute functional plant  $Mg^{2+}$  transporters (Schock et al., 2000; Li et al., 2001; Drummond et al., 2006). Transport capacities are similar to those of the bacterial CorA proteins; besides  $Mg^{2+}$ ,  $Mn^{2+}$  and  $Co^{2+}$  are transported as well, and  $Al^{3+}$  inhibits  $Mg^{2+}$  uptake (Li et al., 2001). RT-PCR analyses showed a more or less ubiquitous expression of the AtMRS2 proteins across the plant (Li et al., 2001) which is not confirmed by our promoter-GUS data (K. Meschenmoser, unpublished results) showing highly distinct expression patterns for each of the genes. *In silico* analyses predict three of the proteins to be localized to organelles: AtMRS2-11 is clearly said to be expressed in the chloroplast membrane, whereas the predictions for AtMRS2-4 and AtMRS2-6 are not unequivocal, but rather hint to a mitochondrial localization for both proteins. Subcellular localization data exist for three proteins (I. Schock, unpublished results; Li et al. (2001); Drummond et al. (2006)) confirming the organellar targeting of AtMRS2-6 and AtMRS2-11 (mitochondria and chloroplasts, respectively) and showing a plasma membrane localization for AtMRS2-10.

Many open questions concerning the molecular and functional analysis of the AtMRS2 gene family remain. An important issue is the determination of the subcellular localization of each member of the gene family so that together with the expression data a model of magnesium uptake into and distribution within the plant can be established. Further complementation assays should confirm the functionality of the remaining AtMRS2 proteins as  $Mg^{2+}$  transporters. Electrophysiological analysis of the transporters in *Xenopus* oocytes could give more detailed insights into the nature of the  $Mg^{2+}$  transport. The diversification into a gene family and the knowledge of pentamerisation to build a functional 2-TM-GxN transporter raise the possibility that not only homo- but also heteropentamerisation may be realised with the plant proteins. These questions were in the focus of the present PhD thesis.



## 2. Materials and Methods

### 2.1 Materials

#### 2.1.1 Plant material

- *Arabidopsis thaliana* ecotype Columbia (Col-0 and Col-5 (glabrous))
- *Nicotiana benthamiana*
- *Nicotiana tabacum*

#### 2.1.2 Bacterial strains

- *Escherichia coli* XL1-Blue (Stratagene)  
genotype: *endA1 gyrA96(nal<sup>R</sup>) thi-1 recA1 relA1 lac glnV44 F'[::Tn10 proAB<sup>+</sup> lacI<sup>q</sup> Δ(lacZ)M15 (Tet<sup>R</sup>)] hsdR17(r<sub>K</sub><sup>-</sup> m<sub>K</sub><sup>+</sup>)*
- *Escherichia coli* DH5α (Invitrogen Inc.)  
genotype: F<sup>-</sup> *endA1 glnV44 thi-1 recA1 relA1 gyrA96 deoR nupG Φ80dlacZΔM15 Δ(lacZYA-argF)U169 hsdR17(r<sub>K</sub><sup>-</sup> m<sub>K</sub><sup>+</sup>) λ<sup>-</sup>*
- *Agrobacterium tumefaciens* GV3101 (pMP90)  
non-oncogenic, displays resistance against rifampicin and gentamycin (Koncz and Schell, 1986)

#### 2.1.3 Yeast strains

- *Saccharomyces cerevisiae* DBY747 Δ*mrs2*  
genotype: *MATa leu2-3 leu2-112 his3-1 ura3-52 trp1-289 mrs2::HIS3 [rho<sup>+</sup> mit<sup>+</sup>]*  
The strain originates from the strain ATCC 44774. For further description see Wiesenberger et al. (1992) and Bui et al. (1999).
- *Saccharomyces cerevisiae* THY.AP4  
genotype: *MATa ura3 leu2 lexA::lacZ::trp1 lexA::HIS3 lexA::ADE2*  
For further description see Obrdlik et al. (2004).
- *Saccharomyces cerevisiae* THY.AP5  
genotype: *MATa URA3 leu2 trp1 his3 loxP::ade2*  
For further description see Obrdlik et al. (2004).

#### 2.1.4 Vectors

- **pDONR221** (Invitrogen Inc.): donor vector for Gateway™ system
- **pK7FWG2** (Karimi et al., 2002): plant expression vector for gene-GFP fusion behind 35S promoter
- **pMDC83** (Curtis and Grossniklaus, 2003): plant expression vector for gene-GFP fusion behind 35S promoter
- **YEpl351** (Hill et al., 1986): expression vector for yeast, native promoter
- **pVT103-U** (Vernet et al., 1987): expression vector for yeast, ADH promoter
- **pMetYCgate** (Obrdlik et al., 2004): fusion to C-terminal part of ubiquitin for use with mating-based split ubiquitin system
- **pNXgate33-3HA** (Cappellaro and Boles, unpublished): fusion to N-terminal part of ubiquitin for use with mating-based split ubiquitin system
- **pGEMHE** (Liman et al., 1992): *Xenopus* expression vector
- **pcDNA3.1D/V5-His** (Invitrogen Inc.): mammalian expression vector, suitable for *Xenopus* expression
- **pDK148** (Zeuthen, University of Copenhagen, unpublished): *Xenopus* expression vector with improved expression background

Detailed maps of the vectors are found in the respective sections in the Methods or the Results chapter.

#### 2.1.5 Oligonucleotides

The sequences of the oligonucleotides used throughout this work are found in the appendix (see section 8.1). Oligonucleotides were purchased from the companies Invitrogen, biomers.net, Thermo Electron, and Qiagen Operon.

#### 2.1.6 Laboratory equipment

Standard laboratory instruments and equipment have been used during this thesis and will not be listed here. Worth mentioning are some plant-specific tools:

- The **plant growth cabinet KBW400 (Binder)** has been used to grow *Arabidopsis* under defined temperature and light conditions of 24 °C and 110  $\mu\text{mol photons} \times \text{m}^{-2} \text{s}^{-1}$  using the Osram L 18W/77 fluorescent tubes.

- 
- The *Arabidopsis* growth chamber is equipped with **Osram LUMILUX Daylight** FQ 39W/860 fluorescent tubes and a R410A Split Series FTKS35CVMB **room air conditioner (Daikin Industries, Ltd.)** to provide appropriate light and temperature conditions of  $110 \mu\text{mol photons} \times \text{m}^{-2} \text{s}^{-1}$  and  $24 \text{ }^\circ\text{C}$ .
  - Adult *Arabidopsis* plants have been grown in the **Arasystem (Betatech)** to offer support for the inflorescences and to prevent seeds from uncontrolled distribution.

### 2.1.7 Bioinformatics tools

There is a growing number of software useful for the analysis of DNA and protein sequences. The following programs have been used frequently during the work on this thesis and also for the preparation of figures within the thesis dealing with sequences in one way or the other:

- MEGA 3.1 (Kumar et al., 2004)
- Vector NTI (Invitrogen Inc.)
- BioEdit 7.0.1 (Hall, 1999)

## 2.2 Methods

### 2.2.1 Established methods in molecular biology

In the past decades numerous methods were developed and became essential tools for everyday work in molecular biology. These methods include, for example, gel electrophoreses (both of DNA and of proteins), purification of nucleic acids, restriction endonuclease cleavage, cloning techniques (blunting, ligation), performance of a western blot, handling of *Escherichia coli* laboratory strains, and of course the widely used PCR (polymerase chain reaction) technique. Detailed descriptions of these standard methods can be found in the compilation of Sambrook et al. (1989) and, regarding PCR, in the book by Newton and Graham (1994) and will not be specified in this thesis. The following chapters will describe miscellaneous plant specific applications and several cloning designs.

Some applications in this thesis were performed with reaction kits according to the manufacturers' protocols. The kits are listed below, as well as the PCR polymerases used during this thesis.

- Isolation of plant DNA: DNeasy Plant Mini Kit, Qiagen  
NucleoSpin®-Plant, Macherey-Nagel
- Isolation of plant RNA: RNeasy Plant Mini Kit, Qiagen  
NucleoSpin®-RNA Plant, Macherey-Nagel
- Isolation of plasmid DNA: QIAprep Spin Miniprep Kit, Qiagen  
NucleoSpin®-Plasmid, Macherey-Nagel  
FastPlasmid® Mini, Eppendorf
- Gel extraction of DNA: QIAquick Gel Extraction Kit, Qiagen  
NucleoSpin®-Extract II, Macherey-Nagel  
Perfectprep® Gel Cleanup, Eppendorf
- Polymerases for PCR: SilverStar DNA Polymerase, Eurogentec  
Taq DNA Polymerase, Fermentas  
Herculase Polymerase, Stratagene  
Pfu Polymerase, Biomaster  
Taq Polymerases S & E, Genaxxon  
FastStart High Fidelity PCR System, Roche  
BD Advantage™ 2 PCR Enzyme System, BD  
Biosciences

- Reverse transcription of mRNA: Omniscript RT Kit, Qiagen  
Transcriptor Reverse Transcriptase, Roche

Sequencing of the constructs cloned in this thesis was performed both manually and by an external company. Manual sequencing was accomplished on the ALFexpress II DNA Sequencer (Amersham Biosciences) using the ReproGel Long Read gel matrix and the Thermo Sequenase Cy5 Dye Terminator Cycle Sequencing Kit (both Amersham Biosciences) or alternatively the SequiTherm EXCEL™ II Long-Read™ DNA Sequencing Kit-ALF™ (Epicentre) according to the manufacturers' protocols. External sequencing was assigned to the Macrogen Corporation in South Korea (see <http://www.macrogen.com> for further information).

### 2.2.2 Designing plant expression constructs with the Gateway™ technology

Cloning of PCR products into the vector of choice was immensely facilitated when Invitrogen Inc. introduced their Gateway™ technology. It is based on the site-specific recombination system used by phage lambda ( $\lambda$ ) to integrate into and excise from the *E. coli* chromosome. The attachment sites necessary for the homologous recombination event are provided by the PCR products and vectors, respectively; the corresponding enzymes can be purchased. The cloning process occurs in a two step reaction:

In the first reaction (the BP reaction) the PCR product flanked by attachment sites of the type B (“bacterial” attB sites) is recombined into a donor vector containing attP (“phage”) sites via the BP Clonase™ enzyme mix (see Figure 2.2.1). This enzyme mix consists of the phage  $\lambda$  Integrase and the *E. coli* Integration Host Factor proteins. Following the BP reaction the PCR product, now flanked by the recombined attL sites, is found within the donor vector; the construct is called entry clone.



**Figure 2.2.1: BP reaction**

Image taken from the Invitrogen Instruction Manual for the Gateway™ Technology, Version D.

In the second reaction (the LR reaction) this entry clone is recombined with the destination vector of choice containing attR sites via the LR Clonase™ enzyme mix which contains, additionally to the two proteins mentioned above, the phage  $\lambda$  Excisionase protein. This reaction yields the PCR product within the desired vector, again flanked by attB sites (see Figure 2.2.2).



**Figure 2.2.2: LR reaction**

Image taken from the Invitrogen Instruction Manual for the Gateway™ Technology, Version D.

An additional feature of the Gateway™ technology facilitating the identification of recombined clones is the usage of the ccdB gene as a negative selection marker in addition to the antibiotic resistance genes present on the vectors used. The ccdB gene is provided within the Gateway™ cassette in between the two attachment sites (see Figure 2.2.1 and Figure 2.2.2) in the original vector before recombination. After a successful recombination the ccdB gene is replaced by the PCR product of choice. The CcdB protein (ccd stands for coupled cell division) interacts with the *E. coli* DNA gyrase subunit A thus causing double strand breaks in the *E. coli* DNA. This protein is naturally encoded on the F plasmid together with the CcdA protein; the two proteins are involved in the stable maintenance of the F plasmid after cell division: CcdA inhibits the lethal action of CcdB in cells containing the F plasmid whereas cells not having received an F plasmid after segregation are killed due to the prolonged action of CcdB. CcdA's half life time is shorter than CcdB's hence CcdB persists longer within the progeny cells (Bernard and Couturier, 1992). For usage with the Gateway™ technology solely the ccdB gene is provided on the original vector thus leading to death of those cells transformed with the non-recombined vector. In theory only *E. coli* cells having been transformed with a recombined donor or destination vector should be able to grow on the appropriate selection plates.

The original vectors can be amplified in the *E. coli* strain DB3.1 carrying a mutation within subunit A of the *E. coli* gyrase which leads to a resistance to the lethal effects of CcdB (Bernard and Couturier, 1992).

One of the advantages of the Gateway™ technology is given by the possibility to transfer the PCR product of choice from the donor vector into multiple destination vectors for different



applications. Thus numerous destination vectors have been constructed both by Invitrogen Inc. and by independent research groups. So far, for the plant sector there are no vectors commercially available but can be obtained from other research groups, generally via material transfer agreements. The destination vectors used in this thesis come from the sets designed by Karimi et al. (2002) and Curtis and Grossniklaus (2003). The donor vector pDONR221 on the other hand was purchased from Invitrogen Inc. Maps of the respective vectors can be found in Figure 2.2.3.

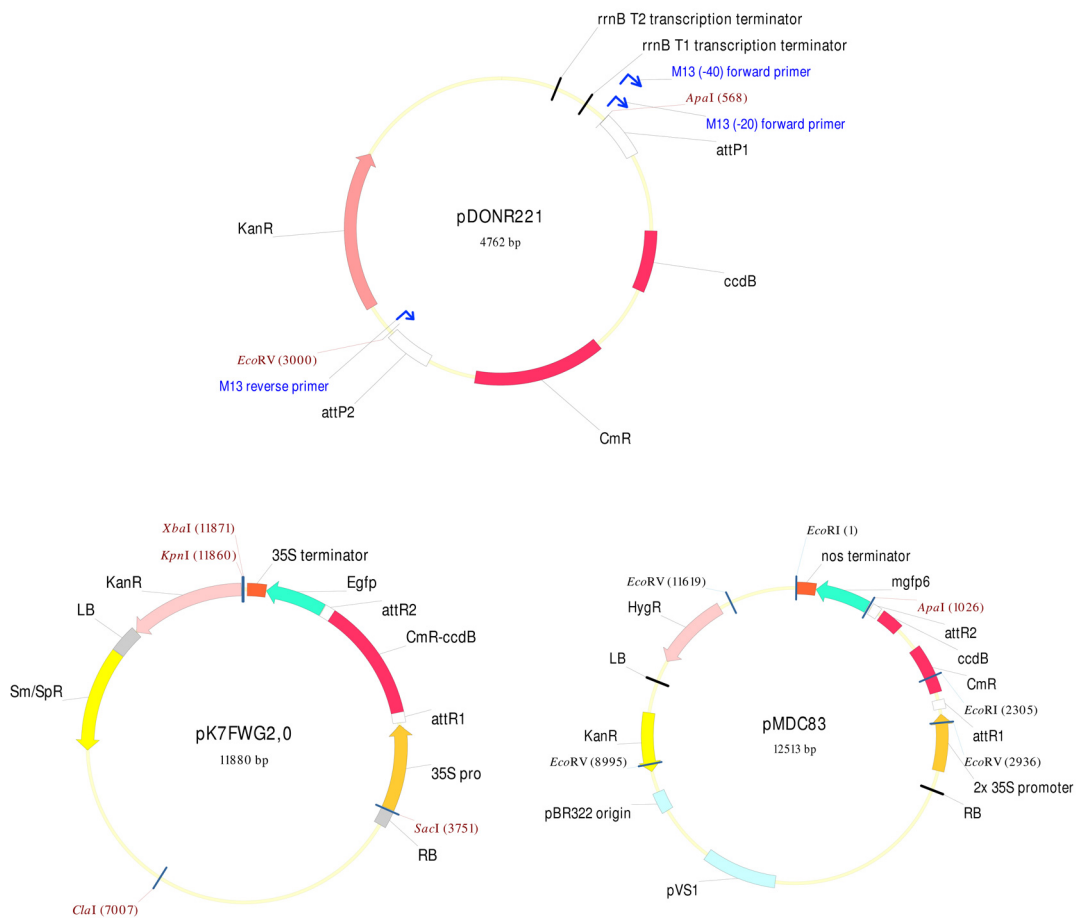


**Figure 2.2.3: Maps of the Gateway™ vectors for gene-GFP fusion construct expression**

Shown are the donor vector pDONR221 (top; Invitrogen Inc.) and the two destination vectors pK7FWG2 (bottom left; Karimi et al. (2002)) and pMDC83 (bottom right; Curtis and Grossniklaus (2003)).

The BP and LR clonase™ reactions were performed according to the Invitrogen manual with appropriate amounts of the two DNA species to be recombined.

### 2.2.3 Transformation of *Arabidopsis thaliana* via *Agrobacterium tumefaciens*

In the last century a naturally occurring process was modified to produce transgenic plants: the ability of the soil bacterium *Agrobacterium tumefaciens* to transfer its DNA into plant hosts and induce growth of a tumour within these plants. Today disarmed Ti plasmids (Ti = tumour inducing) are used in combination with a second vector containing the genes for the transfer of the T-DNA (transfer DNA) from *Agrobacterium* into the plant (a so-called binary vector system). *Agrobacterium* no longer produces virulent tumours but is merely a vehicle for the transfer of a defined portion of DNA into a host plant and the stable integration of this DNA into the plant's genome. If reproductive tissues have been transformed with the T-DNA the progeny will contain the transgenic allele in every cell forming stably transformed plants (contrary to transiently transformed plants).

In order to transform *Arabidopsis thaliana*, *Agrobacterium tumefaciens* needs to be transformed with a plasmid containing the desired T-DNA. Hence competent *Agrobacterium* cells of the strain GV3101 (pMP90) (Koncz and Schell, 1986) were produced following the protocol of Höfgen and Willmitzer (1988). *A. tumefaciens* GV3101 (pMP90) carries resistances against rifampicin (chromosomally encoded) and gentamycin (encoded on the helper plasmid pMP90) both of which are used as selection markers.

In brief, a starter culture of 20 ml **YEB medium** containing the appropriate antibiotics is inoculated with a single colony of *Agrobacterium tumefaciens* and incubated overnight at 28 °C and 170 rpm. The starter culture is transferred into a main culture of 200 ml YEB medium with antibiotics and incubated for 3 to 4 hours at 28 °C and 170 rpm. The bacteria are harvested via centrifugation (5000 rpm, 10 min, 20 °C), washed once with 20 ml of **TE buffer**, resuspended in 2 ml of YEB medium without antibiotics, and aliquots of 200 µl are shock-frozen in liquid nitrogen. The competent cells can be stored for several months at -70 °C.

Höfgen and Willmitzer (1988) also introduced a protocol for the temperature-mediated transformation of the competent *Agrobacterium* cells with the desired plasmid carrying the T-DNA which was used in this thesis. Competent *A. tumefaciens* cells are thawed on ice, mixed with 1 µg of the plasmid to be transformed, and subsequently incubated for 5 min each under the following conditions: on ice, in liquid nitrogen, and at 37 °C. After the addition of 1 ml of YEB medium without antibiotics the cells are incubated at 28 °C and 800 rpm for 3 to 4 hours before plating 200 µl (and the remainder separately) on selection plates containing, besides rifampicin and gentamycin, a third antibiotic for selection of the *Agrobacterium* cells containing the desired plasmid. The plates are incubated at 28 °C for 2 days.

---

<b>YEB medium:</b>	0.5 % beef extract (w/v)
	0.1 % yeast extract (w/v)
	0.1 % peptone (w/v)
	0.5 % sucrose (w/v)
	pH 7.0 with NaOH
for selection plates:	1.5 % agar-agar (w/v)
add after autoclaving:	20 mM MgSO <sub>4</sub>
	rifampicin (100 µg/ml)
	gentamycin (25 µg/ml)
	spectinomycin (100 µg/ml) or
	kanamycin (50 µg/ml) if necessary
<b>TE buffer:</b>	10 mM Tris (Tris(hydroxymethyl)aminomethane)
	1 mM EDTA (ethylenediamine tetraacetic acid)
	pH 8.0 with HCl

Transformation of *Arabidopsis thaliana* with the appropriate *Agrobacterium tumefaciens* cells was accomplished following the protocol of Clough and Bent (1998). Basically this protocol relies on dipping of the above ground parts of the plant into a solution of *Agrobacterium* cells. The bacteria enter the plant tissues through the stomata and infect diverse plant cells. If the floral meristem is affected stably transformed seeds will be produced and can be selected for the appropriate antibiotic resistance. The transformation efficiency of this method is rather low, but due to the high number of *Arabidopsis* floral meristems and seeds approximately 20 transgenic seedlings on average can be obtained from the transformation of a pot containing 4 plants.

In brief, *A. thaliana* Col-0 or Col-5 wild type seeds are sown in pots with standard cultivation soil containing 1/5 of vermiculite, and 4 to 5 plants per pot are grown until flowers develop. Growth conditions are 24 °C and a light intensity of 110 µmol photons × m<sup>-2</sup> s<sup>-1</sup> for 16 h per day. To further increase the number of flowers the inflorescences can be cut 1 to 2 times before transformation. Two days before transformation a 10 ml starter culture of YEB medium with the appropriate antibiotics is inoculated with *Agrobacterium* cells harbouring the desired vector and incubated at 28 °C and 170 rpm overnight. On the following day a main culture of 200 ml YEB medium with antibiotics is inoculated with the starter culture and incubated overnight under the same conditions. On the day of transformation the bacterial culture is harvested by centrifugation (5000 rpm, 10 min, 20 °C) and resuspended in **infiltration medium**. The *Agrobacterium* solution is transferred to a 250 ml beaker, filled to 200 ml with infiltration medium, and the *Arabidopsis* plants are dipped into the solution upside down 3 times for 3 min each. Two pots of plants are used per *Agrobacterium* strain. After transformation the plants are kept lying in a tray covered with a plastic dome for 24 hours before setting them upright again and watering a little. After the production of new

inflorescences the plants are wrapped in light-penetrable paper bags, cultivated until siliques develop and not watered anymore before harvesting the seeds. These seeds are kept at 4 °C for 4 to 7 days to vernalize before sowing on **selection medium**.

<b>Infiltration medium:</b>	1 × Murashige and Skoog (MS) salts with Gamborg vitamins 5 % sucrose (w/v) 0.025 % MES ( <u>m</u> orpholine <u>e</u> thane <u>s</u> ulfonic acid) (w/v) pH 5.7 with KOH
add after autoclaving:	0.044 μM BAP ( <u>b</u> enzyl <u>a</u> minopurine) 0.05 % Silwet L-77 (v/v)
<b>Selection medium:</b>	1 × MS salts with Gamborg vitamins 0.5 % sucrose (w/v) 0.05 % MES (w/v) pH 5.7 with KOH
agar-agar for solid medium:	0.8 % for soft plates 1.5 % for hard plates
add after autoclaving:	kanamycin (50 μg/ml) or hygromycin (30 μg/ml) ampicillin (100 μg/ml)

#### 2.2.4 Transformation of *Arabidopsis* protoplasts

Besides transformation of *Arabidopsis* floral meristems to obtain stably transformed plant lines, several methods exist to produce transiently transformed plant cells. One method used in this thesis is the PEG-mediated transformation of *Arabidopsis* leaf protoplasts. It was accomplished following the protocol of Abel and Theologis (1994) with minor deviations.

In brief, 1 to 2 g of *Arabidopsis* leaves are surface-sterilised with 70 % ethanol, dried under a sterile hood, and cut into approximately 1 mm wide bands with a sharp razor blade. The leaf pieces are incubated overnight in 15 ml of **enzyme solution** in a 90 mm petri dish under gentle agitation, filtered through a 120 μm and a 60 μm mesh, and collected in a 15 ml falcon tube. After centrifugation (800 rpm, 3 min, 20 °C) the supernatant is discarded and the protoplasts are washed with 10 ml of **W5 solution** without disturbing the pellet. Following a second centrifugation step the protoplasts are resuspended in 6 ml of W5 solution and kept on ice for 30 min. After centrifugation (800 rpm, 1 min, 20 °C) the protoplasts are resuspended in 4 ml of **MMG solution** and kept on ice until further utilisation (for at least 20 min). A portion of the protoplast solution is counted in a Fuchs-Rosenthal counting chamber and the concentration is adjusted to  $5 \times 10^6$  protoplasts/ml.

For transformation 200 μl of the protoplast solution is provided in a 60 mm petri dish to provide easy accessibility and carefully mixed with 20 μl of plasmid DNA (containing 80 to 100 μg DNA). 220 μl of **PEG solution** is added and carefully mixed. After incubation for

15 min, 0.5 ml of W5 solution is added, followed by incubation for 15 min, addition of 1 ml of W5 solution, incubation for 15 min, addition of 2 ml of W5 solution, incubation for 15 min, and addition of 4 ml of W5 solution. The transformation mix is carefully transferred to a 15 ml falcon tube and incubated overnight at room temperature in the dark. On the following day the solution above the sedimented protoplasts is nearly completely discarded and the protoplasts are resuspended in the remaining 2 ml of medium prior to fluorescence microscopy.

**Enzyme solution:** 1.5 % cellulase “Onozuka R-10” (w/v) (Serva, # 16419)  
0.4 % macerozyme R-10 (w/v) (Serva, # 28302)  
400 mM mannitol  
20 mM KCl  
20 mM MES  
heat to 55 °C for 10 min, let cool down  
10 mM CaCl<sub>2</sub>  
0.1 % BSA fraction V (w/v)  
pH 5.7 with KOH  
filter sterilise (pore size 0.45 µm)

**W5 solution:** 154 mM NaCl  
125 mM CaCl<sub>2</sub>  
5 mM KCl  
2 mM MES  
5 mM glucose  
pH 5.7 with KOH

sterilise by autoclaving

**MMG solution:** 400 mM mannitol  
15 mM MgCl<sub>2</sub>  
4 mM MES  
pH 5.7 with KOH

sterilise by autoclaving

**PEG solution:** 40 % PEG 3550 (polyethylene glycol) (w/v)  
200 mM mannitol  
100 mM CaCl<sub>2</sub>

filter sterilise (pore size 0.45 µm)

### 2.2.5 Tobacco leaf infiltration with *Agrobacterium tumefaciens*

Another method to transiently transform plants is the infiltration of tobacco leaves with an *Agrobacterium* suspension carrying the plasmid of choice. Complete leaves of *Nicotiana benthamiana* and leaf sections of *Nicotiana tabacum*, respectively, are infiltrated, incubated and inspected under a fluorescence microscope.

The protocol used in this thesis is based on the one given in Batoko et al. (2000) with minor modifications. *Agrobacterium tumefaciens* cells are grown in 5 ml YEB medium containing the appropriate antibiotics at 28 °C and 200 rpm until they reach the stationary phase (after 24 to 48 hours). 1.5 ml of the culture is transferred to an Eppendorf tube, centrifuged for 5 min at 7600 rpm (5500 g) and 20 °C, and the pellet is resuspended in 1 ml of **infiltration solution**. This washing step is repeated once, the OD<sub>600</sub> of a 1/10 dilution is measured, and the bacterial solution adjusted to an OD<sub>600</sub> of 0.1 for *N. benthamiana* and 0.03 for *N. tabacum*, respectively.

The lower epidermis of a tobacco leaf is scratched very carefully with a sharp razor blade producing a fine cut only on the lower epidermal side. The *Agrobacterium* solution is infiltrated into the leaf or leaf section through this cut with a 1 ml syringe without a needle. After infiltration the plants are incubated under the same conditions as before, and fluorescence is observed 48 hours afterwards at the earliest.

**Infiltration solution:** 10 mM MgCl<sub>2</sub>  
100 µM acetosyringone

### 2.2.6 Tobacco protoplast transformation

As well as *Arabidopsis* protoplasts, protoplasts of *Nicotiana benthamiana* and *Nicotiana tabacum* can be transformed via a PEG-mediated method. In this thesis the method described in Koop et al. (1996) was used.

Briefly, *N. benthamiana* or *N. tabacum* leaves are surface-sterilised with 70 % ethanol, dried under a sterile hood, and cut into 1 mm wide bands at right angles to the midrib with a sharp razor blade. 9 ml of **PIN solution** are added to 0.5 % each of **cellulase “Onozuka R-10”** and **macerozyme R-10** in a 90 mm petri dish and the cut leaves are incubated in this solution overnight at room temperature under gentle agitation. On the following day the solution is filtered through a 120 µm and a 60 µm mesh, collected in a 15 ml falcon tube, and 2 ml of **PCN solution** are carefully added as the top layer. After centrifugation at 500 rpm and 20 °C for 10 min intact protoplasts are collected from the interphase between the two media and transferred to a fresh 15 ml falcon tube. The volume is adjusted to 10 ml with PIN medium, overlaid with 2 ml of PCN medium and centrifuged again. Intact protoplasts from the interphase are transferred to a fresh 15 ml falcon tube, resuspended in 10 ml of **PTN medium**, and counted in a Fuchs-Rosenthal counting chamber. After centrifugation for 10 min at 700 rpm and 20 °C the protoplast number is adjusted to  $5 \times 10^6$ /ml with PTN medium.

Per transformation 100 µl of protoplast solution are placed into a 60 mm petri dish and the protoplasts are allowed to settle for a few minutes. 18 µl of plasmid DNA (50 µg) in TE buffer and 7 µl of PCN medium are carefully added to the protoplast solution, followed by careful addition of 125 µl of **PEG solution**, mixture, and incubation for 7.5 min. 125 µl of PCN solution are added and the mix is incubated for 2 min. Then 2.6 ml of PCN solution are added, the suspension is mixed and incubated overnight in the dark at room temperature.

On the following day the protoplasts are observed under a fluorescence microscope.

**Enzyme stock solutions:** 10 % (w/v) of cellulase “Onozuka R-10” (Serva) or macerozyme R-10 (Serva) dissolved in 400 mM sucrose  
filter sterilise (pore size 0.45 µm), store at 4 °C

**PIN medium:** 1 × MS salts with Gamborg vitamins  
1.36 mM CaCl<sub>2</sub>  
5 mM MES  
0.0001 % BAP (w/v)  
400 mM sucrose  
pH 5.7 with KOH

autoclave to sterilise

**PCN medium:** 1 × MS salts with Gamborg vitamins  
1.36 mM CaCl<sub>2</sub>  
5 mM MES  
0.0001 % BAP (w/v)  
400 mM glucose  
pH 5.7 with KOH

autoclave to sterilise

**PTN medium:** 400 mM mannitol  
15 mM CaCl<sub>2</sub>  
pH 5.6 with KOH

autoclave to sterilise

**PEG solution:** 67 mM Ca(NO<sub>3</sub>)<sub>2</sub>  
270 mM mannitol  
dissolve in 17 ml Milli-Q H<sub>2</sub>O, then add  
40 % PEG 1550 (w/v)  
pH 9.75 with KOH

ad 26 ml with Milli-Q H<sub>2</sub>O

filter sterilise (pore size 0.45 µm), store in aliquots at -20 °C

### 2.2.7 Fluorescence microscopy

To detect fluorescence emitted by the green fluorescent protein (GFP) it needs to be excited by UV light of a certain wavelength. This light is provided in fluorescence microscopes either by a mercury lamp and certain filters or generated by a laser. In this thesis plant pieces and protoplasts were mainly investigated with the Zeiss Axioplan microscope using two different

filter sets and documented with the Nikon Digital Camera DXM1200 and the Nikon ACT-1 software, version 2.10. The filter sets used have the following properties:

- Filter set 09: excitation: BP 450-490  
beamsplitter: FT 510  
emission: LP 515
- Filter set 10: excitation: BP 450-490  
beamsplitter: FT 510  
emission: BP 515-565.

Thus, filter set 09 enables to observe the red autofluorescence of the chloroplasts alongside the green fluorescence of GFP, whereas filter set 10 efficiently emits only the green fluorescence of GFP.

Occasionally the Leica TCS 4D confocal microscope, equipped with an argon/krypton laser, was used to observe GFP fluorescence at an excitation wavelength of 488 nm and a 530 nm band pass emission filter.

### 2.2.8 Yeast complementation assays

A possibility to gain insight into the functionality of a protein is a complementation assay of a mutant defective in a homologous gene. The AtMRS2 proteins belong to a large family of magnesium transporters termed the 2-TM-GxN family (Knoop et al., 2005) present in every domain of life. Well characterised are the prokaryotic homologue CorA in *S. enterica* and the yeast homologues ALR1 and MRS2 and their respective mutants. The yeast  $\Delta$ msr2 strain was established in the Schweyen laboratory in Vienna (Wiesenberger et al., 1992) and displays a  $pet^-$  phenotype when grown on synthetic medium lacking a fermentable carbon source, e.g. YPdG containing glycerol as the sole carbon source. This yeast strain was successfully used for complementation assays with the prokaryotic CorA protein (Bui et al., 1999), the yeast MSR2 homologue LPE10 (Gregan et al., 2001a), the human MRS2 protein (Zsurka et al., 2001), and the first discovered plant homologue AtMRS2-1 (Schock et al., 2000) each restoring growth of the mutant strain on YPdG medium.

To demonstrate their functionality as magnesium transporters the two presumably organellarly localized *Arabidopsis* proteins AtMRS2-4 and AtMRS2-6 and the AtMRS2-3 protein were cloned into *E. coli*/yeast shuttle vectors and heterologously expressed in the  $\Delta$ msr2 strain. The cloning work was done in Bonn whereas the yeast work (transformation, trickle tests, mag-fura 2 measurements) was performed at the Vienna Biocenter by Julian Weghuber and Soňa Svidová in the group of Prof. Rudolf Schweyen.



As the ScMRS2 protein constitutes the magnesium uptake system of the inner mitochondrial membrane the complementation assays followed two different strategies: cloning of the complete coding sequences of AtMRS2-4 and AtMRS2-6 driven by the constitutive alcohol dehydrogenase (ADH) promoter into the vector pVT103-U; and fusion of the AtMRS2-3, 2-4 and 2-6 genes devoid of their N-termini behind the yeast MRS2 promoter and targeting sequence into the vector YEp351. The second approach directs the yeast-plant hybrid protein to the inner mitochondrial membrane whereas the first approach relies on the native plant amino terminus for targeting the protein to the correct yeast membrane. Figure 2.2.4 displays the maps of the two vectors used in these approaches.

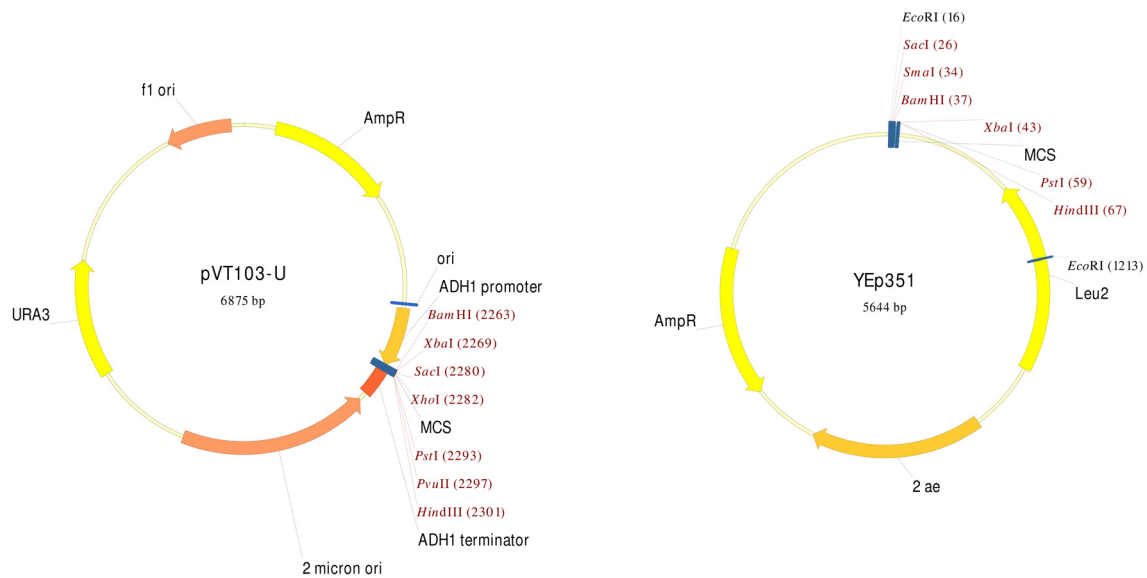


**Figure 2.2.4: Maps of the yeast expression vectors used for complementation assays**

On the left: vector pVT103-U (Vernet et al., 1987) used for expression of the native AtMRS2 coding sequences. On the right: vector YEp351 (Hill et al., 1986) used for expression of the N-terminally shortened AtMRS2 coding sequences fused to the yeast MRS2 promoter and targeting sequence.

The cloning strategies for the full length and the N-terminally shortened constructs followed the approaches described in the dissertations of Steinhauser (1999) and Schock (2000) and are summarized in Figure 2.2.5.

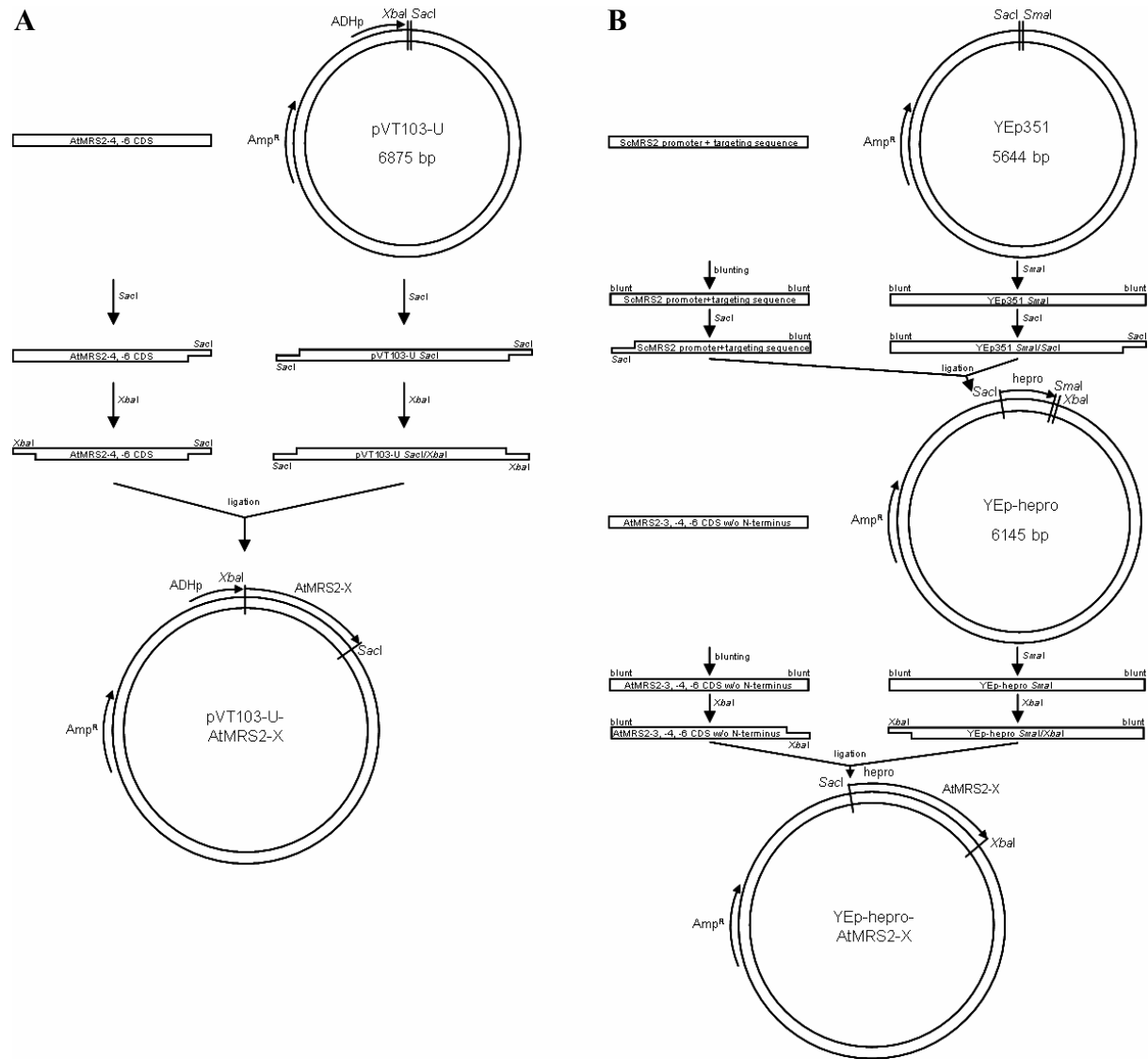


**Figure 2.2.5: Cloning strategies for yeast complementation constructs**

**A:** Cloning of full length constructs into pVT103-U. **B:** Cloning of N-terminally shortened constructs fused to yeast MRS2 promoter and targeting sequence into YEp351. Further explanations are found in the text.

For cloning into pVT103-U (see Figure 2.2.5 A) the complete coding sequence of AtMRS2-4 and AtMRS2-6, respectively, is amplified from cDNA with primers adding restriction endonuclease sites for *XbaI* upstream of the start codon and *SacI* downstream of the stop codon. Both PCR product and vector are digested with the two restriction enzymes in successive reactions, each followed by purification via phenol/chloroform extraction and ethanol precipitation. The fragments are ligated yielding a construct in which expression of AtMRS2-4 or AtMRS2-6 is driven by the constitutive ADH promoter.

Cloning into YEp351 is a two-step process (see Figure 2.2.5 B): in the first step the *Saccharomyces* MRS2 promoter and the first 94 amino acids (aa) of the MRS2 coding sequence containing the mitochondrial targeting sequence are amplified from yeast DNA, the

PCR product is blunted using T4 polynucleotide kinase and T4 polymerase, and digested with *SacI*. Likewise YEp351 is cut with *SmaI* yielding blunt ends and with *SacI*, and the fragments are ligated. This construct, termed YEp-hepro for yeast promoter, is used to clone the N-terminally shortened fragments of AtMRS2-3, 2-4, and 2-6. These are amplified from cDNA via PCR with primers starting at aa 74 for AtMRS2-3, aa 92 for AtMRS2-4, and aa 82 for AtMRS2-6, and adding an *XbaI* restriction site downstream of the stop codon. The PCR products are blunted (see above) and cut with *XbaI*, the YEp-hepro vector is cut with *SmaI* and *XbaI*, each step is followed by phenol/chloroform extraction and ethanol precipitation. The fragments are ligated yielding constructs in which the N-terminally shortened coding sequence of the respective AtMRS2 gene is fused to the mitochondrial targeting sequence of the yeast MRS2 gene and whose expression is driven by the yeast MRS2 promoter.

The constructs described above were sequenced to ensure the correctness of the cloning reactions. Subsequently, they were used to transform the  $\Delta$ mrs2 yeast strain described in Wiesenberger et al. (1992) and to observe whether the AtMRS2 genes can complement the  $\Delta$ mrs2 phenotype.

Preparation of competent yeast cells and transformation follows the protocol given in Gietz and Woods (2002). Transformants are selected on **SD medium** depleted of uracil for pVT103-U constructs or leucine for YEp351 constructs at 28 °C for 3 days.

To perform growth assays positive transformants are grown in selective SD medium and resuspended in water at a defined OD<sub>600</sub> of 2.0. This solution is diluted in a 1:10 series ending with 10<sup>-4</sup>, and 5 µl of each dilution is trickled on a **YPD** (positive control) and a **YPdG** (complementation) plate, respectively. The plates are incubated at 28 °C for the times indicated.

**SD medium:**            1 × YNB (Difco Laboratories)  
                                 1 × SD (synthetic dropout, Bio 101 Incorporation)  
                                 2 % glucose (w/v)

**YPD medium:**        1 % yeast extract (w/v)  
                                 2 % peptone (w/v)  
                                 2 % glucose (w/v)

**YPdG medium:**      1 % yeast extract (w/v)  
                                 2 % peptone (w/v)  
                                 3 % glycerol (w/v)

To solidify, the media are supplemented with 2 % agar (w/v).

A way to quantify transport via the MRS2 proteins is the measurement of magnesium uptake into isolated yeast mitochondria expressing the respective MRS2 protein. This method, established in the group of Prof. Schweyen in Vienna, is based on the usage of the magnesium-sensitive, fluorescent dye mag-fura 2 (Molecular Probes). This dye possesses different excitation wavelengths depending on whether magnesium is bound to the dye or not: 340 nm for the  $Mg^{2+}$ -bound form, 380 nm for the free form. The acetoxymethyl (AM) ester of mag-fura 2 is membrane-permeant, and isolated yeast mitochondria can be loaded with it. According to the amount of  $Mg^{2+}$  within the mitochondrion the ratio of bound and unbound mag-fura 2 changes. This is measured with the spectrofluorometer LS-55 (Perkin-Elmer) using the fast filter accessory (FFA) which allows quick change of excitation at 340 and 380 nm in 20 ms intervals with an emission measured at 509 nm. The system is calibrated by the addition of SDS (10 % (w/v)) in the presence of high magnesium concentrations (25 mM), leading to lysis of the mitochondria and accordingly the maximum 340/380 nm ratio ( $R_{max}$  of ca. 3; mag-fura 2 completely complexed with  $Mg^{2+}$ ), and subsequently of EDTA (50 mM, pH 8) complexing the  $Mg^{2+}$  and leading to the minimum 340/380 nm ratio ( $R_{min}$  of ca. 0.5; maximal amount of free mag-fura 2). The 340 and 380 nm excitation data are continuously recorded, the ratio (R) is calculated, and the magnesium concentration inside the mitochondria is determined using the following formula (first established by Grynkiewicz et al. (1985)):

$$[Mg^{2+}]_m = K_D \cdot (R - R_{min}) / (R_{max} - R)$$

with  $K_D$  being the effective dissociation constant of the mag-fura 2/ $Mg^{2+}$  complex of 1.52 in the buffer used.

Isolation of yeast mitochondria and mag-fura 2 measurements were done according to the methods described in Kolisek et al. (2003).

### **2.2.9 Analysis of protein interactions via the mating-based split ubiquitin system**

Several methods have been employed to detect possible interactions of two proteins. A system described by Johnsson and Varshavsky (1994) is based on the action of ubiquitin-specific proteases (UBPs or USPs) which generally cleave proteins attached to ubiquitin moieties (see Figure 2.2.6 A). The ubiquitin molecule itself can be split into two halves which are able to spontaneously reassemble (see Figure 2.2.6 B) and still build a functional ubiquitin which is recognized by the UBPs (see Figure 2.2.6 C). For detection of protein interactions a modification was introduced to the N-terminal half of ubiquitin ( $N_{ub}$ ): amino acid Ile-13 is replaced by Gly ( $N_{ubG}$ ), thereby preventing the spontaneous reconstitution of a functional

ubiquitin molecule (see Figure 2.2.6 D). This functional molecule can only be built if the two proteins of interest fused to each half of ubiquitin interact with each other and bring  $C_{ub}$  and  $N_{ubG}$  in close proximity to each other (see Figure 2.2.6 E). Attached to the C-terminus of  $C_{ub}$  is a reporter protein which is in turn cleaved off by the action of the ubiquitin-specific proteases and denotes the interaction of the two proteins of interest.

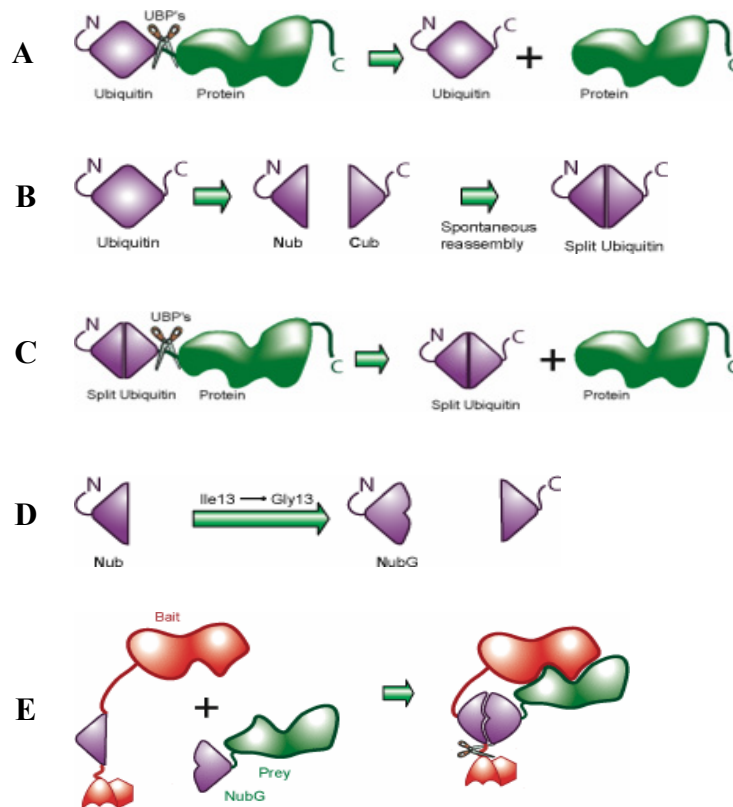


**Figure 2.2.6: Principle of the split ubiquitin system**

Basic steps undertaken to modify ubiquitin for detection of protein interactions. Further explanations are found in the text. Images taken from [http://www.dsbiotech.ch/site/technologies/split\\_ubiquitin/index.html](http://www.dsbiotech.ch/site/technologies/split_ubiquitin/index.html).

This basic principle has been adopted for the investigation of membrane protein interactions by Stagljar and colleagues (1998) and further modified by Obrdlik and colleagues (2004). Other methods like e.g. the yeast two-hybrid system are limited to the analysis of soluble proteins or soluble domains only of membrane proteins (Stagljar et al., 1998). The reporter protein released by the action of the UBPs is an artificial transcription factor termed PLV (for proteinA-LexA-VP16) which activates lexA-driven reporter genes. In the original system by Stagljar and colleagues (1998) the two genes *HIS3* and *lacZ* are expressed; Obrdlik and colleagues (2004) added the *ADE2* gene. A further improvement is the utilisation of two different yeast strains for a mating-based large-scale approach. These strains (THY.AP4 for  $C_{ub}$  fusions and THY.AP5 for  $N_{ub}$  fusions, see section 2.1.3 for genotypes) allow for *in vivo*

recombination of the PCR products of interest into the respective vectors by parallel transformation of PCR product and linearized vector. As the two strains have different mating types (MATa for THY.AP4, MAT $\alpha$  for THY.AP5) the N<sub>ub</sub> construct can easily be transferred from THY.AP5 into THY.AP4 by mating of the respective yeasts.

The *in vivo* cloning process is based on the same principle as the Gateway™ system (cf. section 2.2.2): both PCR product and vector contain attachment sites which are fused by the native yeast recombination ability saving laborious *in vitro* cloning procedures. Maps of the vectors used are given in Figure 2.2.7. The N<sub>ub</sub> vector pNXgate33-3HA is a low copy plasmid recommended for the first test of the screening system. If interactions cannot be detected, high copy vectors are available as well (e.g. pNXgate32-3HA). The C<sub>ub</sub> vector pMetYCGate is a low copy plasmid which contains the *MET25* promoter regulating the expression of the C<sub>ub</sub> fusion protein. The promoter is sensitive to elevated methionine concentrations allowing a titration of the amount of C<sub>ub</sub> fusion protein and therefore of the detection of interactions via reporter gene activity.

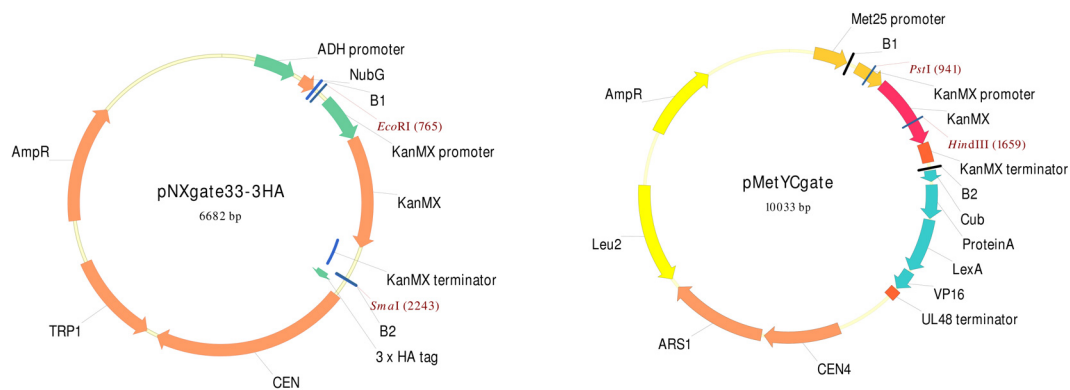


**Figure 2.2.7: Maps of the vectors used in the mating-based split ubiquitin system**

On the left: vector pNXgate33-3HA (Cappellaro and Boles, unpublished) for fusion of the protein of interest to the N-terminus of ubiquitin. On the right: vector pMetYCGate (Obrdlik et al., 2004) for fusion of the C-terminus of ubiquitin to the protein of interest.

The mating-based split ubiquitin system (mbSUS) as presented by Obrdlik et al. (2004) thus provides a useful platform for the screening of possible interactions of a large number of membrane proteins, as for example the AtMRS2 gene family of magnesium transporters.

The mbSUS as used by Petr Obrdlik (ZMBP, University of Tübingen) was adopted for usage in our group during this thesis. First screens were accomplished in the laboratory in Tübingen, followed by repetitions and expansions in our laboratory. The detailed protocols are described

in the “Manual for the use of mating-based Split ubiquitin system “mbSUS”, version B, December 2004” by Petr Obrdlik available together with the components of the system.

Figure 2.2.8 gives an overview of the experimental steps of the mbSUS with the possible methods to detect interactions.

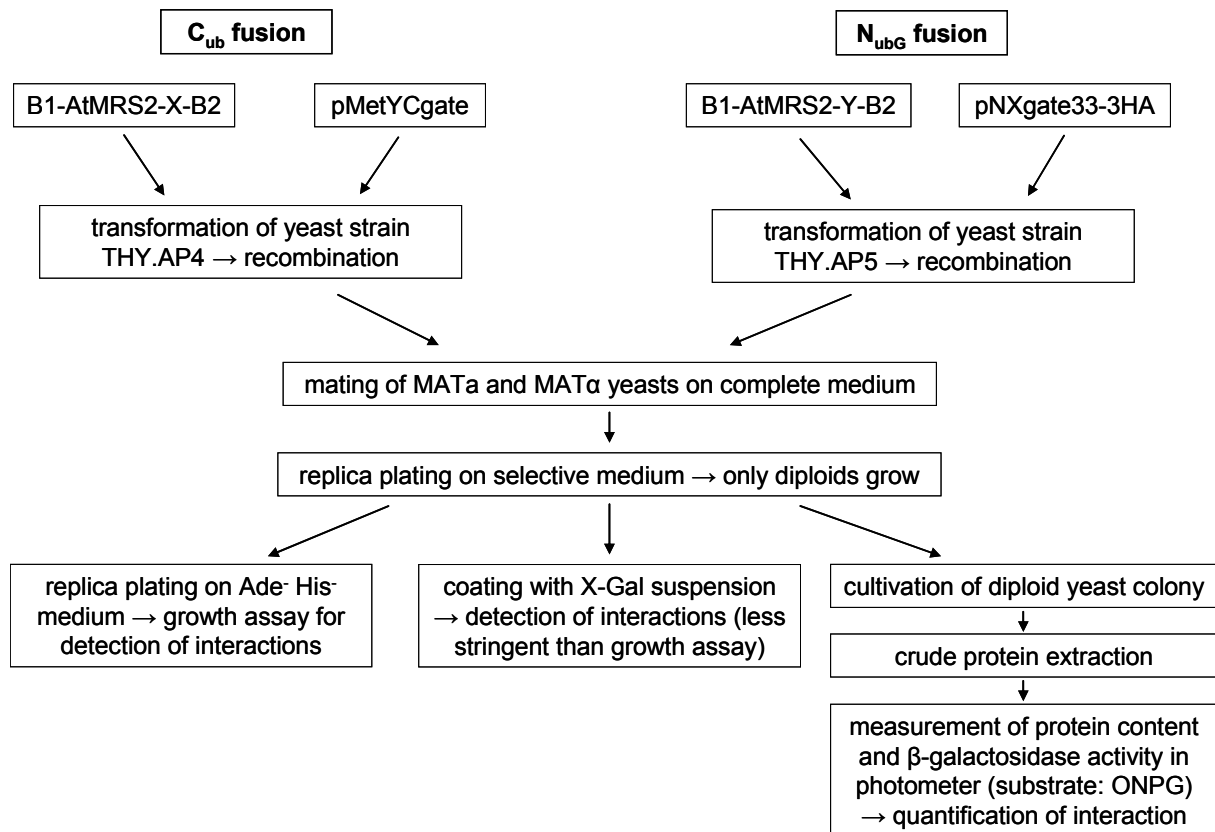


**Figure 2.2.8: Flow chart of the mbSUS approach**

The basic steps of the application of the mating-based split ubiquitin system (Obrdlik et al., 2004) are: Transformation of the respective yeast strains with PCR products containing the B1 and B2 linkers and linearized vector, mating of the two yeast strains, selection of diploid yeast cells, and test for interaction via different methods (growth assay, X-Gal assay, and quantitative ONPG assay).

The method was performed according to the manual mentioned above; the quantitative  $\beta$ -galactosidase assay was not applied.

### 2.2.10 Heterologous expression in *Xenopus* oocytes

The oocytes of the clawed frog *Xenopus laevis* became a widely used tool to study the electrogenic properties of ion channels and transporters via electrophysiological methods. They can be prepared easily from female clawed frogs, kept stable for a couple of days and due to their relatively large diameter (1.1 to 1.3 mm) are easy to handle in subsequent

applications (for a review see Wagner et al. (2000)). The oocytes are equipped with the complete protein expression machinery and are thus able to translate endogenous mRNA into proteins. For heterologous protein expression the oocytes are injected with the cRNA (copy-RNA) of choice, the protein is synthesized, and in case of a membrane protein integrated into the oocyte plasma membrane. Transport of its substrates via this membrane protein can, if the transport is electrogenic, be measured by electrophysiological methods such as DEVC, the double electrode voltage clamping technique.

For the synthesis of cRNA the coding sequence of the protein of interest needs to be cloned into an oocyte expression vector such as pGEMHE (Liman et al., 1992) which provides 5' and 3' UTRs (untranslated regions) of a well-translated *Xenopus* mRNA, usually  $\beta$ -globin (Wagner et al., 2000) and a T7, T3, or SP6 RNA polymerase promoter. After linearization downstream of the 3' UTR, the CDS is transcribed with the respective RNA polymerase *in vitro* yielding cRNA to be injected into the oocytes.

The oocyte experiments described in this thesis were performed in cooperation with the group of Prof. Hedrich at the University of Würzburg. Designing and cloning of the expression constructs was accomplished in Bonn, whereas the measurements were conducted in Würzburg.

In a first attempt the coding sequences of AtMRS2-1, 2-3, and 2-5 were amplified from cDNA and directionally cloned into the *Xenopus* expression vector pGEMHE (Liman et al. (1992); see Figure 2.2.9) via different restriction enzyme sites added to the primer sequences. Transcription is accomplished by the T7 RNA polymerase recognizing the T7 promoter upstream of the cassette consisting of 5' UTR, CDS, and 3' UTR.

In a second experiment a V5-His6 tag (V5 being the GKPIPPLLGLDST epitope from the P and V proteins of Simian parainfluenza virus 5 (SV5); His 6 being six histidine residues in succession) was added downstream of the CDS of AtMRS2-1 and 2-5 by in-frame cloning into the vector pcDNA3.1D/V5-His (Invitrogen Inc.; see Figure 2.2.9). The cassette is preceded by the T7 promoter. The V5His6 tag allows for the detection of the expressed protein in a western blot with anti-V5 antibodies.

In a third experiment the coding sequences of AtMRS2-1, 2-5, and a mutated version of AtMRS2-5 harbouring an AMN motif instead of the GMN motif were cloned into pDK148 which provides an improved expression background (T. Zeuthen, University of Copenhagen; see Figure 2.2.9).





**Figure 2.2.9: Maps of the vectors used for heterologous expression in *Xenopus* oocytes**

Displayed are the vectors pGEMHE (top left; Liman et al. (1992)), pcDNA3.1D/V5-His (top right; Invitrogen Inc.), and pDK148 (bottom; Zeuthen, unpublished).

The respective plasmids were verified via restriction enzyme digestion and sequencing and sent to the laboratory of Prof. Hedrich in Würzburg. After linearization, cRNA is synthesized following the protocol of the T7 mMessage™ mMachin™ Kit (Ambion Inc.). 30-50 ng of this cRNA is injected into oocytes isolated from *Xenopus laevis* frogs using a General Valve Picospritzer II microinjector. Two to six days after injection, these oocytes can be applied to the double electrode voltage clamping technique using a Turbotec-01C two-microelectrode voltage-clamp amplifier (NPI instruments) with pipettes filled with 3 M KCl having an input resistance of about 0.5 to 2 MΩ.

The DEVC technique uses one of the electrodes to measure the membrane potential of the oocyte plasma membrane in relation to the potential of the bathing electrode and to compare this potential to the voltage clamp command given by a generator. If the two potentials differ,

a current resetting the membrane potential to the desired value is delivered through the second electrode. This current is amplified and recorded; it can be read as the counter current induced by electrogenic ion or substrate fluxes across the oocyte membrane. Comparison to non-injected control oocytes makes sure that the currents measured are indeed caused by transport through the protein heterologously expressed within the oocyte (for a review, see Wagner et al. (2000)).

The oocytes are placed into the recording chamber, the glass microelectrodes impaled into the opposite poles of the oocyte by use of micromanipulators and a stereomicroscope, and the membrane potential clamped to a voltage usually around -20 to -30 mV. While keeping the oocyte in the recording chamber, it needs to be surrounded by either control solutions or the solutions designed for the respective measurements.

Two different types of DEVC measurements are performed: in the first type, the membrane potential is clamped to a fixed voltage, and the currents delivered after the application of defined solutions are recorded. Table 2.2-1 summarizes the solutions used both for storage of the injected oocytes and for the DEVC recordings. A typical experiment looks like this: the membrane potential is clamped to -100 mV, and three different solutions are applied, starting with 1 mM MgCl<sub>2</sub>, then 0 mM MgCl<sub>2</sub>, 10 mM MgCl<sub>2</sub>, 0 mM MgCl<sub>2</sub>, and 1 mM MgCl<sub>2</sub>. This is repeated at different membrane potentials, e.g. -60 mV, 0 mV, -120 mV. As a result, currents depending on the membrane potential and/or the extracellular magnesium concentration can be recorded.

In the second type of measurement, a range of different solutions is used as well, but, starting at a potential of -30 mV, the membrane voltage is successively changed from +60 mV to -120 mV in 10 mV steps for a duration of 2 s per step. Afterwards, the voltage-current relationship dependent on the extracellular solution can be plotted.

As can be seen in Table 2.2-1, a wide range of magnesium concentrations is used for the measurements, mostly as MgCl<sub>2</sub>, but also as Mg-Gluconate and Mg-ATP to test whether the transport might be energy-dependent. The first couple of solutions (denoted “x Mg<sup>2+</sup> / y Ca<sup>2+</sup>”) are designed to have the same ionic strength independent of the magnesium concentration; CaCl<sub>2</sub> is used to complete the amount of ions. Where indicated, buffers are used at two different pH values to test the possibility of a pH-dependent transport. Also addition of NaCl to some buffers is used to study potential effects of this cation on the transport. Co(III)-hexaammine, known as a potent inhibitor of bacterial CorA magnesium transporters (Kucharski et al., 2000), is used in the buffers indicated to block possible magnesium-induced currents.

**Table 2.2-1: Composition of the solutions used for *Xenopus* oocyte storage and DEVC measurements**

Solution	NaCl (mM)	KCl (mM)	CaCl <sub>2</sub> (mM)	MgCl <sub>2</sub> (mM)	Mg-Gl. (mM) <sup>1</sup>	Mg-ATP (mM)	HEPES (mM)	MES (mM) <sup>2</sup>	Tris (mM) <sup>3</sup>	pH
ND96 (storage)	96	2	1	1			5			7.4
ND96 low Mg <sup>2+</sup>	96	2	1	0.2			5			7.4
control solution		30	1	1.5				10		5.6
0 Mg <sup>2+</sup> / 11 Ca <sup>2+</sup>		30	11	0				10		5.6
0 Mg <sup>2+</sup> / 11 Ca <sup>2+</sup>		30	11	0					10	7.5
1 Mg <sup>2+</sup> / 10 Ca <sup>2+</sup>	(10) <sup>4</sup>	30	10	1				10		5.6
5 Mg <sup>2+</sup> / 6 Ca <sup>2+</sup>		30	6	5				10		5.6
10 Mg <sup>2+</sup> / 1 Ca <sup>2+</sup> <sup>5</sup>	(10) <sup>4</sup>	30	1	10				10		5.6
10 Mg <sup>2+</sup> / 1 Ca <sup>2+</sup>		30	1	10					10	7.5
1 Mg <sup>2+</sup> / 50 Ca <sup>2+</sup>		30	50	1				10		5.6
50 Mg <sup>2+</sup> / 1 Ca <sup>2+</sup>		30	1	50				10		5.6
0 mM MgCl <sub>2</sub>	10	30	1	0				10		5.6
1 mM MgCl <sub>2</sub>	10	30	1	1				10		5.6
5 mM MgCl <sub>2</sub>	10	30	1	5				10		5.6
10 mM MgCl <sub>2</sub> <sup>5</sup>	10	30	1	10				10		5.6
25 mM MgCl <sub>2</sub> <sup>5</sup>	10	30	1	25				10		5.6
1 mM Mg-Gl.	10	30	1		1			10		5.6
10 mM Mg-Gl.	10	30	1		10			10		5.6
1 mM Mg-ATP	10	30	1			1		10		5.6
10 mM Mg-ATP	10	30	1			10		10		5.6
1 mM Mg-ATP + 9 mM Mg-Gl.	10	30	1		9	1		10		5.6

<sup>1</sup>: Mg-Gl. = Mg-Gluconate; <sup>2</sup>: pH adjusted with 1 M Tris; <sup>3</sup>: pH adjusted with 0.5 M MES; <sup>4</sup>: these buffers are used both with and without 10 mM NaCl; <sup>5</sup>: these buffers are additionally prepared with 1 mM Co(III)-hexaammine

The storage solutions (ND96/ND96 low Mg<sup>2+</sup>) are filter sterilised after adjustment of the pH with 1 M Tris. After addition of all components and adjustment of the pH, the osmolarity of the DEVC solutions is measured and adjusted to 200-220 mOsmol/kg by the addition of D-sorbitol.

For more detailed descriptions of oocyte loading, DEVC measurements, and data analysis, compare the following references: Becker et al. (1996), Hoth et al. (1997), and Marten et al. (1999).

### 2.2.11 *Xenopus* oocyte protein extraction and immunoblot

One possibility to check the site of expression of the protein of interest in the *Xenopus* oocyte is co-expressing the protein of interest with a tag, here the V5 tag (see above), and detecting this tag in an immunoblot after extraction of microsomal protein fractions from the oocyte.

This experiment was performed in the laboratories of Prof. Hedrich in Würzburg by Andreas Latz according to the protocol given here.

Fifty *Xenopus* oocytes previously injected with the cRNA of interest are homogenised on ice in 500 µl of **Homog buffer** containing protease inhibitors. After centrifugation for 10 min at 2500 g and 4 °C, the supernatant is used for either whole protein extraction or extraction of the microsomal fraction.

- For whole protein extraction, the supernatant is mixed with Triton X-100 (Sigma) in a final concentration of 4 % and shaken for 15 min at 37 °C. After centrifugation for 15 min at 1000 g and 4 °C, the protein concentration in the supernatant is determined. The protein extract is stored at -20 °C.
- For extraction of the microsomal fraction, the supernatant is centrifuged again for 10 min at 2500 g and 4 °C to remove remaining yolk proteins. The microsomal fraction is pelleted through ultra-centrifugation at 100000 g and 4 °C and resuspended in 200 µl of Homog buffer. The solution is homogenised with a glass potter on ice, the protein concentration is determined, and the protein extract is stored at -20 °C.

50 µg of the protein extracts are separated on a denaturing SDS-PAGE, and the gel is blotted onto a Hybond-P PVDF membrane (Amersham Biosciences). The membrane is incubated with anti-V5 antibody (diluted 1:5000) for one hour and with anti-mouse alkaline phosphatase antibody (diluted 1:30000) overnight. Detection of the alkaline phosphatase is mediated by the NBT/BCIP system: the 5-Bromo-4-chloro-3'-indolyphosphate p-toluidine salt (BCIP) is hydrolysed to an intermediate by the alkaline phosphatase. By reduction of Nitro-blue tetrazolium chloride (NBT), the intermediate becomes the purple-black indigo dye 5,5'-Dibromo-4,4'-dichloro-indigo white, thus marking the protein bands that have interacted with both antibodies.

**Homog buffer:**           20 mM Tris pH 7.4  
                              5 mM EDTA  
                              5 mM EGTA  
                              100 mM NaCl

### 3. Results

#### 3.1 Investigating subcellular AtMRS2 protein localizations via gene-GFP fusions

One of the obvious questions to ask after the discovery of a family of genes in plants is that for the subcellular localization of each of the family's members. Around the time when the AtMRS2 gene family was first described in 2000 (Schock et al., 2000), localization patterns were known or beginning to become clear for the prokaryotic and yeast homologues: in prokaryotes CorA is, of course, expressed in the plasma membrane, and in yeast two distinct patterns are found with ALR1/2 in the plasma membrane and MRS2/LPE10 in the inner mitochondrial membrane (Graschopf et al., 2001; Bui et al., 1999; Gregan et al., 2001a). The increased complexities of plant cells offer further possibilities for membrane localizations in the various compartments present within the cell.

*In silico* predictions using the Aramemnon server (<http://aramemnon.botanik.uni-koeln.de>; Schwacke et al. (2003)), which combines eight different prediction programs, give hints for intracellular localization of three AtMRS2 proteins: AtMRS2-11 is clearly predicted to be localized to the chloroplast, whereas the predictions for AtMRS2-4 and AtMRS2-6 are more ambiguous with similar likelihoods both for chloroplast and mitochondrial localization. There are no similar predictions for the further members of the gene family (data not shown).

Determination of localization patterns of proteins can be achieved by a variety of methods; the most common approach nowadays is probably fusion of the protein of interest to a reporter protein and monitoring of the reporter protein's expression. For detection of tissue-specific expression in plants the reporter protein GUS ( $\beta$ -glucuronidase) is especially suited whereas for detection of subcellular localization the most commonly used reporter is the green fluorescent protein, GFP, originally isolated from the jellyfish *Aequorea victoria* and adopted for usage in molecular and cell biological investigations. GFP is a relatively small protein (27 kDa) possessing the intrinsic feature of autofluorescence when correctly folded and illuminated with UV or blue light (Cody et al., 1993). This fluorescence can be utilised to show the subcellular localization of the protein of interest translationally fused to the GFP protein. Fusion can occur both at the N- and at the C-terminus of the GFP protein, depending on the properties of the protein to be studied.

Initial studies on the subcellular localization of the first two characterised plant proteins, AtMRS2-1 and AtMRS2-2, were performed with full length- and C-terminally shortened gene-GFP constructs transiently expressed in *Arabidopsis* and tobacco protoplasts (Schock, 2000). If fluorescing at all, they revealed ambiguous localization patterns with a diffuse fluorescence within the cytoplasm which could not be assigned to a distinct membrane (Schock, 2000; Schock et al., 2000). Here, the question of subcellular localization should be approached with a completely new set of constructs for all members of the AtMRS2 family.

### 3.1.1 Full length gene-GFP constructs: cloning and transformation of *A. thaliana*

In a first approach the coding sequence of GFP was fused to the carboxytermini of the full length coding sequences of the AtMRS2 genes. Fusion to the aminotermini of the AtMRS2 genes might, at least in the cases of the chloroplast or mitochondrially localized proteins, prevent the proper protein localization and was not considered for that reason. Cloning of the constructs was performed with the Gateway™ technology developed by Invitrogen Inc., for which appropriate plant vectors became available at the beginning of this thesis. The advantages of this cloning system are described in the Materials and Methods chapter (see 2.2.2). Following the early steps of innovation several research groups constructed expression vectors suitable for different applications within the plant research field, e.g. promoter-GUS and gene-GFP fusions, RNAi applications, overexpression, etc. The vector of choice for the approach outlined above was designed by Karimi et al. (2002); it is called pK7FWG2 and suited for fusion of GFP to the C-terminus of the protein of interest and stable integration into the plant genome. A vector map can be found in Figure 2.2.3 on page 19.

Amplification of the full length coding sequences of the AtMRS2 genes was performed with the oligonucleotide pairs gate2-Xup and gate2-Xdown; sequences of the primers can be found in the appendix (see section 8.1.1). The primer pairs amplify the respective AtMRS2 gene coding sequences starting four to seven codons upstream of the ATG and terminating one codon upstream of the stop codon so that an in-frame fusion with the GFP coding sequence is maintained (see section 8.2.1 for the sequence of an exemplary construct). Added to the oligonucleotides are the bacterial attachment sites (attB) necessary for the Gateway™ recombination reactions. They produce an artificial sequence of eleven amino acids (NPAFLYKVVIS) between the C-terminus of the respective AtMRS2 protein and the N-terminus of GFP. Amplification was performed either with cDNA from rosette leaves or, in cases where no cDNA product could be obtained, with genomic DNA, resulting in the PCR product sizes given in Table 3.1-1.

**Table 3.1-1: Templates and sizes of the full length PCR products for the gene-GFP fusions**

The sizes of the PCR products include the attB attachment sites (58 bp).

PCR product	Amplification from	Size (bp)
gate2-1	rosette leaf cDNA	1399
gate2-2	rosette leaf cDNA	1255
gate2-3	genomic DNA	2206
gate2-4	genomic DNA	1578
gate2-5	genomic DNA	1747
gate2-6	genomic DNA	1583
gate2-7	genomic DNA	2123
gate2-8	not amplified	
gate2-9	not amplified	
gate2-10c	rosette leaf cDNA	1402
gate2-10g	genomic DNA	1652
gate2-11	rosette leaf cDNA	1450

AtMRS2-9, being the pseudogene within the AtMRS2 family, was not considered to be included in the localization studies. AtMRS2-8, on the other hand, was not included in the initial amplification and cloning and should be cloned later on, which was omitted when problems with the completed constructs appeared (see below).

The PCR products obtained were employed first in the BP and then in the LR reaction of the Gateway™ system leading first to entry clones and subsequently to expression clones. AtMRS2-10 was amplified both from cDNA and from genomic DNA (cf. Table 3.1-1) to ideally confirm the possibility of using both cDNA and genomic DNA products for a successful gene-GFP fusion and to address potential differences in expression levels. The constructs were sequenced to ensure the correctness of the recombination reactions in which the respective PCR product was translationally fused to the GFP coding sequence of pK7FWG2. Figure 3.1.1 on page 44 shows the binding sites of the oligonucleotides used for sequencing, namely PBJs for amplification starting upstream of the 5' end of the PCR product and gfp-pK7FWG2 anchoring within the GFP coding sequence. An exemplary sequence can be seen in the appendix (see section 8.2.1 on page 129); all constructs proved to be correct.

The expression constructs were used to stably transform *Arabidopsis thaliana* via the floral dip method (cf. section 2.2.3). After harvesting, the seeds were spread on selective medium allowing the discrimination of transformed versus non-transformed seeds via the kanamycin resistance encoded on the T-DNA integrated into the transgenic seed's genome. The numbers of transgenic plants received for each construct and further analysed through successive generations are given in Table 3.1-2.

**Table 3.1-2: Number of transgenic plants received after transformation of *A. thaliana* with the full length gene-GFP constructs**

The small letters "c" and "g" following the gene denomination refer to the PCR template, cDNA and genomic DNA, respectively.

Construct	Number of transgenic plants
AtMRS2-1c-GFP	3
AtMRS2-2c-GFP	9
AtMRS2-3g-GFP	4
AtMRS2-4g-GFP	6
AtMRS2-5g-GFP	10
AtMRS2-6g-GFP	7
AtMRS2-7g-GFP	4
AtMRS2-10c-GFP	7
AtMRS2-10g-GFP	8
AtMRS2-11c-GFP	8

These plants were further analysed to examine the fluorescence of the gene-GFP fusion protein.

### 3.1.2 Fluorescence of the full length gene-GFP fusion plants

The GFP constructs used here are driven by the cauliflower mosaic virus 35S promoter (cf. Figure 3.1.1 on page 44), a constitutive promoter ensuring high expression of the downstream coding sequences in all plant cells. Thus principally every plant tissue is suitable for examination of the fluorescence theoretically omitted by the gene-GFP fusion protein. One needs to consider the autofluorescence of certain cell compartments and compounds: chloroplasts exhibit a strong red fluorescence when excited with UV light, and cell walls, due to the phenolic compounds, show a weak green fluorescence very similar to the GFP fluorescence also under UV light. With the fluorescence microscope mostly used during this thesis, the Zeiss Axioplan kindly made available by the neighbouring group of Prof.



Schreiber, the chloroplast autofluorescence can be excluded using one of the two GFP filter sets available (cf. section 2.2.7). Fluorescence emitted by GFP is supposed to be several times stronger than the green autofluorescence of the cell walls which means that detection of the fluorescence emitted by the gene-GFP fusion proteins should be well possible with the technical means available during this thesis.

Different parts of the stably transformed plant lines obtained for each of the full length gene-GFP constructs were used for fluorescence microscopy: sections of rosette leaves cut with a razor blade, roots of several days old seedlings grown on kanamycin-containing MS (Murashige & Skoog) plates, and protoplasts gained from rosette leaves. As a negative control, the same parts of *A. thaliana* wild type plants were likewise observed under the microscope. The plant vector pK7FWG2, as being a Gateway™ vector, cannot be used as a positive control in its non-recombined version due to the *ccdB* gene and the chloramphenicol resistance gene inserted between 35S promoter and the GFP coding sequence (cf. vector map in Figure 2.2.3) as these two genes are not in frame with the GFP gene. Therefore a positive control for the vector was not given in this thesis.

Extensive fluorescence microscopy of each obtained plant line was performed, but gained no results. No GFP fluorescence could be detected for any of the constructs. GFP expressing plants kindly provided by other research groups in the institute excluded any obvious experimental errors. Examination of transgenic AtMRS2-X-GFP seedling roots with the confocal microscope of the group of Prof. Menzel in the IZMB gave the same negative results.

In parallel to new approaches with different constructs, the transgenic plant lines were further analysed to gain insight into the question why no fluorescence could be detected.

### 3.1.3 Transcription and translation of the transgene

Successful transformation of *A. thaliana* with a desired gene construct does not necessarily lead to expression of the transgene. As the site of insertion cannot be predicted when *Agrobacterium*-mediated transformation is used, it is possible that the transgene is inserted into a heterochromatic region of the genome and thus, although equipped with its own promoter, never gets transcribed.

This scenario, however, is rather improbable here as the transgenic lines obtained were isolated via the expression of the kanamycin resistance gene co-integrated into their genome. To test whether these plant lines exhibit transcription of their respective GFP-fusion transgene, RT-PCRs were performed. For this purpose, RNA was isolated from rosette leaves, reverse-transcribed into cDNA, and PCR reactions were carried out with the oligonucleotides *gate2-Xup* and *gfp-pK7FWG2*. As can be seen in Figure 3.1.1, the amplified product consists of the full length *AtMRS2-X* coding sequence and the 5' end of the GFP coding sequence which can accordingly only be amplified from the transcribed transgene, not from an endogenous cDNA.

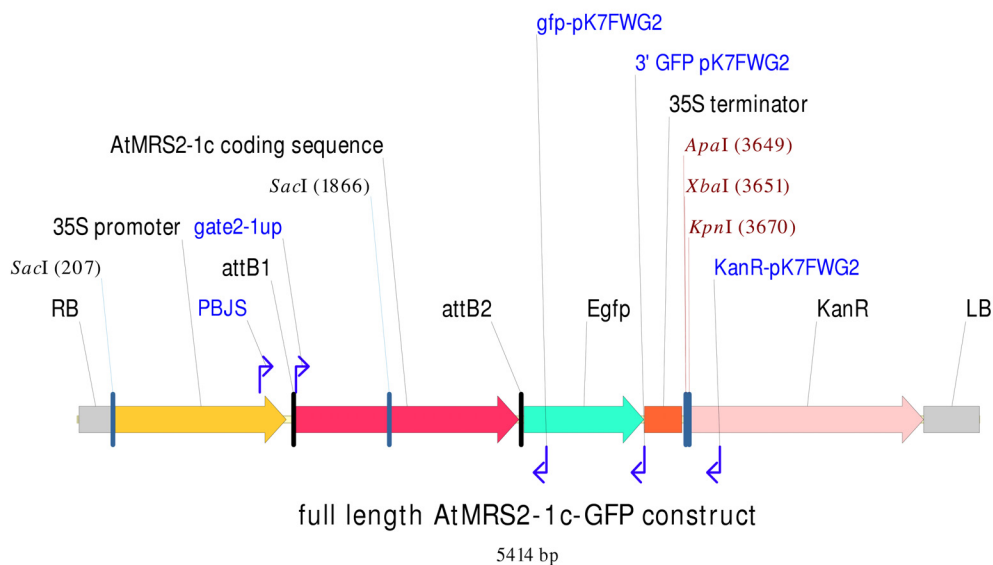


**Figure 3.1.1: Description of the expression clone of the full length *AtMRS2-1*-GFP construct**

Only the part of the vector being transferred into the plant's genome is shown, i.e. the part from right border (RB) to left border (LB). In between the two border sequences there are (from left to right) the 35S promoter containing the binding site for primer PBJS, the *AtMRS2-1* cDNA PCR product flanked by attB sites (attB1 and attB2) with the binding site for primer *gate2-1up*, the coding sequence for enhanced GFP (*Egfp*) translationally fused to *AtMRS2-1* containing the binding site for primer *gfp-pK7FWG2* and flanked by primer 3' GFP pK7FWG2, the 35S terminator, and the kanamycin resistance gene for selection of transgenic plants containing the binding site for primer *KanR-pK7FWG2*. Also given are the recognition sites for the four restriction enzymes *SacI*, *ApaI*, *XbaI*, and *KpnI* used to analyse the clones after plasmid miniprep.

Discrimination between the genomic copy and the transcript of the transgene, which might be necessary if trace amounts of genomic DNA are still present after DNase treatment of the RNA, is easily achieved in the cases where genomic DNA was used as a template in the initial PCR reaction (cf. Table 3.1-1 on page 41): the introns present in the genomic copy of the construct are spliced in the cDNA copy, resulting in a significantly smaller PCR product. In the four cases where cDNA was used as the initial template (cf. Table 3.1-1), the second RT-

PCR performed with every cDNA should give information on residual genomic DNA in the samples: this PCR reaction used an unrelated primer pair, either *gate2-10up/down* or *gate2-11up/down*, which should amplify distinct products from rosette leaf cDNA. In cases where genomic DNA was still present, a second, larger product would appear. Figure 3.1.2 gives an example of the RT-PCRs performed with plant lines of two different constructs, full length *AtMRS2-10c-* and *AtMRS2-10g-GFP*.

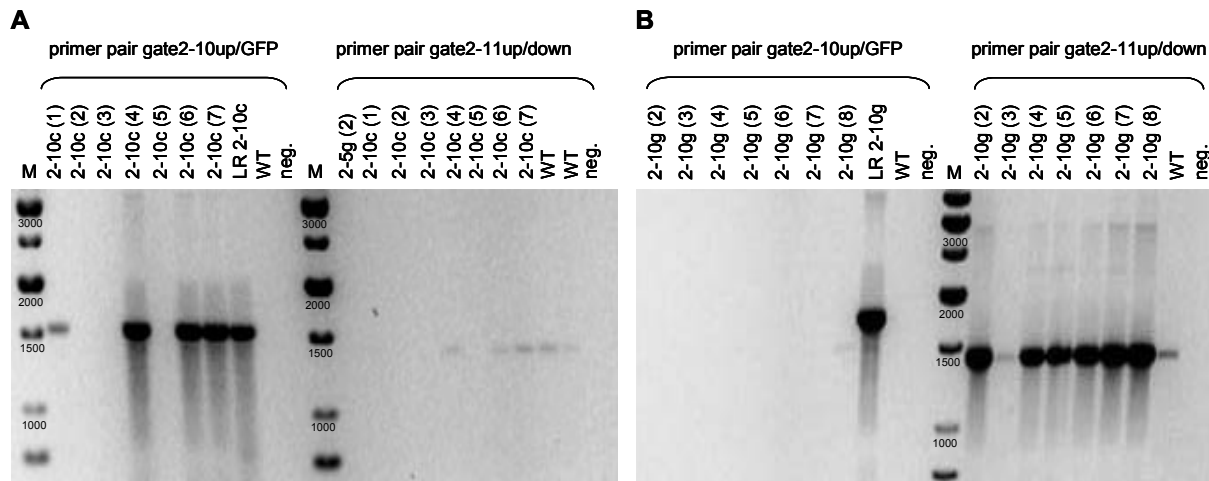


**Figure 3.1.2: Exemplary transcriptional analysis of full length gene-GFP plant lines**

RT-PCRs performed with cDNAs from the full length gene-GFP plant lines for *AtMRS2-10c* (A) and *AtMRS2-10g* (B) and with the respective expression clones used for plant transformation (denoted “LR 2-10c/g”). Left of the marker in the middle of the gels (“M”, Gene Ruler 1kb-ladder, Fermentas) are the RT-PCRs performed with the primer pair *gate2-10up* and *gfp-pK7FWG2* (“GFP”), right of the marker are RT-PCRs performed with the independent primer pair *gate2-11up* and *gate2-11down* to check the quality of the cDNAs. Negative controls (“neg.”) contain all components except for the template. Gel A also shows the control of the unrelated *AtMRS2-5g(2)* cDNA with primer pair *gate2-11up/down*; a double wild type control is included here.

These two constructs differ in the template originally used for PCR: *AtMRS2-10* was amplified both from cDNA and from genomic DNA. The expected PCR product sizes for the original expression clones (LR 2-10c/g) are 1.58 kb for the cDNA and 1.76 kb for the genomic DNA construct, respectively. The RT-PCR product amplified from the isolated cDNAs should have the size of 1.58 kb in all cases, as introns should be spliced from the genomic constructs.

Concerning the control with the unrelated primer pair *gate2-11up* and *gate2-11down*, the expected sizes are 1.42 kb for the cDNA product and 2.96 kb for a product resulting from residual genomic DNA. This PCR checks the quality of the cDNA, and for the two different approaches shown, a difference in the cDNA quality can be observed: the cDNAs of the genomic *AtMRS2-10-GFP* constructs (see Figure 3.1.2 B) give very distinct cDNA products

in all cases (weaker for line 2-10g (3) and for the wild type) and, in the cases with the strong products, also weak bands of the size of the genomic product hinting at remnants of genomic DNA present in the synthesized cDNAs. The cDNAs of the AtMRS2-10c-GFP plant lines (see Figure 3.1.2 A) seem to have a less good quality as only for three of the seven cDNAs a weak cDNA product for AtMRS2-11 is present, together with the product from the two wild type cDNAs used. No genomic DNA products are visible.

The three AtMRS2-10c-GFP cDNAs showing the control RT-PCR products (plant lines 4, 6, and 7) also produce very distinct bands of the correct size (1.58 kb) with the primer pair gate2-10up/gfp-pK7FWG2 (see Figure 3.1.2 A), a weaker product can be seen for plant line 2-10c (1). These products are most likely due to the high number of transgene cDNAs resulting from expression from the 35S promoter and not due to a possibly present small amount of genomic DNA harbouring a far reduced number of transgene copies. The unrelated AtMRS2-11 gene used as a control is expressed from its own promoter with a probably greatly reduced efficiency compared to the 35S promoter. Thus, four out of seven plant lines harbouring the full length AtMRS2-10c-GFP construct show transcription of the transgene.

The cDNAs of the full length AtMRS2-10g-GFP plant lines give nearly no products with the transgene-specific primer pair (see Figure 3.1.2 B). Only one weak RT-PCR product of the correct size (1.58 kb after splicing of the introns) can be observed for line 2-10g (8). As the quality of the respective cDNAs seems to be very good (see above), this result most likely represents the true transcriptional state of the examined plant lines: six out of seven lines seem not to transcribe the transgene. Plant line 2-10g (1), which was tested independently, did show transcription of the transgene.

Similar RT-PCRs were performed for the further transgenic plant lines resulting in proof of transcription of the transgene in at least one plant line per construct. In average more than 50 % of the plant lines show transcription of the transgene. The results are summarized in Table 3.1-3 on the following page.

**Table 3.1-3: Number of transgenic full length gene-GFP plants showing transcription of the construct**

<b>Construct</b>	<b>Number of transgenic plants</b>	<b>Number of plants showing transcription</b>
AtMRS2-1c-GFP	3	3
AtMRS2-2c-GFP	9	7
AtMRS2-3g-GFP	4	3
AtMRS2-4g-GFP	6	1
AtMRS2-5g-GFP	10	9
AtMRS2-6g-GFP	7	1
AtMRS2-7g-GFP	4	3
AtMRS2-10c-GFP	7	4
AtMRS2-10g-GFP	8	2
AtMRS2-11c-GFP	8	1

As all of the plant lines were examined under the microscope (cf. section 3.1.2 on page 42), the possibility that only plants showing no transcription were coincidentally chosen can be ruled out.

A lack of transcription thus seems not to be the explanation for the lack of fluorescence of the full length gene-GFP constructs. As successful transcription does not necessarily lead to a protein, the translation of the transgene was checked for exemplary plant lines. The plant lines chosen were AtMRS2-1c (1), AtMRS2-2c (1), AtMRS2-4g (2), and AtMRS2-7g (1), each of them showing transcription of the transgene. To test for translation, total proteins were extracted from green plant material (mainly rosette leaves supplemented by green siliques and stems), separated on a denaturing SDS-PAGE, and blotted onto a nitrocellulose membrane via the wet western blot technique. The membrane was hybridized with mouse anti-GFP antibody (Roche), and bands were visualized with the Fast Red substrate (Sigma) turned over by the alkaline phosphatase provided by the secondary antibody (goat anti-mouse IgG, alkaline phosphatase conjugate; Promega) allowing a colorimetric detection of interacting protein bands.

Figure 3.1.3 shows the protein gel (A) and the nitrocellulose membrane after detection (B). The sizes expected for GFP, the AtMRS2 proteins, and the respective fusion proteins are summarized in Table 3.1-4. Staining of the nitrocellulose membrane with the detection solution Fast Red led to one distinct band per lane around 70 kDa in size, which is weaker in case of AtMRS2-4g (2)-GFP (see Figure 3.1.3). This band is fitting very well to the expected

sizes for the gene-GFP fusion proteins. The size differences between the AtMRS2 proteins are also visible. Further visible is a band of nearly 35 kDa in the lanes of AtMRS2-1c (1)-GFP and AtMRS2-7g (1)-GFP and a band of about 28 kDa in the lane of AtMRS2-1c (1)-GFP (see Figure 3.1.3). These bands might be unspecific, or they might be caused by degraded fusion proteins or, in case of the smallest band for AtMRS2-1c (1)-GFP, by GFP expressed alone.

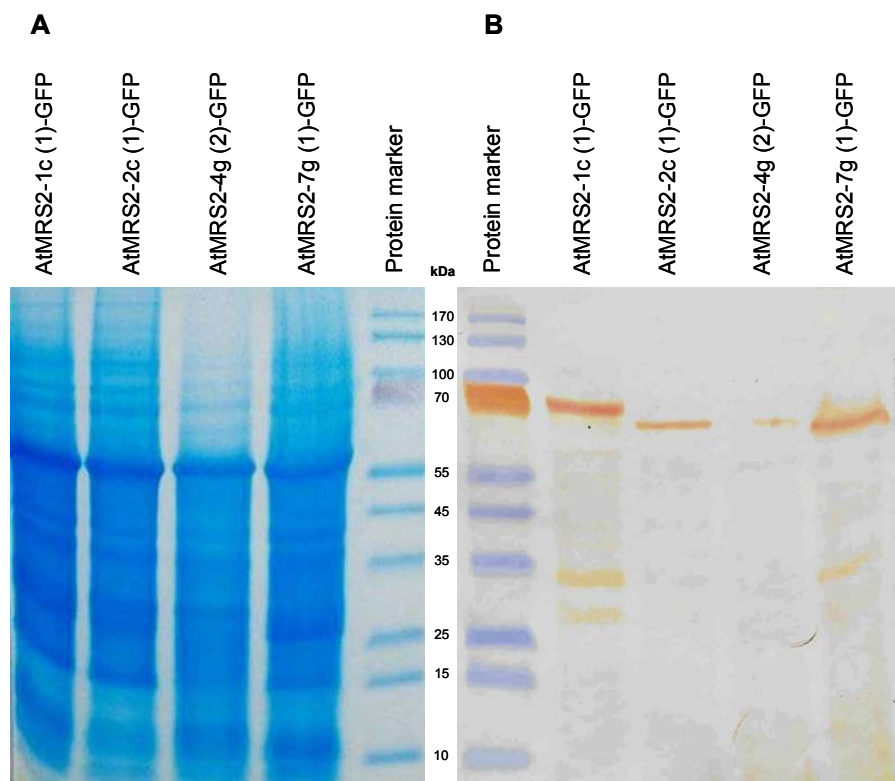


**Figure 3.1.3: Test for translation of the transgene in four selected full length gene-GFP plant lines**

SDS-PAGE (A) and Western Blot after detection with Fast Red (B) of the protein extracts of plant lines AtMRS2-1c (1), AtMRS2-2c (1), AtMRS2-4g (2), and AtMRS2-7g (1). The protein marker used is the PeqGold Protein Marker IV (prestained; Peqlab), the sizes of the bands are given in kDa.

**Table 3.1-4: Expected sizes of the AtMRS2, GFP, and fusion proteins**

Construct	Size of AtMRS2 protein	Size of GFP	Size of fusion protein
AtMRS2-1c-GFP	50,4 kDa	27 kDa	77,4 kDa
AtMRS2-2c-GFP	43,7 kDa	27 kDa	70,7 kDa
AtMRS2-4g-GFP	48,4 kDa	27 kDa	75,4 kDa
AtMRS2-7g-GFP	43,4 kDa	27 kDa	70,4 kDa

Nonetheless, the experiment suggests that the desired gene-GFP fusion protein is indeed expressed within the cell. No statement concerning the site of expression can be made as the protein extraction method chosen here does not separate soluble and membrane proteins. This

result, although demonstrated here for only four of the transgenic plant lines, can most probably be expected for the further plant lines.

Hence, a lack of expression cannot be the reason for not detecting any fluorescence of the fusion proteins.

### **3.1.4 C-terminally shortened gene-GFP constructs**

In parallel to the investigations of the non-fluorescent full length gene-GFP plants a second approach was followed in which the C-terminal part of the coding sequences was omitted for fusion to the GFP coding sequence. This approach resulted from considerations that the C-terminal transmembrane regions might interfere with the correct folding of the green fluorescent protein, thus preventing its fluorescence. Moreover, within the Gateway™ system, entry clones consisting of the promoter region along with the first exon of the coding sequence for each AtMRS2 gene in pDONR221 (cf. Figure 2.2.3 on page 19 for the vector map) already existed and could be used for this second approach. They were originally designed for promoter-GUS fusions within the Gateway™ vector pKGWFS7 (Karimi et al. (2002); diploma and PhD thesis of Karoline Meschenmoser). The first exon was thought to be sufficient to direct the GFP protein into the cellular compartment in which the corresponding AtMRS2 protein is expressed; the additional promoter sequence would be disregarded as the constructs are again driven by the 35S promoter provided by destination vector pK7FWG2 (cf. Figure 2.2.3 for the vector map).

Table 3.1-5 on the following page summarizes the key data for each construct, giving the nucleotide length of the promoter sequences and the protein lengths of the respective first exons.

**Table 3.1-5: Key data for the C-terminally shortened GFP constructs**

The PCR product (size including the attachment sites) is further subdivided into the length of the promoter sequence preceding the start codon in bp and the length of the amplified first exon in aa compared with the length of the entire protein (in parentheses).

Construct	Promoter sequence in bp	First exon in aa	Length of PCR product in bp
AtMRS2-1short-GFP	1082	196 (442)	1729
AtMRS2-2short-GFP	789	81 (394)	1091
AtMRS2-3short-GFP	294	143 (484)	782
AtMRS2-4short-GFP	1201	108 (436)	1584
AtMRS2-5short-GFP	1022	146 (421)	1519
AtMRS2-6short-GFP	1422	96 (408)	1769
AtMRS2-7short-GFP	550	83 (386)	858
AtMRS2-8short-GFP	837	76 (380)	1124
AtMRS2-9short-GFP	746	77 (328)	1036
AtMRS2-10short-GFP	1272	196 (443)	1918
AtMRS2-11short-GFP	706	130 (459)	1155

The length of the first exon varies considerably between the members of the AtMRS2 family; the shortest one is found for AtMRS2-8 with 76 amino acids, similar lengths occur for the closely related proteins AtMRS2-7, AtMRS2-2, and AtMRS2-9 (which although being a misspliced pseudogene was included in this study), and the longest first exons are found for AtMRS2-1 and AtMRS2-10 with 196 amino acids each. The overall protein lengths of the AtMRS2 family are in a narrower range between 380 aa (AtMRS2-8) and 459 aa (AtMRS2-11); AtMRS2-9 would be a C-terminally shortened protein lacking the conserved GMN motif if it was translated. Thus the first exon comprises at least 20 % and maximally 44 % of the overall protein sequence.

To gain stably transformed *Arabidopsis* plants, the existing entry clones were used for the Gateway™ LR clonase reaction as described before (see section 2.2.2), correct expression clones were identified via restriction endonuclease digestion and further verified via sequencing. The primers used for sequencing were 35S-Prom. pK7FWG2 and gfp-pK7FWG2, their binding sites are illustrated in Figure 3.1.4 on page 52. An exemplary sequence of an AtMRS2short-GFP construct can be found in section 8.2.2 on page 133; the further constructs proved to be correct as well. After transformation of *A. tumefaciens* with the expression clones the bacteria were used to transform *Arabidopsis* wild type plants. Upon



selective growth of their seeds on kanamycin-containing MS plates, different numbers of transgenic plant lines per construct were obtained; the numbers are displayed in Table 3.1-6.

**Table 3.1-6: Number of transgenic plant lines obtained for the C-terminally shortened GFP constructs**

Construct	Number of transgenic lines
AtMRS2-1short-GFP	5
AtMRS2-2short-GFP	9
AtMRS2-3short-GFP	9
AtMRS2-4short-GFP	3
AtMRS2-5short-GFP	6
AtMRS2-6short-GFP	8
AtMRS2-7short-GFP	6
AtMRS2-8short-GFP	4
AtMRS2-9short-GFP	7
AtMRS2-10short-GFP	no transgenic seeds
AtMRS2-11short-GFP	no transgenic seeds

For AtMRS2-10short-GFP and AtMRS2-11short-GFP no kanamycin-resistant seeds could be gained from two independent transformations of two pots of *Arabidopsis* wild type plants each. Thus no stably transformed plants were on hand for further analyses.

### 3.1.5 Transcription and translation within the AtMRS2short-GFP plant lines

The transgenic plant lines harbouring the C-terminally shortened GFP constructs were, similarly to the full length gene-GFP plant lines, analysed for transcription and translation of the transgene.

Transcriptional analysis was performed with RT-PCR reactions on cDNA synthesized from one plant line each per construct. Three different oligonucleotide combinations were used (cf. Figure 3.1.4 on the following page): the gate2-Xup primer binding around the start codon of the AtMRS2 gene was combined both with the gfp-pK7FWG2 primer and with the 3' GFP pK7FWG2 primer binding within and downstream of the GFP coding sequence, respectively. These reactions would amplify the fusion transcript of AtMRS2 first exon plus GFP coding sequence, with a size difference of 585 bp between the two downstream oligonucleotides. A third reaction was performed with the gfp-pK7FWG2 primer and a gate2-Yup primer for a

further AtMRS2 gene. No PCR product should be amplified here, the approach served as the negative control.

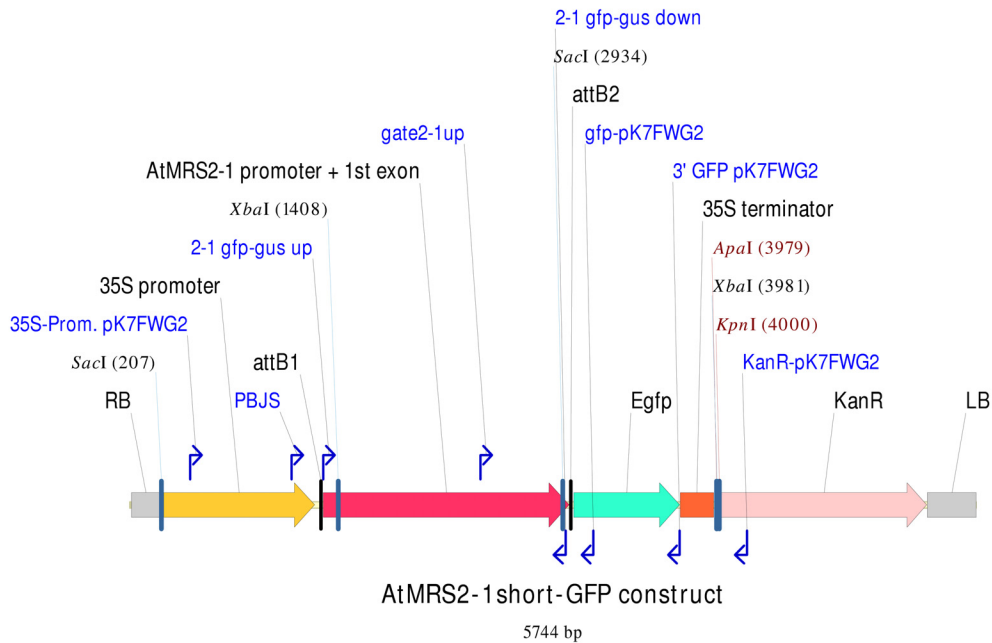


**Figure 3.1.4: Description of the expression clone of the C-terminally shortened AtMRS2-1-GFP construct**

Only the part of the vector being transferred into the plant's genome is shown, i.e. the part from right border (RB) to left border (LB). In between the two border sequences there are (from left to right) the 35S promoter containing the binding sites for primers 35S-Prom. pK7FWG2 and PBJs, the AtMRS2-1 promoter plus first exon PCR product flanked by attB sites (attB1 and attB2) with the binding sites for primers 2-1 gfp-gus up, gate2-1up, and 2-1 gfp-gus down, the coding sequence for enhanced GFP (Egfp) translationally fused to AtMRS2-1 containing the binding site for primer gfp-pK7FWG2 and flanked by primer 3' GFP pK7FWG2, the 35S terminator, and the kanamycin resistance gene for selection of transgenic plants containing the binding site for primer KanR-pK7FWG2. Also given are the recognition sites for the four restriction enzymes *SacI*, *XbaI*, *ApaI*, and *KpnI* used to analyse the clones after plasmid miniprep.

Figure 3.1.5 on the following page summarizes the results of the RT-PCR for nine different AtMRS2short-GFP plant lines. A single plant line per construct was used for RNA extraction, cDNA synthesis, and RT-PCR analysis except for the AtMRS2-6short-GFP constructs where two more plant lines were analysed.

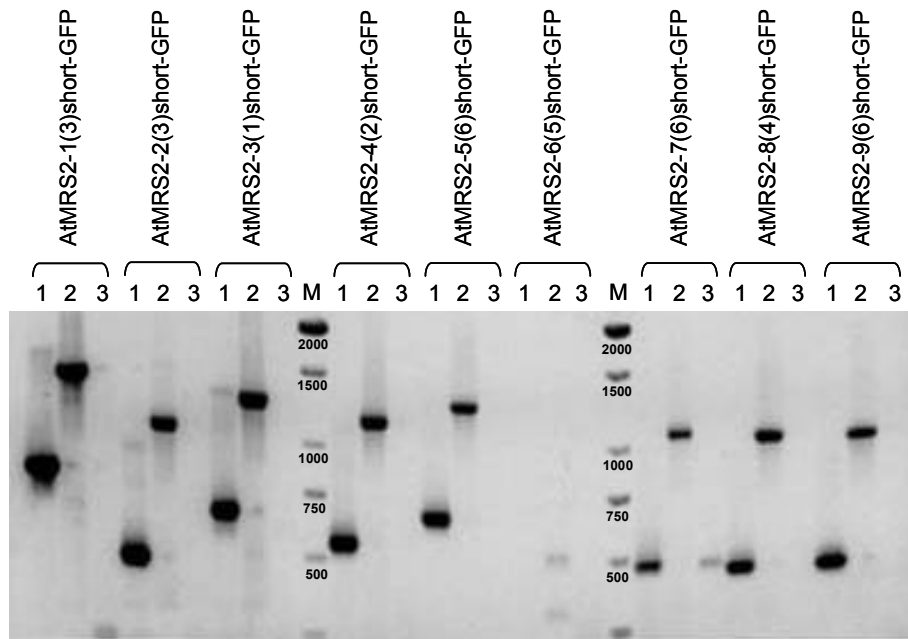


**Figure 3.1.5: Test for transcription within the AtMRS2short-GFP plant lines**

RT-PCR analysis of nine C-terminally shortened GFP plant lines with three different primer combinations. 1: gate2-Xup + gfp-pK7FWG2; 2: gate2-Xup + 3' GFP pK7FWG2; 3: gate2-Yup (different from gate2-Xup) + gfp-pK7FWG2. The size difference between PCR products 1 and 2 is 585 bp. PCR approach 3 with an unrelated gate2-Yup primer is meant to be the negative control. M: size marker Gene Ruler 1 kb-ladder (Fermentas).

All plant lines except for AtMRS2-6(5)short-GFP show RT-PCR products of the expected sizes (exact sizes not given here) and the size shift of 585 bp between products 1 and 2. The negative controls are negative; in the case of AtMRS2-7(6)short-GFP the signal in lane number 3 is caused by a spill-over from lane 1 of AtMRS2-8(4)short-GFP, the size difference is due to the different amounts of PCR product found in the two lanes.

Further analyses of AtMRS2-6short-GFP plant lines revealed that line AtMRS2-6(7)short-GFP shows transcription of the transgene. To summarize, transcription of the C-terminally shortened GFP fusion gene could be shown for one plant line per construct. Analyses of additional plant lines were not carried out, but it can be assumed that most of the further lines would show transcription of the transgene as well, according to the results achieved for the full length gene-GFP plant lines (cf. section 3.1.3).

Translation of the fusion gene was examined in the same way as for the full length gene-GFP plants (cf. section 3.1.3), that is via extraction of total proteins from green parts of the respective plant line, separation through an SDS-PAGE, western blotting onto a nitrocellulose membrane, hybridization with anti-GFP antibody (Roche), and detection of the interacting bands with the Fast Red system (Sigma). Plant lines examined in a first attempt were

AtMRS2-4(2)short-GFP, AtMRS2-5(6)short-GFP, AtMRS2-6(7)short-GFP, AtMRS2-8(4)short-GFP, and AtMRS2-9(6)short-GFP. The signals on the nitrocellulose membrane were not as strong as for the full length gene-GFP plants (cf. Figure 3.1.3 on page 48); bands of nearly 35 kDa in size appeared in the lanes for the particular AtMRS2-6 (very weak) and AtMRS2-8 plant lines, as shown in Figure 3.1.6. The expected sizes for the first exon-GFP fusion proteins are around 40 kDa, thus larger than the bands on the membrane.

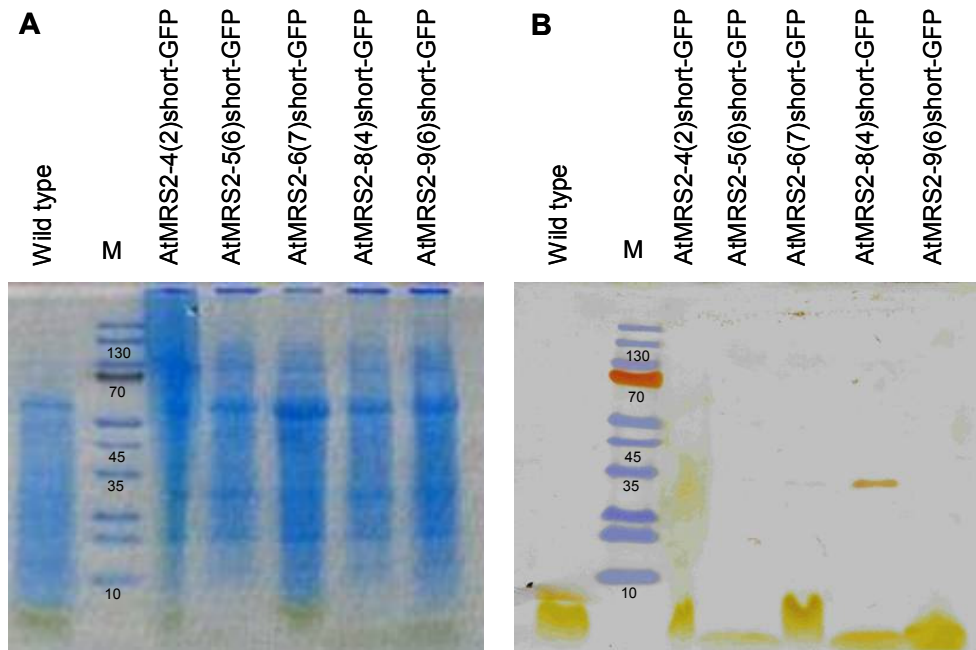


**Figure 3.1.6: Test for translation of the transgene in five selected shortened gene-GFP plant lines**

SDS-PAGE (A) and Western Blot after detection with Fast Red (B) of the protein extracts of plant lines AtMRS2-4(2)short-GFP, AtMRS2-5(6)short-GFP, AtMRS2-6(7)short-GFP, AtMRS2-8(4)short-GFP, and AtMRS2-9(6)short-GFP. The protein marker used is the PeqGold Protein Marker IV (prestained; Peqlab), the sizes of the bands are given in kDa.

A second approach used plant material both from the full length and the C-terminally shortened GFP plants for the genes AtMRS2-4 and AtMRS2-6. The plant lines examined were full length AtMRS2-4g (2)-GFP, AtMRS2-4(2)short-GFP, full length AtMRS2-6g (3)-GFP, and AtMRS2-6(7)short-GFP. Once again the signals on the nitrocellulose membrane were very weak. This time no bands of the expected sizes (around 75 kDa for the full length and around 40 kDa for the C-terminally shortened constructs) could be detected. Thus, the result previously achieved for full length AtMRS2-4g (2)-GFP (cf. Figure 3.1.3 on page 48) could not be repeated. The only distinct specific signal was a band of nearly 35 kDa in the lane of full length AtMRS2-6g (3)-GFP (data not shown), similar to the result achieved in the

first approach (see above) and to the smaller bands observed in the first western blot. It might result from a degraded fusion protein.

In summary, translation of the C-terminally shortened gene-GFP constructs could not be detected. Two out of five plant lines examined showed a signal of around 35 kDa, too small for a first exon-GFP fusion protein.

### **3.1.6 Fluorescence of the C-terminally shortened GFP plant lines**

In parallel to the transcriptional and translational analyses, all plant lines were examined under the fluorescence microscope after generating protoplasts to obtain single cells. Protoplasting is simplest for the rosette leaves as they can easily be cut into thin stripes before applying them to the enzyme solution. As a negative control, *Arabidopsis* wild type rosette leaves were treated and examined in the same manner.

For none of the transgenic plant lines (see Table 3.1-6 on page 51 for the numbers of transgenic lines obtained for each construct) fluorescence different from the background fluorescence also seen for the wild type protoplasts could be detected. This result parallels the findings for the full length gene-GFP constructs where no fluorescence was detected, either. Sequencing of the full length transcript of the GFP coding sequence from RT-PCRs of the transgenic plants AtMRS2-2(6)short-GFP and AtMRS2-5(6)short-GFP revealed the integrity of the GFP coding sequence with no nucleotide difference between the given vector and the actual transcript sequence.

### **3.1.7 A third approach: full length constructs in a new vector backbone**

Gateway™ vector pK7FWG2 from the Karimi series (Karimi et al., 2002) places, as mentioned before (see section 3.1.1 on page 40), eleven amino acids between the end of the gene of interest's coding sequence and the start codon of the GFP sequence. A different vector providing a longer spacer in between the two coding sequences might be helpful for the correct folding of the GFP and therefore enable to detect fluorescence of the fusion protein.

The vector chosen for this approach is pMDC83 from the Curtis series (Curtis and Grossniklaus, 2003), also suitable for usage with the Gateway™ system. A map of the vector can be found in Figure 2.2.3 on page 19. Similar to pK7FWG2 the construct is driven by a constitutive promoter, in this case a double 35S promoter. The respective AtMRS2 gene is fused to the N-terminus of the GFP coding sequence which is termed “mgfp6” here: it is a

modified version of GFP which is improved in its maturation and spectral properties (Schuldt et al., 1998). It differs in six amino acids from the enhanced GFP (Egfp) sequence of pK7FWG2. Additionally the mgfp6 is tagged with six histidines at its C-terminus. The construct is terminated by the nos (nopaline synthase) terminator; selection of transgenic plants occurs via the hygromycin resistance encoded on the T-DNA.

The spacer between the C-terminus of the AtMRS2 gene and the start codon of GFP is 24 amino acids long in pMDC83 (NPAFLYKVVIAWRASRGGPVPVEK), more than double the length of that in pK7FWG2.

Application of this vector to recombination with the existing full length AtMRS2 entry clones (see section 3.1.1) in the Gateway™ system proved not to be as straightforward as with pK7FWG2: selection for positive bacterial clones occurs in both vector backgrounds (pDONR221 and pMDC83) via kanamycin resistance so that it cannot easily be differentiated between entry and expression clones. To circumvent this problem, the entry clones in pDOR221 (cf. Figure 2.2.3) were linearized with either *ApaI* or *EcoRV*, depending on the intrinsic restriction enzyme recognition sites of the respective AtMRS2 coding sequences, and afterwards used for recombination with pMDC83. The probability of a linear vector fragment to be taken up by *E. coli* cells during transformation via electroporation is significantly lower than that of a circular vector fragment; besides for successful replication within the cell the linear vector would have to be re-ligated first. The probability that via this strategy a moderately large part of the kanamycin-resistant *E. coli* clones does indeed harbour the recombinated pMDC83 vector is comparatively high.

This approach was followed with the entry clones used for the full length gene-GFP fusions in pK7FWG2 (see section 3.1.1). After linearization, LR clonase reaction, and transformation of *E. coli* DH5 $\alpha$  four kanamycin-resistant colonies per approach were amplified, their plasmid DNA isolated and analysed via restriction enzyme digestion. Correct expression clones were immediately identified for AtMRS2-1c, AtMRS2-2c, AtMRS2-6g, and AtMRS2-10c coding sequences in pMDC83. No further approaches were made to get hold of correct expression clones of the remaining AtMRS2 genes; these four constructs were further analysed.

Figure 3.1.7 gives an overview of the AtMRS2-1c-mgfp6 construct in pMDC83. The four expression clones were sequenced with primer pMDC202 GFP to confirm the correct linker sequence between the C-terminus of the AtMRS2 gene and the start of the GFP coding

sequence. All four constructs proved to have the correct translational fusion to GFP with 24 amino acids linker between the two coding sequences.

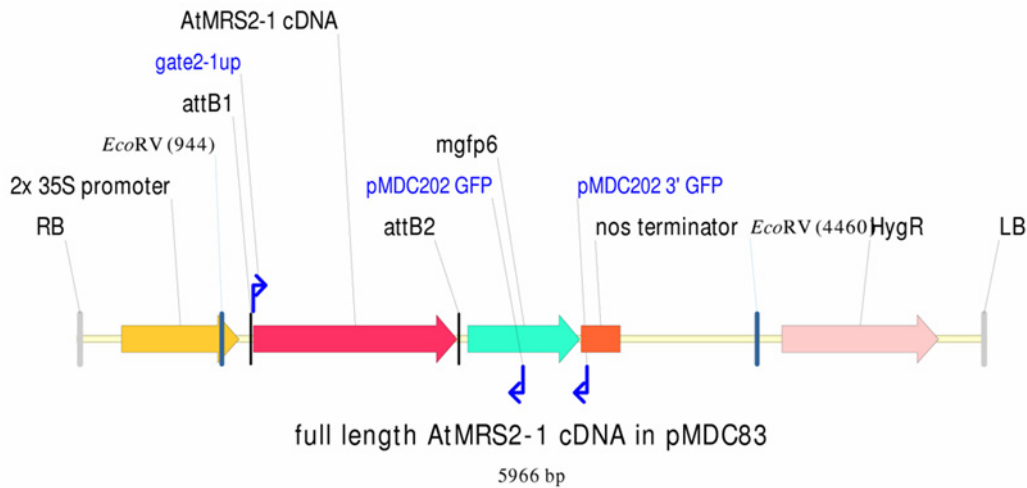


**Figure 3.1.7: Description of the expression clone of full length AtMRS2-1 coding sequence in pMDC83**

Only the part of the vector being transferred into the plant's genome is shown, i.e. the part from right border (RB) to left border (LB). In between the border sequences there are (from left to right) the double 35S promoter, the AtMRS2-1 cDNA coding sequence flanked by attB sites (attB1 and attB2) with the binding site for primer gate2-1up, the coding sequence for the modified GFP (mgfp6) translationally fused to AtMRS2-1 containing the binding site for primer pMDC202 GFP and flanked by primer pMDC202 3' GFP, the nos terminator, and the hygromycin resistance gene for selection of transgenic plants. Also given are the recognition sites for the restriction enzyme *EcoRV* used to analyse the clones after plasmid preparation.

*Agrobacterium tumefaciens* was transformed with the four expression clones, and correct *Agrobacterium* colonies were used for the transformation of *Arabidopsis thaliana* wild type plants. Two pots of *Arabidopsis* plants were used for transformation per construct; the seeds of these plants have been harvested and will be analysed for their transgenic status and GFP fluorescence soon. Thus no statements can be made at the moment concerning the gaining of transgenic plants and their potential fluorescence.

The expression constructs were furthermore used to transiently transform tobacco protoplasts and to observe the potential fluorescence of the fusion protein. Description of these experiments can be found in the following sections.

### 3.1.8 Transient transformation approaches I: tobacco leaf infiltration

Regardless of multiple trials with two different gene-GFP constructs, no GFP fluorescence could be observed for the stably transformed *Arabidopsis* plants (see above). To test whether the plant background might be responsible for this lack of fluorescence despite the correct

transcription and translation of the constructs, a second plant species was chosen for transient transformation assays: tobacco. Both *Nicotiana tabacum* and *Nicotiana benthamiana* are well-known model plants for a wide range of applications. One of them is the transient transformation via infiltration with *Agrobacterium tumefaciens* harbouring the construct of interest. The agrobacteria solution is infiltrated into the plant tissue via a small scratch on the leaf lower epidermis, some of the leaf cells are invaded by a bacterium, and the T-DNA, in this case the gene-GFP construct, is inserted into the genome of this single plant cell (method described in section 2.2.5 on page 23). After approximately 48 hours, expression of the transgene within the leaf area can be monitored via fluorescence microscopy.

To make sure that the method itself functions reliably, a vector expressing GFP alone was kindly provided by Dr. Guillaume Pilot. This vector, pPGTkan (see Figure 3.1.8 for a map), harbours between its T-DNA borders the coding sequence for mGFP (which differs in one amino acid from mgfp6 of pMDC83) driven by the 35S promoter and terminated by the Rbcs (RuBisCO small subunit) terminator, and the kanamycin resistance gene driven by the Mas (mannopine synthase) promoter and terminated by the Mas terminator as a selection marker in the plant. Outside of the T-DNA lies the spectinomycin resistance for selection of positive bacterial colonies. Due to the 35S promoter, soluble GFP should be expressed in the transfected cells regardless of cell type or plant tissue.

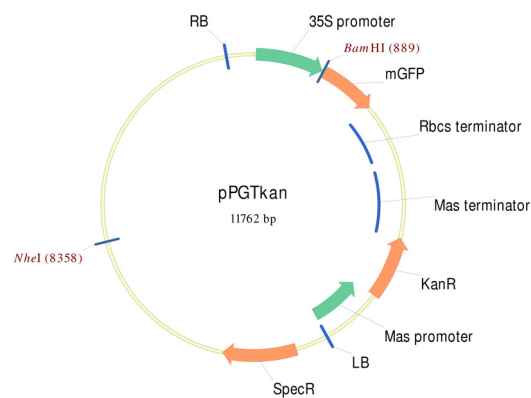


**Figure 3.1.8: Map of the vector pPGTkan used for expression of soluble GFP**

This vector was kindly provided by Dr. Guillaume Pilot, IZMB, Bonn.

Both leaves of *Nicotiana benthamiana* and leaf sections of *Nicotiana tabacum* (whose leaves have several times the surface than those of *N. benthamiana*) were used for infiltration with *Agrobacterium tumefaciens* harbouring different gene-GFP constructs and the control plasmid pPGTkan.

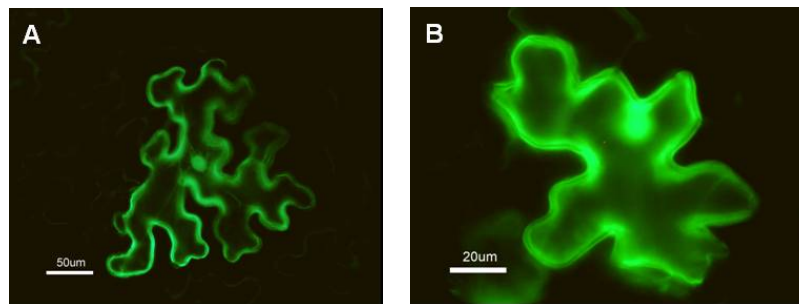


Table 3.1-7 gives an overview of the constructs that were used for the transient transformation and the tobacco species that was used.

**Table 3.1-7: Transient transformation of tobacco leaves via *Agrobacterium* infiltration**

Construct	<i>Nicotiana benthamiana</i>	<i>Nicotiana tabacum</i>
full length AtMRS2-4g-GFP (pK7FWG2)	✓	
full length AtMRS2-5g-GFP (pK7FWG2)	✓	
full length AtMRS2-6g-GFP (pK7FWG2)	✓	
full length AtMRS2-11c-GFP (pK7FWG2)	✓	✓
AtMRS2-1short-GFP (pK7FWG2)	✓	
AtMRS2-6short-GFP (pK7FWG2)	✓	
AtMRS2-11short-GFP (pK7FWG2)	✓	✓
35S::GFP (pPGTkan)	✓	✓

Transformation via leaf infiltration was mostly performed with *N. benthamiana* leaves; two of the constructs were likewise used to transform leaf sections of *N. tabacum* as well. The control with the 35S::GFP construct was applied in every transformation approach, and it reliably always gave the same result. An example of the 35S::GFP expression can be seen in Figure 3.1.9.



**Figure 3.1.9: Fluorescence of tobacco epidermal cells transformed with the 35S-GFP construct**

Leaves of *Nicotiana benthamiana* (A) and *Nicotiana tabacum* (B) were infiltrated with agrobacteria harbouring the pPGTkan plasmid which expresses GFP under control of the 35S promoter. 48 hours after transfection the leaves were observed with the fluorescence microscope, and green fluorescent epidermal cells were photographed as described in section 2.2.7 with exposure times of 0.5 s in (A) and 1 s in (B).

In both *N. benthamiana* and *N. tabacum*, whose epidermal cells are smaller than those of *N. benthamiana*, GFP expressed alone from the 35S promoter can be found soluble within the cytoplasm and in the nucleus of the transfected epidermal cell. The transformation efficiency

was, roughly estimated, quite high with more than 50 transformed cells per square centimetre of leaf material showing that the method principally worked well.

Transformation with the gene-GFP constructs mentioned in Table 3.1-7 did not result in fluorescent epidermal cells in any case, independent of the tobacco species used.

The design of the gene-GFP and the 35S::GFP constructs is very similar; each of them is around eleven kilo base pairs in size, is a binary T-DNA plasmid which harbours the same resistances for selection in bacteria and plants, and expresses the fusion protein or GFP alone under the control of the 35S promoter. The non-fluorescence of the gene-GFP fusion proteins is therefore likely not due to the design of the constructs but must have different reasons maybe lying in the nature of the fusion protein itself.

### **3.1.9 Transient transformation approaches II: protoplast transformation**

A further possibility for transient genetic modification is the transformation of protoplasts and subsequent analysis of the transformed cells. Protocols for this method are available both for *Arabidopsis* and for tobacco; the methods used in this thesis (cf. sections 2.2.4 and 2.2.6) are for both plant species based on PEG-mediated uptake of the plasmid of choice which is found in solution together with the respective protoplasts. After subsequent dilution steps and incubation of the reaction mixture overnight in the dark, the protoplasts can be observed under a fluorescence microscope.

The former PhD student Irene Schock used the methods to transform tobacco and *Arabidopsis* protoplasts with different AtMRS2 gene-GFP constructs in the vector psmGFP4 (Davis and Vierstra, 1998). The results she obtained were varying; for AtMRS2-1 and AtMRS2-2 with C-terminally shortened constructs there were no clear patterns of fluorescence so that no cellular compartment could be assigned to the respective protein (Schock et al., 2000; Schock, 2000), whereas for a C-terminally shortened AtMRS2-6 construct the observed fluorescence correlated with the MitoTracker-caused fluorescence of the mitochondria (I. Schock, unpublished results). This result should be replicated and the GFP constructs of this thesis should be transformed into protoplasts as a last attempt to gain insight into the subcellular localization of the AtMRS2 proteins.

Preliminary tests with the pPGTkan plasmid and both *Arabidopsis* and *N. benthamiana* protoplasts using the methods described in sections 2.2.4 and 2.2.6 showed that transformation of tobacco protoplasts gave the better results: first the differential centrifugation step included in the tobacco protoplast purification effectively separated the

intact protoplasts from broken ones and tissue debris, and second more transformed, i.e. fluorescent protoplasts were observed with tobacco than with *Arabidopsis*. Therefore for transformation with the gene-GFP constructs only tobacco protoplasts were used.

Table 3.1-8 gives an overview of the gene-GFP constructs used to transform *Nicotiana benthamiana* protoplasts. As large amounts of plasmid DNA (50 µg) are necessary for each transformation, plasmid maxi preparations were performed to obtain enough plasmid DNA for several transformation approaches.

**Table 3.1-8: Gene-GFP constructs used for transient transformation of tobacco protoplasts**

<b>Construct type</b>	<b>Representative</b>
full length gene-GFP fusions in pK7FWG2	full length AtMRS2-3g-GFP
	full length AtMRS2-4g-GFP
	full length AtMRS2-6g-GFP
	full length AtMRS2-7g-GFP
	full length AtMRS2-11c-GFP
C-terminally shortened fusions in pK7FWG2	AtMRS2-3short-GFP
	AtMRS2-4short-GFP
	AtMRS2-6short-GFP
	AtMRS2-11short-GFP
full length gene-GFP fusions in pMDC83	full length AtMRS2-1c-mgfp6
	full length AtMRS2-2c-mgfp6
	full length AtMRS2-6g-mgfp6
	full length AtMRS2-10c-mgfp6
controls	35S::GFP (pPGTkan)
	GFP2-6 short (Irene Schock)

The tobacco protoplast transformation protocol principally worked reliably, but there were some unforeseen problems: for some time, although fresh solutions were used, the transformation assays were contaminated with fission yeast obviously living on the leaf surface. Different protocols for surface sterilisation were applied, but the problem disappeared independently after some time, and common surface sterilisation (rinsing in 70 % ethanol and subsequent drying) was enough to keep the assays sterile. If the solutions used for protoplast production, clean-up, and transformation became too old, the protoplasts looked normal on the day of transformation, but had lost their regular shape and the cell turgor on the next day

following the overnight incubation so that analysis under the fluorescence microscope was impossible.

In each transformation approach, the 35S::GFP plasmid pPGTkan kindly provided by Dr. Guillaume Pilot was used as a positive control and a standard for the transformation efficiency. Similar to the results achieved after tobacco leaf infiltration (see section 3.1.8), expression of GFP under the control of the 35S promoter can be seen within the cytoplasm and in the nucleus of the transformed protoplast. An image of a 35S::GFP expressing protoplast is shown in Figure 3.1.10.

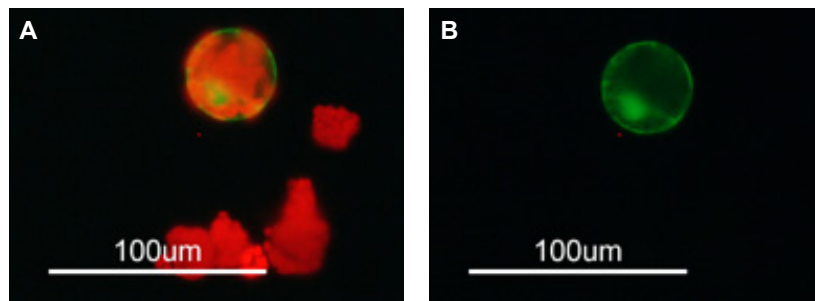


**Figure 3.1.10: Fluorescence of an *N. benthamiana* protoplast transformed with pPGTkan**

Protoplasts of *N. benthamiana* transformed with the 35S::GFP construct pPGTkan and observed under the fluorescence microscope 24 hours after transformation. The picture in (A) was taken with filter set 09 (cf. section 2.2.7) allowing both the red autofluorescence of the chloroplasts and the green GFP fluorescence, whereas the same protoplasts were regarded with filter set 10 in (B) cutting off the red autofluorescence. The two pictures were taken with the same exposure time of 1 s.

Transformation of the protoplasts with pPGTkan usually always led to a positive result, at least if the protoplasts were still intact on the day after transformation. The assays contaminated with fission yeast were nonetheless regarded under the microscope, and fluorescence could be observed there as well.

During the approaches contaminated with fission yeast, distinct fluorescence patterns could be observed both for the full length and for the C-terminally shortened AtMRS2-4-GFP constructs in pK7FG2. An example for these observations is shown in Figure 3.1.11 on the following page.

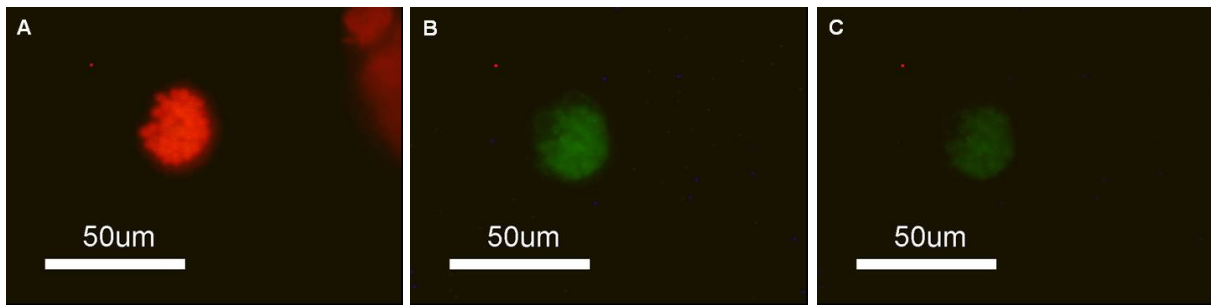


**Figure 3.1.11: Fluorescence of an *N. benthamiana* protoplast transformed with full length AtMRS2-4g-GFP**

Protoplasts of *N. benthamiana* transformed with the full length AtMRS2-4g-GFP construct in pK7FWG2 and observed under the fluorescence microscope 24 hours after transformation. The picture in (A) was taken with filter set 09 (cf. section 2.2.7) allowing both the red autofluorescence of the chloroplasts and the green GFP fluorescence, whereas the same protoplasts were regarded with filter set 10 in (B) and (C) cutting off the red autofluorescence. The picture in (A) was taken with an exposure time of 1 s whereas the exposure time was tripled to 3 s in (B); in (C) it is 2 s.

The observed green fluorescence clearly corresponds to the red autofluorescence of chlorophyll, thus making a localization of AtMRS2-4 to the chloroplasts very likely. As mentioned above, the same pattern was seen both for the full length and the C-terminally shortened construct in two independent transformation approaches each time contaminated with fission yeast. The transformation was repeated several times, mostly contamination-free, but although the 35S::GFP control gave positive results, the fluorescence for AtMRS2-4-GFP could not be detected again. Approaches with protoplasts from *Nicotiana tabacum* gave the same negative results. The same holds true for the further gene-GFP constructs in pK7FWG2 (cf. Table 3.1-8 on page 61) transformed into *N. benthamiana* protoplasts: no fluorescence could be observed there, either.

Concerning the full length gene-GFP fusions in pMDC83, at least for full length AtMRS2-1c-mgfp6 and full length AtMRS2-2c-mgfp6 some fluorescence could be detected as shown in Figure 3.1.12 for AtMRS2-1 (the same picture emerged for AtMRS2-2): some indefinable cellular compartments showed GFP fluorescence, but a statement as to which compartments are affected cannot be made. The further two gene-GFP fusions in pMDC83 showed no fluorescence at all.

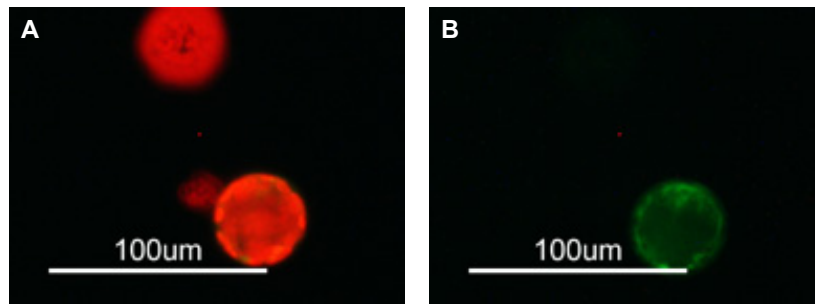


**Figure 3.1.12: Fluorescence of an *N. benthamiana* protoplast transformed with the full length AtMRS2-1c-GFP construct in pMDC83**

Protoplasts of *N. benthamiana* transformed with the full length AtMRS2-1c-GFP construct in pMDC83 and observed under the fluorescence microscope 24 hours after transformation. The picture in (A) was taken with filter set 09 (cf. section 2.2.7) allowing both the red autofluorescence of the chloroplasts and the green GFP fluorescence, whereas the same protoplasts were regarded with filter set 10 in (B) cutting off the red autofluorescence. The picture in (A) was taken with an exposure time of 1 s whereas the exposure time was doubled to 2 s in (B).

The GFP2-6 short construct of Irene Schock was likewise used for transformation of *N. benthamiana* protoplasts. Although repeated several times, none of the transformations led to detection of any fluorescence. Sequencing of the plasmid revealed that the linker sequence between the last codon of the AtMRS2-6 genomic sequence comprising the first 143 amino acids and the first codon of the GFP coding sequence of psmGFP4 (Davis and Vierstra, 1998) is ten base pairs long, thus no functional fusion protein could be translated. During this thesis there was no time to look at two more GFP2-6 clones that are available from Irene Schock, one of which at least should have the correct linker between the two coding sequences.

### 3.1.10 Summary of the results obtained with the numerous gene-GFP fusions

To gain insight into the subcellular localization of the AtMRS2 magnesium transporter family of *Arabidopsis thaliana*, a multitude of gene-GFP fusions were constructed in two different vector backgrounds. *Arabidopsis* was stably transformed with two of these construct types; transgenic plants were analysed for transcription and translation of the transgene and for fluorescence, both with microscopic sections and after protoplasting. All construct types were used for transient transformation approaches, either via tobacco leaf infiltration or via transformation of tobacco protoplasts. Table 3.1-9 recapitulates the different approaches and the results achieved.

**Table 3.1-9: Summary of the results obtained with the entire gene-GFP fusions in different expression systems**

Construct type	Transcription	Translation	Fluorescence		
			Stably transformed <i>Arabidopsis</i>	Tobacco leaf infiltration	Tobacco protoplast transformation
full length gene-GFP fusions in pK7FWG2	yes (34/66 plant lines)	yes (4/4 lines tested)	none	none (four constructs tested)	2-4: 2/10 approaches fluorescent; rest: none <sup>1</sup>
C-terminally shortened fusions in pK7FWG2	yes (9/57 plant lines <sup>2</sup> )	no (5/5 lines tested)	none	none (three constructs tested)	2-4: 2/4 approaches fluorescent; rest: none <sup>3</sup>
full length gene-GFP fusions in pMDC83		no stably transformed <i>Arabidopsis</i> lines		not performed	2-1 & 2-2: patchy pattern; rest: none <sup>4</sup>

<sup>1</sup>: five constructs tested; <sup>2</sup>: one plant line tested per construct; <sup>3</sup>: four constructs tested; <sup>4</sup>: four constructs tested

Although transcribing and partly translating the gene-GFP fusion protein, none of the stably transformed *Arabidopsis* plants showed any fluorescence under the fluorescence microscope of Prof. Schreiber's group or the confocal laser scanning microscope of Prof. Menzel's group. Transient transformation via *Agrobacterium* infiltration of tobacco leaves did not lead to detection of fluorescence, either, but with transient transformation of *Nicotiana benthamiana* protoplasts for two constructs fluorescence of chloroplasts could be observed: for the full length and the C-terminally shortened AtMRS2-4-GFP constructs in pK7FWG2. However, these results, seen in two approaches each, could not be repeated in a couple of further transformations. None of the further gene-GFP constructs showed any fluorescence, except for two constructs in pMDC83, full length AtMRS2-1c- and AtMRS2-2c-GFP: the fluorescence patterns observed there were rather patchy, no distinct membrane localization could be assigned to them. The patterns were identical for the two different constructs, rather pointing to an unspecific fluorescence maybe caused by a degraded fusion protein.

In parallel to the approaches performed in Bonn, the two plasmids that showed fluorescence in tobacco protoplasts, full length and C-terminally shortened AtMRS2-4-GFP in pK7FWG2, were sent to the ZMBP in Tübingen for transient transformation of *Arabidopsis* protoplasts.

Dr. Wolfgang Koch performed the experiment, but was not able to detect any fluorescence of the two fusion proteins.

Despite the numerous attempts made to determine the subcellular localization of the members of the AtMRS2 gene family, no positive results can be given at this point.



## 3.2 Heterologous expression in yeast: complementation and measurement of transport capacities

One of the possibilities to gain insight into the functional nature of an ion transporter is its expression in an optimally unicellular system which does not carry an endogenous transporter of the same kind and measurement of the transporter's capacities within this system. The yeast *Saccharomyces cerevisiae* does carry MRS2-like magnesium transporters itself (cf. the introduction for further details), but mutant strains exist allowing the functional characterization of heterologously expressed magnesium transporters.

One of these strains is the  $\Delta mrs2$  mutant established by Wiesenberger et al. (1992) which does not express the mitochondrial MRS2 gene anymore causing a defect in the respiratory system. This strain does not grow on non-fermentable carbon sources like glycerol (e.g. in YPdG medium), whereas growth is restored to wild type levels on fermentable carbon sources like glucose (e.g. in YPD medium). The growth defect on non-fermentable carbon sources can be compensated by heterologous expression of functional magnesium transporters, as was shown for AtMRS2-1 by Irene Schock in her dissertation: the first identified member of the AtMRS2 gene family can complement the  $\Delta mrs2$  mutant when expressed under the control of the yeast MRS2 promoter and with the yeast MRS2 targeting sequence replacing the AtMRS2-1 N-terminus (Schock et al., 2000; Schock, 2000). The second gene tested in this work, AtMRS2-2, was not able to complement the mutant, which was later found to be due to a non-functional expression construct resulting from incorrect predictions of the AtMRS2-2 coding sequence.

One aim of this PhD thesis was to continue the complementation assays of the yeast  $\Delta mrs2$  strain and to extend the experiments with a method newly developed in the group of Prof. Rudolf Schweyen from the Vienna Biocenter. As described in Kolisek et al. (2003), isolated yeast mitochondria can be used to measure the uptake of magnesium via the fluorescent dye mag-fura 2 (see also section 2.2.8 for a detailed description), thus providing a way to quantify the magnesium uptake mediated by the transporter expressed in the inner mitochondrial membrane.

### 3.2.1 Selection of AtMRS2 proteins and cloning of the expression constructs

AtMRS2-4 and AtMRS2-6 were chosen for complementation of the yeast  $\Delta mrs2$  mutant. Both proteins are predicted to be targeted to the chloroplast or the mitochondrion, respectively, so that two different expression constructs per gene were designed: as mentioned

before, N-terminally shortened coding sequences were fused to the yeast MRS2 mitochondrial targeting sequence and driven from the yeast MRS2 promoter within vector YEp351 (Hill et al. (1986); see Figure 2.2.4 on page 27 for a vector map) to ensure the expression of the AtMRS2 gene within the inner mitochondrial membrane. A second construct should demonstrate whether the native plant organellar targeting sequences were able to direct expression of the AtMRS2 genes into the yeast mitochondrion. Therefore the complete coding sequences were cloned behind the constitutive ADH (alcohol dehydrogenase) promoter in vector pVT103-U (Vernet et al. (1987); see Figure 2.2.4 for a vector map).

Later on during this thesis, a third gene, AtMRS2-3, was additionally included for the approach with the yeast mitochondrial targeting sequence and cloned into YEp351 as well.

The experiments described here were carried out in cooperation with two PhD students in the group of Prof. Schweyen, Julian Weghuber and Soňa Svidová. Cloning of the constructs was performed in Bonn, these constructs were sent to Vienna, and the following steps were performed there. During this thesis, I was able to spend some days in the laboratory of Prof. Schweyen and perform some of the experiments myself.

The cloning strategies for the two different approaches are described in detail in the Materials and Methods chapter (see section 2.2.8 on page 26 ff). Assembly of the expression constructs in YEp351 proved to be fairly straightforward: the N-terminally shortened PCR products were amplified from rosette leaf cDNA (AtMRS2-4), flower cDNA (AtMRS2-6), and an existing cDNA clone originally amplified from root cDNA in the case of AtMRS2-3 using the oligonucleotides denoted “YEP 2-X up/down“ in section 8.1.3. The *S. cerevisiae* MRS2 promoter and targeting sequence (the first 94 amino acids as described before by Steinhäuser (1999) in his dissertation) were amplified from wild type yeast genomic DNA, digested as described in section 2.2.8, and ligated into the likewise digested YEp351 vector to obtain YEp-hepro. This vector was used for ligation with the respective AtMRS2 RT-PCR product digested with the two restriction enzymes of choice. Correct clones as verified by restriction enzyme digestion and PCR assays were obtained for each of the three AtMRS2 genes. These clones were subsequently sequenced to ensure the accuracy of the constructs before sending them to the laboratory of Prof. Schweyen.

The full length AtMRS2-4 product to be cloned into pVT103-U was amplified from rosette leaf cDNA with primer pair “pVT 2-4 up/down” (oligonucleotides given in section 8.1.3). Amplification of the full length coding sequence of AtMRS2-6 proved to be more difficult than amplification of the N-terminally shortened sequence : as known from promoter-reporter

gene fusions (K. Meschenmoser, unpublished data) and from publicly available microarray data (<https://www.genevestigator.ethz.ch/>; Zimmermann et al. (2004)), this gene is only expressed in the pollen of the flowers. Flower cDNA reversely transcribed with only AtMRS2-6 oligonucleotides was prepared; the full length coding sequence was subdivided into two overlapping PCR products; but no full length RT-PCR product could be obtained in various attempts. Hence, for the full length AtMRS2 genes in pVT103-U, only AtMRS2-4 could be cloned as described in section 2.2.8. The correct clone was once again verified via restriction enzyme digestion, PCR assay, and finally by sequencing of the construct before sending it to the laboratory of Prof. Schweyen.

### 3.2.2 Complementation of the yeast $\Delta$ mrs2 mutant strain

The yeast expression constructs cloned in Bonn were used for transformation of the  $\Delta$ mrs2 mutant strain (Wiesenberger et al., 1992) in Vienna by Julian Weghuber and Soňa Svidová. As described in the Materials and Methods chapter (see section 2.2.8), competent  $\Delta$ mrs2 yeast cells were prepared and transformed; transformants were grown on selective medium. To test for the ability to complement the  $\Delta$ mrs2 phenotype, positive transformants were grown in selective medium, diluted in a series of 1:10 steps, and trickled onto two different plates: YPD medium containing the fermentable carbon source glucose, and YPdG medium containing the non-fermentable carbon source glycerol. Several controls were included:  $\Delta$ mrs2 yeast transformed with the yeast MRS2 gene in the respective vector background served as a positive control, and non-transformed  $\Delta$ mrs2 yeast cells served as a negative control.

Figure 3.2.1 shows the results of the growth assays performed with the N-terminally shortened *Arabidopsis* constructs in YEp351 fused to the yeast MRS2 promoter and targeting sequence. Growth is monitored on the two different media mentioned above. As expected, each yeast strain used grows well on the fermentable carbon source glucose (left panel). The yeast wild type strain is able to grow on the non-fermentable carbon source as well, whereas the  $\Delta$ mrs2 mutant strain cannot grow on this medium. Growth is restored to wild type levels when the mutant strain is transformed with the yeast MRS2 protein. Targeting of the *Arabidopsis* MRS2 proteins to the yeast mitochondria leads to a complementation of the mutant phenotype for AtMRS2-3 and AtMRS2-6, but not for AtMRS2-4; growth there is as little as that of the mutant strain itself.

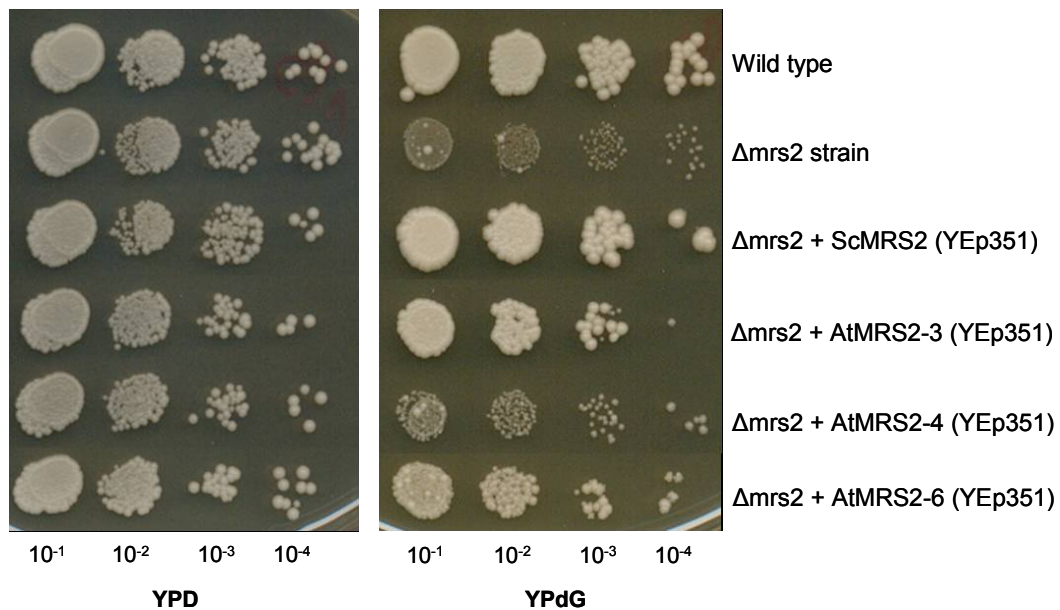


**Figure 3.2.1: Complementation of the  $\Delta mrs2$  mutant with AtMRS2 proteins targeted to the mitochondria**

Growth of the respective yeast cells in four different dilutions ( $10^{-1}$  to  $10^{-4}$ ) on YPD medium containing glucose (left panel) and on YPdG medium containing glycerol (right panel). The yeast cells trickled on the plates are (from top to bottom) a yeast wild type strain, the mutant  $\Delta mrs2$  strain alone, and the mutant strain transformed with four different constructs all driven by the yeast MRS2 promoter: yeast MRS2 protein, and *Arabidopsis* AtMRS2-3, AtMRS2-4, and AtMRS2-6 each N-terminally shortened and fused to the yeast mitochondrial targeting sequence. All constructs are found within vector YEp351.

Thus, when targeted to the yeast mitochondria, the *Arabidopsis* proteins AtMRS2-3 and AtMRS2-6 are able to complement the  $\Delta mrs2$  phenotype by restoring a functional magnesium transport into the mitochondrion. AtMRS2-4 seems not to be able to complement the mutant.

This gene was also cloned with its full length coding sequence behind the constitutive ADH promoter in vector pVT103-U and employed in growth assays. Figure 3.2.2 shows the results of these assays. All yeast strains used are able to grow well on the fermentable medium containing glucose. As expected, the wild type yeast strain grows equally well on the non-fermentable medium containing glycerol, whereas growth of the  $\Delta mrs2$  mutant strain is inhibited there. This phenotype is fully reverted by expression of the yeast MRS2 gene from the strong ADH promoter; and the *Arabidopsis* AtMRS2-4 gene can complement the phenotype as well, although to a lower degree than the yeast homologue.

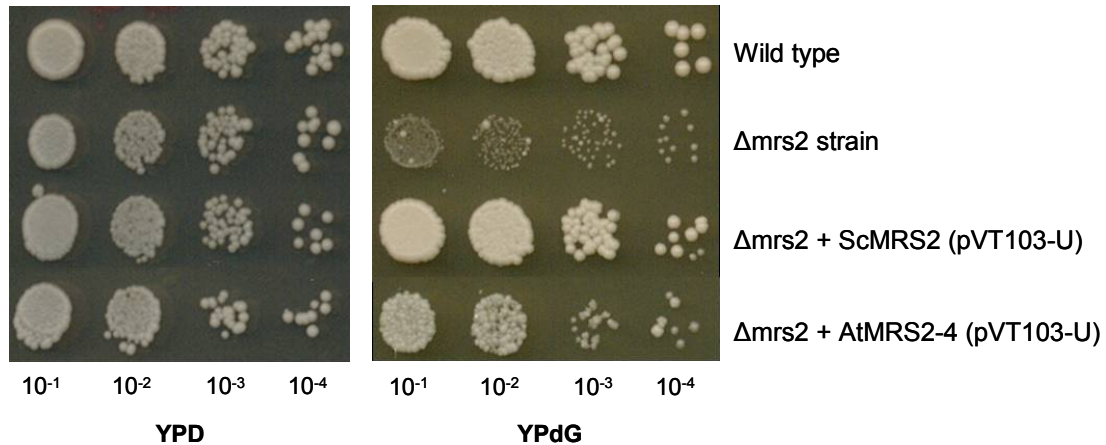


**Figure 3.2.2: Complementation of the  $\Delta mrs2$  mutant with the native AtMRS2-4 protein**

Growth of the respective yeast cells in four different dilutions ( $10^{-1}$  to  $10^{-4}$ ) on YPD medium containing glucose (left panel) and on YPdG medium containing glycerol (right panel). The yeast cells trickled on the plates are (from top to bottom) a yeast wild type strain, the mutant  $\Delta mrs2$  strain alone, and the mutant strain transformed with two different constructs driven by the ADH promoter: yeast MRS2 protein, and full length *Arabidopsis* AtMRS2-4. The constructs are found within vector pVT103-U.

Hence, opposing the results obtained for the N-terminally shortened construct fused to the yeast mitochondrial targeting sequence, the full length AtMRS2-4 construct is able to complement the yeast mutant phenotype. Obviously the native *Arabidopsis* organellar targeting sequence is able to direct expression of the AtMRS2-4 protein into the yeast inner mitochondrial membrane. The same result would be expected for the full length AtMRS2-6 construct which is predicted to be targeted to the plant mitochondria. Unfortunately, due to the amplification problems from cDNA (see above), this construct could be neither cloned nor tested.

### 3.2.3 Measurement of transport capacities via the mag-fura 2 system

The fluorescent dye mag-fura 2 is magnesium-sensitive and changes its excitation wavelength depending on whether magnesium is bound to it or not. As acetoxymethyl ester (AM), mag-fura 2 is membrane-permeant, so that it can be used to “load” cells or organelles with the dye. As described in Kolisek et al. (2003), the group of Prof. Schweyen makes use of mag-fura 2 to measure the uptake of magnesium into isolated yeast mitochondria.

The yeast strains described in the complementation section (see above) were used for these measurements. Mitochondria were isolated from yeast cell cultures, loaded with the AM ester of mag-fura 2, and measured in a spectrofluorometer with a fast filter accessory which allows the simultaneous recording of the emissions obtained at two different excitation wavelengths (cf. section 2.2.8 for a detailed description). Mag-fura 2 is excited at 380 nm in its free form

and at 340 nm if magnesium is bound to it. The ratio of bound and unbound mag-fura 2 changes according to the amount of magnesium present within the mitochondria. The system is calibrated by determining maximal and minimal ratios, and the concentration of magnesium inside the mitochondria  $[Mg^{2+}]_m$  is calculated via the formula given in the Materials and Methods section. During the recording of the emission at the two wavelengths, the extramitochondrial magnesium concentration is increased stepwise from nominally free medium to 1 mM, 3 mM, and 9 mM  $MgCl_2$ . After calculation of the innermitochondrial concentrations, the capacities of the magnesium transporters expressed in the respective mitochondria can be monitored.

Figure 3.2.3 shows the results of the mag-fura 2 measurements for the yeast strains expressing AtMRS2-3, AtMRS2-4 and AtMRS2-6 targeted to the mitochondria via the yeast MRS2 targeting sequence, for the strain expressing the yeast MRS2 gene, and for the  $\Delta mrs2$  mutant strain. The measurements were repeated at least twice, one representative graph was selected for each construct.

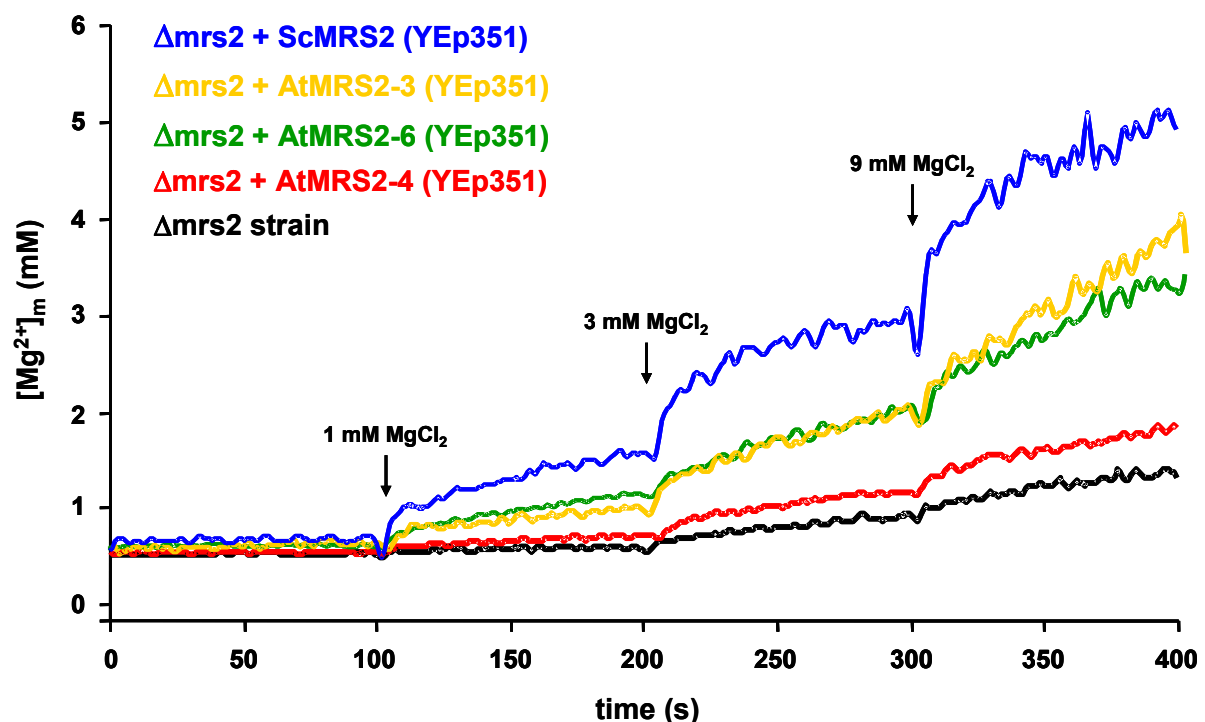


**Figure 3.2.3: Measurement of  $Mg^{2+}$  uptake into isolated yeast mitochondria via mag-fura 2**

Graph showing the magnesium concentrations inside the mitochondria isolated from the respective yeast strains as determined from the mag-fura 2 measurements at the times indicated. Recording started in nominally  $Mg^{2+}$  free medium; after 100 s each the concentration was increased to the given values. The curves shown are measured with (from top to bottom): yeast mitochondria expressing the yeast MRS2 gene, the *Arabidopsis* genes AtMRS2-3, AtMRS2-6, and AtMRS2-4 fused to the yeast mitochondrial targeting sequence, and the mutant  $\Delta mrs2$  strain alone. All constructs are found within vector YEp351.

The innermitochondrial magnesium concentrations are plotted against the time in seconds. At the beginning of the measurement all yeast mitochondria contain approximately the same magnesium concentration of about 0.5 mM. When raising the extramitochondrial  $Mg^{2+}$  concentration, the concentration within the  $\Delta mrs2$  mitochondria rises slowly, reaching approximately 1.4 mM at the maximal extramitochondrial concentration applied of 9 mM  $MgCl_2$ . If this mutant strain is transformed with the yeast MRS2 gene under control of its own promoter, the uptake of magnesium is greatly enhanced. Magnesium concentrations inside the mitochondria rise quickly and reach a plateau soon after raising the extramitochondrial  $MgCl_2$  concentration. At the highest extramitochondrial magnesium concentration, the innermitochondrial level reaches approximately 5 mM, as is reported in Kolisek et al. (2003) under the same conditions, confirming the reliability of the system.

The two *Arabidopsis* proteins AtMRS2-3 and AtMRS2-6, when targeted to the yeast mitochondria and driven from the yeast MRS2 promoter as well, give nearly identical results in the mag-fura 2 measurements. AtMRS2-3 performs a little better than AtMRS2-6, but principally both proteins can take up magnesium with capacities not much smaller than the yeast MRS2 protein. At the end of the recording, the plateau seems not to be reached; AtMRS2-3 accumulates approximately 4 mM  $Mg^{2+}$  within the yeast mitochondria, those complemented with AtMRS2-6 contain approximately 3.5 mM magnesium. These results are well comparable with the complementation assays where ScMRS2 complements the  $\Delta mrs2$  mutant best, followed by approximately equally large yeast colonies expressing AtMRS2-3 and AtMRS2-6 (cf. Figure 3.1.2 on page 70).

The results of the complementation assays and mag-fura 2 measurements are also comparable for AtMRS2-4: no complementation could be observed (see above), and AtMRS2-4 mitochondria perform only a little better in the mag-fura 2 assay than the  $\Delta mrs2$  mutant mitochondria.

Mag-fura 2 measurements have not yet been performed with the native AtMRS2-4 construct in vector pVT103-U which shows complementation of the growth defect. These data, when available, will quantify the uptake capacities of the native AtMRS2-4 protein driven by the constitutive yeast ADH promoter in relation to the uptake mediated by the ScMRS2 gene under control of the same promoter.

The series of AtMRS2 constructs fused to the yeast mitochondrial targeting sequence was completed in a diploma thesis prepared by Karolin Eifler building on this work (Eifler, 2006).

### 3.3 Heterologous expression in *Xenopus* oocytes: electrophysiological measurements

A second possibility for the functional characterization of transporter proteins is the expression of the transporter in oocytes of *Xenopus laevis* and subsequent electrophysiological measurement of the electrogenic properties. *Xenopus laevis* (the clawed frog) oocytes have become a widely used expression system for transporters and channels of all kinds as they are easily prepared from the female frog, have a size well to handle, and can be applied to the various electrophysiological methods developed by now. The oocytes do only express a limited number of endogenous channels and transporters making them an ideal system for the study of heterologously expressed transporters.

In cooperation with Dr. Dirk Becker and Dr. Dietmar Geiger from the group of Prof. Hedrich at the University of Würzburg, a selection of the AtMRS2 magnesium transporters should be expressed in *Xenopus* oocytes and tested for their electrogenic properties by double electrode voltage clamping (DEVCl) measurements. Cloning of the respective constructs was performed in Bonn; the further steps were undertaken in Würzburg, partly by me during a one-week visit in the laboratories of Prof. Hedrich.

#### 3.3.1 Selection of AtMRS2 proteins and cloning of the first constructs

Electrophysiological measurements can only be applied successfully if the transport protein of choice is expressed within the plasma membrane of the oocyte as flux of charges across this membrane is recorded. Thus, four AtMRS2 proteins that are predicted not to be organellarly targeted were chosen for a first trial: AtMRS2-1, 2-2, 2-3, and 2-5. The vector chosen is a classical *Xenopus* expression vector, pGEMHE. A map can be found in Figure 2.2.9 on page 35; typical features also found within alternative *Xenopus* vectors are the 5' and 3' UTRs (untranslated regions) flanking the multiple cloning site (MCS), accordingly flanking the coding sequence of interest after cloning and providing an optimized sequence environment for translation, and of course the promoter region for a DNA-dependent RNA polymerase transcribing the coding sequence of interest, here the T7 promoter derived from phage T7.

The complete coding sequences from ATG to stop codon plus some nucleotides up- and downstream, respectively, were amplified with the oligonucleotides given in section 8.1.4 denoted "Xenopus2-Xup/down". AtMRS2-1 was amplified from rosette leaf cDNA, whereas AtMRS2-2, 2-3, and 2-5 were amplified from cDNA of cauline leaves. Due to the different restriction enzyme recognition sequences included in the 5' parts of the oligonucleotides, the



obtained PCR products could be directionally ligated with the pGEMHE vector as described in the Materials and Methods chapter (see section 2.2.10). Positive transformants were obtained for each PCR product, the plasmid DNA isolated and checked via restriction enzyme digestion and PCR with the original primers. Only after sequencing of the constructs it turned out that in case of AtMRS2-2, a misspliced version of the cDNA had been amplified in which the seventh intron within the coding sequence was not spliced out and caused a premature stop of the protein. Attempts to clone a full length version of AtMRS2-2 were made, but abandoned when results from Würzburg concerning the further constructs were received.

The further three constructs proved to have the correct coding sequences and were sent to the laboratory of Prof. Hedrich for analysis in the *Xenopus* expression system.

### 3.3.2 DEVC measurements of the first constructs

The further experiments were carried out by the former PhD student Dr. Dietmar Geiger in the laboratory of Prof. Hedrich at the University of Würzburg. As described in the Materials and Methods chapter (see section 2.2.10 on page 33), the plasmid DNA was linearized, transcribed into cRNA with the T7 RNA polymerase, checked on an RNA gel, and used for injection of *Xenopus* oocytes. These oocytes together with non-injected control oocytes were incubated for two to six days prior to the DEVC measurements. As mentioned above, solutions using different magnesium concentrations with and without NaCl, at different pH values, and with or without the competitive inhibitor Co(III)-hexaammine were used for the two different DEVC setups. Under none of the conditions tested, magnesium-induced currents could be recorded.

The injected and non-injected oocytes were then used for different uptake experiments: they were kept in modified ND96 solutions (cf. Table 2.2-1 on page 37) containing either 200  $\mu\text{M}$  or 3 mM  $\text{MgCl}_2$  at different pH values for six days and then, after several washing steps, subjected to a determination of the  $\text{Mg}^{2+}$ ,  $\text{Ca}^{2+}$ , and  $\text{K}^+$  concentrations via ICP (inductively coupled plasma) analysis. The ion concentrations did not differ between the injected and non-injected oocytes under the conditions tested.

A reason for the inability to measure magnesium-dependent currents might either be that efficient (plant) protein expression did not work at all in the heterologous system or that the expressed proteins were not properly translocated into the plasma membrane. Hence, new constructs adding a V5-His6 tag were cloned to enable protein detection in western blot analyses.

### 3.3.3 V5-His6 tagged constructs: cloning, DEVC recordings, and oocyte blot

For this second approach the vector pcDNA3.1D/V5-His (see Figure 2.2.9 for a map) from Invitrogen Inc. was chosen. It is a mammalian expression vector also suitable for *Xenopus* oocytes which additionally contains a tag consisting of the V5 epitope and six histidine residues (cf. section 2.2.10 for further descriptions) to be translationally fused to the C-terminus of the coding sequence of interest. The following genes were chosen for cloning: AtMRS2-1, 2-3, and 2-5, as they had been analysed in the first approach in pGEMHE, and additionally AtMRS2-6 to include an *in planta* definitely organellarly localized protein in the studies as no results were obtained so far for the non-organellarly localized proteins.

AtMRS2-1, 2-3, and 2-5 coding sequences were amplified with the oligonucleotides given in section 8.1.4 from rosette leaf cDNA, this time without the stop codon to enable the in frame fusion to the tag. AtMRS2-6 was tried to be amplified from flower cDNA, but as already described in the above part about the heterologous expression in the  $\Delta mrs2$  yeast strain (cf. section 3.2.1), amplification of the full length coding sequence proved to be impossible. PCR verification of the plasmids obtained for the other three genes showed that none of the AtMRS2-3 clones contained the correct sequence. Thus, only AtMRS2-1 and AtMRS2-5 in vector pcDNA3.1D/V5-His, which were shown to be correct via sequencing, were sent to the laboratory of Prof. Hedrich for further analysis.

Largely the same DEVC measurements as already described for the constructs in pGEMHE were conducted by Dr. Dietmar Geiger, i.e. changing the magnesium concentration, pH value, potassium concentration, and using the inhibitor Co(III)-hexaammine under different DEVC setups. Once again, no AtMRS2-mediated currents could be measured.

The V5-His6 tag added to the coding sequences allowed for a western blot analysis giving hints as to whether the AtMRS2 proteins were expressed in the *Xenopus* plasma membrane, a prerequisite for successful DEVC recordings. Oocytes expressing the two proteins and a positive control, the potassium channel KCO4 also tagged with the V5-His6 epitopes, were used for protein extraction and subfractionation into a microsomal fraction enriching membrane proteins (cf. section 2.2.11 for a detailed description of the method). The protein extracts were separated via an SDS-PAGE, blotted, and incubated with anti-V5 antibody. After incubation with the secondary antibody and detection via the NBT-BCIP system, the result shown in Figure 3.3.1 was obtained.

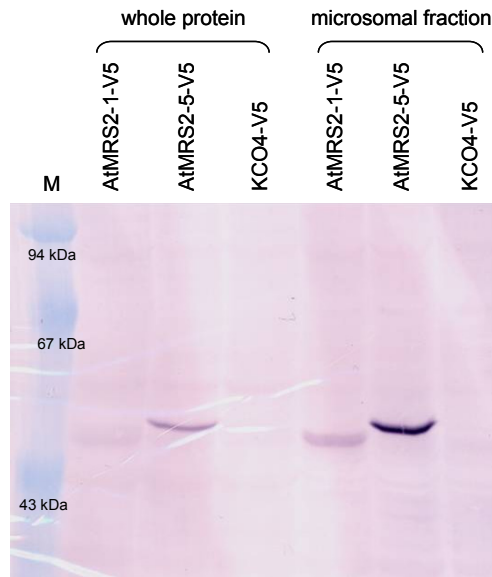


**Figure 3.3.1: Western Blot analysis of V5-His6-tagged AtMRS2-1 and AtMRS2-5 proteins**

*Xenopus* oocytes expressing either AtMRS2-1, AtMRS2-5, or the potassium channel KCO4 in vector pcDNA3.1D/V5-His were used for protein isolation and further subfractionation into a microsomal fraction. Both whole protein extracts and the microsomal fractions were loaded onto a polyacrylamide gel with 50 µg of protein per lane. After blotting, the membrane was incubated with anti-V5 antibody for one hour and anti-mouse alkaline phosphatase-conjugated antibody overnight. The NBT-BCIP system was used for detection of the bands. M designates the protein marker.

Distinct bands are visible in the lanes containing the protein extracts of AtMRS2-1-V5 and AtMRS2-5-V5 expressing oocytes. No bands are visible in the lanes with extracts from KCO4-V5 expressing oocytes. The potassium channel KCO4 from *Arabidopsis thaliana* has been electrophysiologically well characterised by the group of Prof. Hedrich (Becker et al., 2004), and KCO4-V5 expressing oocytes were thought to serve as a positive control for the experiment. A possible explanation for the negative result might be that the cRNA injected into the oocytes was degraded and could thus not be used for translation of a functional channel. Nevertheless, the method must have worked as bands are visible for the two AtMRS2 proteins tagged with the V5 epitope. The bands are stronger in the microsomal fraction than in the whole protein extracts. As equal amounts of protein were loaded per lane, the concentration of the AtMRS2 proteins is higher in the microsomal fraction, indicating that the proteins are indeed expressed in oocyte membranes, most likely in the plasma membrane. The only peculiar point about the result is the size of the proteins: AtMRS2-1-V5 is approximately 45 kDa as estimated from the gel, AtMRS2-5-V5 approximately 47 kDa. The sizes predicted for the native proteins are 50 kDa for AtMRS2-1 and 47 kDa for AtMRS2-5, fitting for AtMRS2-5, but expecting a larger product for AtMRS2-1. A repetition of the experiment led to exactly the same result. A final answer to the question of the size difference for AtMRS2-1 cannot be given.

This experiment showed that it is most likely not due to a mistargeting of the AtMRS2 proteins within the oocyte that no currents could be measured via the DEVC recordings.

### 3.3.4 A week in Würzburg and numerous DEVC measurements

To test a greater variety of DEVC conditions which might produce an electrogenic current through one of the AtMRS2 transporters, I worked in the laboratory of Dr. Dirk Becker in the department of Prof. Hedrich in Würzburg for one week together with Dr. Dietmar Geiger. We used all of the solutions described in the Materials and Methods chapter (cf. Table 2.2-1 on page 37) under the two recording conditions mentioned there. Oocytes were injected with native and V5-His6-tagged cRNAs of AtMRS2-1 and AtMRS2-5 as well as with the native cRNA of AtMRS2-3 and used for measurements minimally four days after injection.

Both AtMRS2-1 constructs (in pGEMHE and in pcDNA3.1D/V5-His) and the AtMRS2-3 construct (in pGEMHE) did not lead to measurable currents under any of the conditions chosen.

The oocytes injected with AtMRS2-5 in pGEMHE were phenotypically different from the other ones: a greater part of them developed a very thin outer membrane and dark spots, became leaky and died as soon as three days after injection. The surviving oocytes still had thinner outer membranes than those injected with the other constructs, so that impaling them with the microelectrodes sometimes led to a leakage and thus destruction of the cells. Those ones that were successfully impaled often showed some basic currents, e.g. of 0.3  $\mu\text{A}$  at -100 mV holding potential, indicative of a little leak. These oocytes were used for the DEVC measurements as described, and opposite to any other oocytes, there were some currents to be recorded.

Figure 3.3.2 shows an example of a measurement at a clamped holding potential of -120 mV using solutions with different concentrations of  $\text{MgCl}_2$ . Per definition, a negative current is equivalent to a cation influx into the oocyte, and a positive current corresponds to a cation efflux from the oocyte.

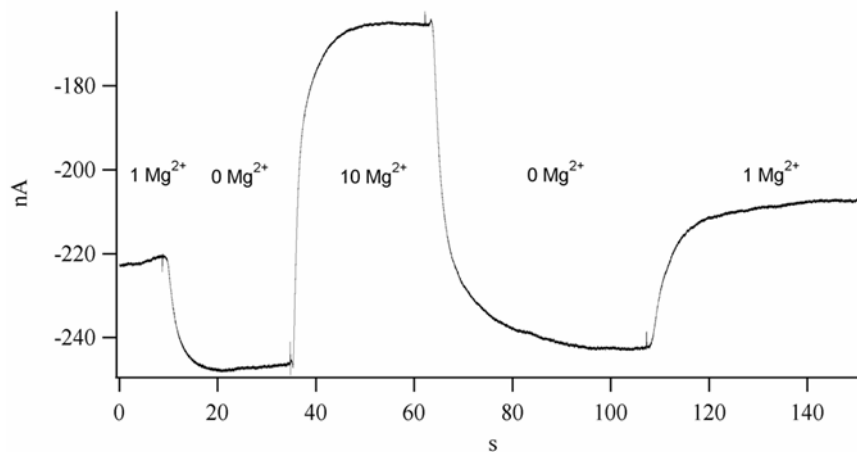


**Figure 3.3.2: DEVC recording of an AtMRS2-5 injected *Xenopus* oocyte**

The oocyte expressing AtMRS2-5 (pGEMHE construct) was clamped at a holding potential of -120 mV, and currents were recorded at extracellular solutions containing different MgCl<sub>2</sub> concentrations. Three of the solutions denoted “x mM MgCl<sub>2</sub>” in Table 2.2-1 were used by turns: those ones containing 1 mM, 0 mM, and 10 mM MgCl<sub>2</sub>, indicated by “x Mg<sup>2+</sup>” in the figure. The currents in nA recorded at the different MgCl<sub>2</sub> concentrations are plotted against the time of the measurement.

At a holding potential of -120 mV, an extracellular concentration of 1 mM MgCl<sub>2</sub> caused an electrical current of approximately -220 nA. Completely removing the Mg<sup>2+</sup> led to a more negative current of more than -240 nA, whereas raising the MgCl<sub>2</sub> concentration to 10 mM led to a more positive current of approximately -170 nA. The oocyte reacted reproducibly to a second lowering to 0 mM Mg<sup>2+</sup>, and reached a little more positive current when exposed to 1 mM MgCl<sub>2</sub> again, approximately -210 nA. Thus, the oocyte expressing AtMRS2-5 reacted in a Mg<sup>2+</sup>-dependent way by producing a positive current when raising the extracellular magnesium concentration, meaning that, as mentioned above, either cations effluxed from the cell or anions influxed into the cell.

These results could be reproduced with different oocytes; the utilisation of different magnesium sources (Mg-gluconate and Mg-ATP) did not change the reaction, either (data not shown), ensuring that the effect seen was due to the change in Mg<sup>2+</sup> and not in the accompanying counter ion. Oocytes injected with the V5-His6-tagged version of AtMRS2-5 (pcDNA3.1D/V5-His construct) gave basically the same recordings, but with a lower amplitude, thus generating weaker currents under the same conditions. No reactions were obtained with non-injected oocytes.

The recordings were carried out at different holding potentials, and more DEVC measurements were done with the second method described in section 2.2.10 (see page 33 ff) so that the voltage-dependence of the electrogenic transport could be determined (data not

shown). The recordings showed that the transport was activated by hyperpolarisation, i.e. clamping the oocyte membrane to voltages more negative than -90 mV.

These results are not in line with the expected transport capacities of AtMRS2-5: with increasing extracellular magnesium concentrations, an increasing influx of  $Mg^{2+}$  into the oocyte via the transporter would be expected, but the opposite behaviour was observed, the oocytes seemed to efflux  $Mg^{2+}$  into the extracellular space. Alternatively, AtMRS2-5 might not only transport magnesium, but additionally a second ion which might be responsible for the currents measured.

To gain further insight into these puzzling DEVC recordings, AtMRS2-1 and AtMRS2-5 were cloned into a third *Xenopus* expression vector providing an improved expression background which might allow for the recording of stronger currents.

### 3.3.5 Stronger expression background: cloning into pDK148 and measurements

Besides cloning of the full length cDNAs of AtMRS2-1 and AtMRS2-5 into the expression vector pDK148 (Dr. Thomas Zeuthen, University of Copenhagen, unpublished), a mutated version of AtMRS2-5 harbouring an AMN motif instead of the conserved GMN motif at the end of the first transmembrane domain (cf. the introduction, page 3 ff) was amplified and cloned into pDK148 as well.

As a template for the PCR amplification and PCR-based mutagenesis, respectively, the corresponding V5-His6-tagged clones were used. The oligonucleotides used are given in section 8.1.4; for amplification of the full length products, the original *Xenopus*2-1/2-5up primers were used in combination with the 2-1/2-5 pDK148 down primers to achieve the suitable restriction enzyme recognition sites for cloning. For the mutagenesis, AtMRS2-5 was amplified in two overlapping halves with the additional primers 2-5AMNmiup/mido both providing the necessary nucleotide modification to change the codon G to A. These two halves were then used in a second PCR reaction with the full length primers to obtain the complete, mutagenised PCR product. After restriction enzyme digestion and ligation with the likewise digested pDK148 vector, correct clones were obtained for the three reactions which were verified via restriction enzyme digestion and sequencing. These clones were sent to the laboratory of Prof. Hedrich for further analysis.

After transcription into cRNA and injection of *Xenopus* oocytes, Dr. Dietmar Geiger performed the same DEVC experiments as described in the preceding section. With none of the constructs, he was able to record any currents. Thus, the results obtained for AtMRS2-5 in

---

pGEMHE and pcDNA3.1D/V5-His could not be repeated when this gene was expressed in pDK148.

To summarize, the experiments performed with *Xenopus* oocytes and multiple expression constructs for the genes AtMRS2-1, 2-3, and 2-5 did not lead to unambiguous results. No electric currents could be measured for AtMRS2-1 and AtMRS2-3. Two of the three AtMRS2-5 expression constructs led to measurement of magnesium dependent currents, but for magnesium as the only ion transported (an assumption based on the results obtained for the bacterial magnesium transporters) the currents would point at efflux rather than uptake of magnesium. These results could not be repeated with the third expression construct for AtMRS2-5.

Taken together, heterologous expression in *Xenopus* oocytes seems not to be the ideal system to test the electrogenic properties of the AtMRS2 magnesium transporters.

### 3.4 Analysis of protein interactions via the mating-based split ubiquitin system

The AtMRS2 proteins as well as the further members of the 2-TM-GxN family of divalent cation transporters (Knoop et al., 2005) form a new class of transport proteins. This becomes apparent for example in their structure: as mentioned in the introduction (cf. section 1.2.2), CorA from *Thermotoga maritima* and most probably every other member of this superfamily is a pentamer consisting of five identical subunits with the central pore being formed by the five aminoterminal out of the total of ten transmembrane domains (Lunin et al., 2006; Eshaghi et al., 2006). In those organisms with only one CorA-like transport protein encoded in their respective genomes the functional protein is necessarily a homopentamer, but in those cases where more than one CorA-like transporter is present, the possibility of heteropentamer formation cannot be ruled out or might even be required to provide a population of functional transporters in a complex organism like *Arabidopsis thaliana*.

To test whether two different AtMRS2 proteins are principally able to interact (a prerequisite for heteropentamer formation) we made use of the mating-based split ubiquitin system (mbSUS). This screening system for interactions of two membrane proteins was modified from the existing split ubiquitin system (Johnsson and Varshavsky, 1994) first by Stagljar and colleagues (1998) and subsequently to the present version by Obrdlik and colleagues (2004) as described in the Materials and Methods chapter (see section 2.2.9 on page 30 ff). In principle, two membrane proteins of interest are fused to the two halves of ubiquitin, expressed within the same yeast cell, and if the two membrane proteins interact, a functional ubiquitin molecule is reconstituted, recognized by ubiquitin-specific proteases, and a reporter protein attached to the C-terminal half of ubiquitin is cleaved off. This reporter protein allows for the detection of the interaction.

For a first test, the two most closely related AtMRS2 proteins, AtMRS2-1 and AtMRS2-10, were chosen. The mbSUS was used in cooperation with Dr. Petr Obrdlik from the ZMBP in Tübingen who built up a large screening of membrane protein interactions which we were able to include our proteins in.

#### 3.4.1 Amplification of the AtMRS2-1 and AtMRS2-10 cDNAs

The high throughput screening nature of the mating-based split ubiquitin system circumvents individual ligation of the cDNAs encoding the proteins of interest with the respective vectors *in vitro* -- this is accomplished via homologous recombination within the yeast cell *in vivo* (cf. section 2.2.9). Hence, the RT-PCR products themselves only need to be provided with the



necessary flanking sequences required for the recombination reaction. Accordingly, oligonucleotides were constructed which contain attachment sites related to the ones used in the Gateway™ system followed by the AtMRS2 specific sequences. The complete coding sequences starting with the ATG and ending upstream of the stop codon (so that translational fusions within the vectors were enabled) were amplified; the oligonucleotide sequences are given in section 8.1.3.

For amplification of AtMRS2-1 cDNA from rosette leaves was used; AtMRS2-10 was amplified with cDNA from cauline leaves. PCR amplification was repeated several times including steps where the original RT-PCR product was used as a template in a second PCR until the required concentration was achieved. The PCR products were eluted from the agarose gel, their concentrations determined and set to 100 ng/μl, and then sent to the laboratory of Dr. Petr Obrdlik.

### **3.4.2 mbSUS: description of the procedure and first results**

Dr. Petr Obrdlik performed the interaction tests as described in his “Manual for the use of mating-based Split ubiquitin system “mbSUS”, version B, December 2004”. Briefly, the RT-PCR products were used for co-transformation together with the respective vectors to gain both fusions to the C- and to the mutated N-terminal half of ubiquitin (cf. the Materials and Methods chapter for further details on the method, page 30 ff). Two different yeast strains are used for either the N<sub>ub</sub> or the C<sub>ub</sub> constructs: PCR products plus linearized pMetYCgate vector were transformed into yeast strain THY.AP4 (mating type Mat a), whereas PCR products plus linearized pNXgate33-3HA vector were transformed into strain THY.AP5 (mating type Mat α). The respective controls (described further below) were included and also transformed. After selection of positive transformants, five to ten colonies each were pooled and grown overnight for the mating assay: in a petri dish, every combination of yeasts containing C<sub>ub</sub> and N<sub>ub</sub> constructs was mixed and trickled on a YPD plate to allow for mating of the Mat a and Mat α yeast cells. Successful mating was monitored after replica plating on selective medium lacking those amino acids whose synthesis is provided by diploid yeast cells. Interaction of the two membrane proteins expressed within one yeast cell was monitored both by growth assays on selective medium containing different concentrations of methionine to titrate the amount of C<sub>ub</sub> fusion protein as pMetYCgate harbours a methionine-sensitive promoter, and via an X-Gal overlay assay performed with the plates used for selective growth of the mated yeast cells. Both interaction tests are possible because the interaction of the two membrane proteins leads to the liberation of the artificial transcription factor proteinA-LexA-VP16

(PLV) which activates the reporter constructs *lexA-His3*, *lexA-Ade2*, and *lexA-lacZ*. The *lacZ* reporter protein can also be used for quantitative determination of the interaction strength utilising the substrate ONPG (o-nitrophenylgalacto-pyranoside), an assay which was not performed in this interaction screen.

Figure 3.4.1 depicts the results of this interaction screen. Part A shows the growth assay performed on medium lacking adenine and histidine, part B illustrates the X-Gal overlay assay carried out with the selected diploid yeast cells.

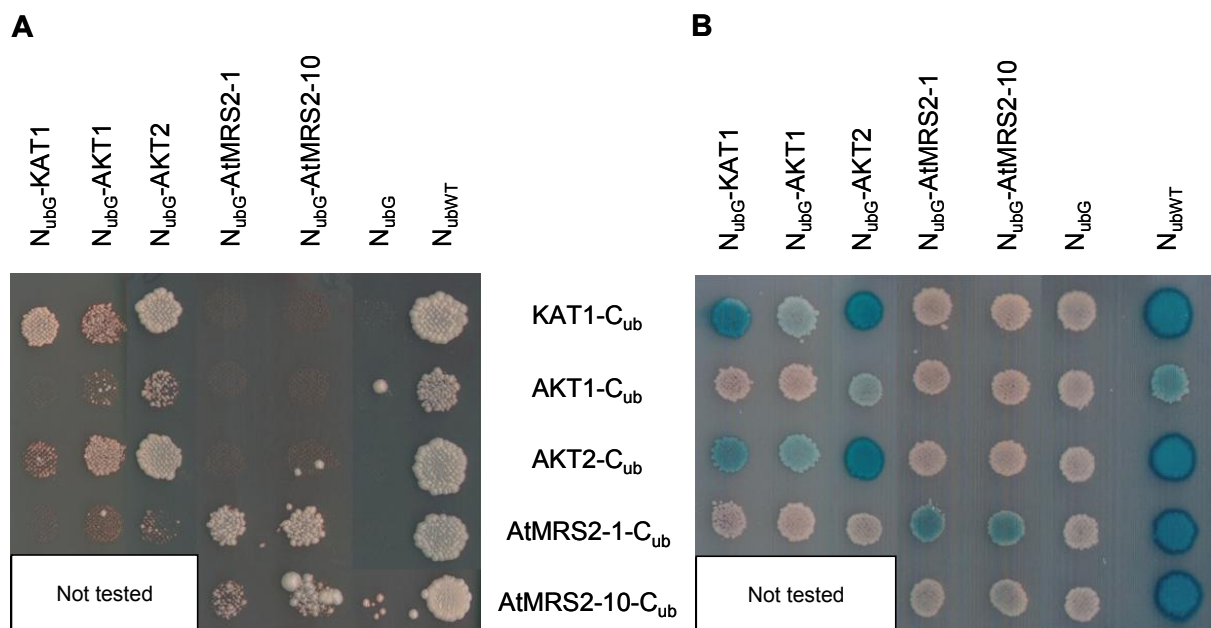


**Figure 3.4.1: mbSUS interaction screening with AtMRS2-1 and AtMRS2-10**

AtMRS2-1 and AtMRS2-10 were both fused to the N-terminal mutated half of ubiquitin, N<sub>ubG</sub>, and to the C-terminal half, C<sub>ub</sub>. Multiple control constructs were used: N<sub>ubG</sub> and C<sub>ub</sub> fusions of three *Arabidopsis* potassium channels, KAT1, AKT1, and AKT2; the mutated N<sub>ubG</sub> half solely expressed; and the wild type half N<sub>ubWT</sub>. The yeast cells expressing the N<sub>ub</sub> constructs were mated with those ones expressing the C<sub>ub</sub> constructs in every possible combination except for mating of AtMRS2-10-C<sub>ub</sub> with the potassium channel N<sub>ub</sub> constructs. After selection of the diploid cells on medium lacking leucine, tryptophane, and uracil, the diploid cells were screened for interaction either via a growth assay on medium lacking histidine and adenine for seven days at 28 °C (A) or via an X-Gal assay on medium containing adenine and histidine by coating with the staining solution (B).

Positive interactions are shown either by an even growth of colonies in the growth assay (A) or by a blue staining of the diploid colonies in the X-Gal assay (B). The last column in each assay harbours the interaction of the C<sub>ub</sub> constructs with the wild type N<sub>ub</sub> half. As the non-mutated N<sub>ub</sub> has a very high affinity to C<sub>ub</sub> regardless of the proteins attached to each half, a functional ubiquitin molecule should be reconstituted whenever N<sub>ubWT</sub> meets a C<sub>ub</sub> construct. Thus, the growth assay shows distinct yeast colonies for every C<sub>ub</sub> protein coexpressed with N<sub>ubWT</sub>, and in the X-Gal assay the colonies are stained dark blue. The interactions are evenly

strong except for the one of AKT1-C<sub>ub</sub> with N<sub>ubWT</sub>. This is due to a lower expression level of AKT1-C<sub>ub</sub> compared to the other C<sub>ub</sub> constructs (P. Obrdlik, personal communication).

The second last column shows the interactions of the C<sub>ub</sub> constructs with the mutated N<sub>ubG</sub> half. This I to G mutation was introduced to circumvent the reconstitution of a functional ubiquitin from both halves without interaction of the two proteins attached to the C- and N-terminal halves (Johnsson and Varshavsky, 1994). If N<sub>ubG</sub> is expressed alone, no interaction with any C<sub>ub</sub> construct should take place. Thus, no distinct yeast colonies are visible in the growth assay, and the colonies stay white in the X-Gal assay.

Further controls are implied in this screen: the potassium channels KAT1, AKT1, and AKT2 from *Arabidopsis thaliana* were studied extensively within the mbSUS (Obrdlik et al., 2004) and are used here as control constructs. KAT1-C<sub>ub</sub> and AKT2-C<sub>ub</sub> interact with each of the potassium channel N<sub>ubG</sub> constructs in different strengths, whereas AKT1-C<sub>ub</sub> only interacts with N<sub>ubG</sub>-AKT2. This is most probably due to the lower expression level of AKT1-C<sub>ub</sub> in comparison to the further two C<sub>ub</sub> constructs (see above). The interaction pattern seen here is as reported in Obrdlik et al. (2004). Taken together, all controls give the expected screening results.

The AtMRS2 N<sub>ubG</sub> constructs do not show any interaction with the potassium channel C<sub>ub</sub> constructs. Interactions would have been very unlikely as the structures of the potassium and magnesium channels are highly different and no functional replacement of a potassium channel subunit with a magnesium transporter subunit or vice versa could be expected. Likewise, the AtMRS2-1-C<sub>ub</sub> construct shows no interaction with the potassium channel N<sub>ubG</sub> constructs, either. The AtMRS2-10-C<sub>ub</sub> construct was not tested in combination with the potassium channel N<sub>ubG</sub> constructs, but no interactions would be expected here as well.

AtMRS2-1-C<sub>ub</sub> shows positive interaction signals both with the N<sub>ubG</sub>-AtMRS2-1 construct and with the N<sub>ubG</sub>-AtMRS2-10 construct. The interactions for AtMRS2-10-C<sub>ub</sub> with the two AtMRS2 N<sub>ubG</sub> constructs are less unequivocal; in the X-Gal overlay assay the colonies might be very light blue. The more sensitive growth assay shows modest growth for the AtMRS2-10-C<sub>ub</sub>/N<sub>ubG</sub>-AtMRS2-1 interaction and yeast colonies of different size for the AtMRS2-10-C<sub>ub</sub>/N<sub>ubG</sub>-AtMRS2-10 interaction. This cannot be due to a reduced expression level of AtMRS2-10-C<sub>ub</sub> as the N<sub>ubWT</sub> control interaction is as strong as those for the further well expressed C<sub>ub</sub> constructs.

Although not completely unambiguous, the results show that the two AtMRS2 proteins tested in this first screen, AtMRS2-1 and AtMRS2-10, can both interact with themselves and with

the second AtMRS2 protein. Thus, the theoretical possibility that the AtMRS2-proteins may form heteropentamers so far finds support from this first experiment.

The yeast cells expressing either the AtMRS2 C<sub>ub</sub> or the N<sub>ubG</sub> construct, which were obtained after the initial transformation of the yeast strains and used for the interaction assays, were also used for isolation of these constructs via a method given in the mbSUS protocol. The isolated plasmids were retransformed into *E. coli* cells to gain a larger amount of plasmid DNA and used for sequencing. Sequencing showed that both C<sub>ub</sub> constructs as well as the N<sub>ubG</sub>-AtMRS2-1 construct carried amino acid exchanges due to mutations in the respective codons. AtMRS2-1-C<sub>ub</sub> had one mutation exchanging Val against Gly at amino acid position 119 in a modestly conserved region with the amino acids Val, Gln, and Arg occurring at this position in *Arabidopsis* and rice. The N<sub>ubG</sub>-AtMRS2-1 construct bore two mutations: Trp was exchanged for Arg at position 149 in a non-conserved region, and Asn was exchanged for Ser at position 346 in a modestly conserved region where other MRS2 proteins naturally carry a Ser residue. Three substitutions were observed for the AtMRS2-10-C<sub>ub</sub> construct: a Glu-Lys exchange at amino acid position 118 in a modestly conserved region where other *Arabidopsis* and rice MRS2-type proteins carry Glu, Gln, or Arg residues, respectively, at this position; a Ser-Leu exchange at position 199 in a non-conserved region; and a Phe-Leu exchange at position 402 directly following the GMN motif. At this position the *Arabidopsis* and rice proteins carry besides Phe also Leu, Ile, and Val.

Although no influences on the protein functions should be expected by these amino acid exchanges, the number of base pair substitutions and mutations is considerably high. This can be due either to mistakes made by the Taq DNA polymerase used for amplification of the PCR product or to problems with the *in vivo* recombination of PCR product and vector within the yeast cell (P. Obrdlik, personal communication). Further RT-PCRs should be carried out with a proofreading DNA polymerase.

### 3.4.3 Extension of the screening system

After the successful first utilisation of the mating-based split ubiquitin system, further AtMRS2 proteins should be analysed to gain an extended interaction pattern for the AtMRS2 family. The very closely related proteins AtMRS2-2 and AtMRS2-7 were chosen, as well as modified versions of AtMRS2-1: to test whether the conserved GMN motif might be relevant for the interaction, a mutated version with an AMN motif instead should be included, and the

N-terminus of the protein should be deleted to examine whether this part of the protein had any influence on the oligomerisation ability.

Due to the problems with mutations occurring within the amplified and recombined coding sequences (see above), a proofreading DNA polymerase was used for the further RT-PCRs (Fast Start High Fidelity PCR System, Roche; see section 2.2.1), and the RT-PCR products were cloned into the Gateway™ vector pDONR221 and sequenced prior to amplification of PCR products from these vectors for the *in vivo* recombination. As an advantage of the mating-based split ubiquitin system, the RT-PCR products gained for usage with the system can also be used with the Gateway™ system due to the employment of the same recombination sequences attached to the oligonucleotides.

For amplification of the new PCR products the oligonucleotides given in section 8.1.3 were used together with cDNA from *Arabidopsis* wild type rosette leaves. To gain mutation-free sequences, AtMRS2-1 and AtMRS2-10 were also included in the amplification assay. To introduce the GMN to AMN mutation in AtMRS2-1, two halves were amplified using the original mbSUS primers and the overlapping 2-1AMNmiup/mido primers, and these two products were recombined in a second PCR reaction. For the N-terminally shortened AtMRS2-1 product a new upstream primer was designed omitting the first 93 amino acids of the protein.

After having obtained the desired PCR products, aliquots were used to perform the BP clonase™ reaction (cf. section 2.2.2 for a description of the Gateway™ system) with pDONR221 (see Figure 2.2.3 on page 19 for a vector map). More or less quickly, correct clones as verified via restriction enzyme digestion were obtained for each PCR product. Sequencing of the constructs revealed that amino acid exchanges still occurred, although a proofreading DNA polymerase had been used. AtMRS2-1, AtMRS2-1 –N, and AtMRS2-7 in pDONR221 bore two amino acid exchanges each, one exchange was found for AtMRS2-1 AMN and AtMRS2-10 in pDONR221. This means a reduction in the rate of amino acid exchanges compared to the directly recombined constructs, but no complete elimination.

To establish the mating-based split ubiquitin system in our group, I visited the laboratory of Dr. Petr Obrdlik and was trained in the usage of the mbSUS. Among other experiments, we used PCR products from the then existing recombined BP clones for a new screening approach. This new screening approach comprised the following AtMRS2 constructs besides the usual controls: AtMRS2-1, AtMRS2-1 AMN, AtMRS2-7, and AtMRS2-10. I had not

been able to identify a correct BP clone for AtMRS2-10 so that the RT-PCR product originally obtained for the first screening and still stored in Tübingen was used. The mbSUS screening was performed according to the manual (as described in the previous section, cf. page 83 ff); both the growth and the X-Gal assay were carried out to determine the possible interactions. The results are displayed in Figure 3.4.2.

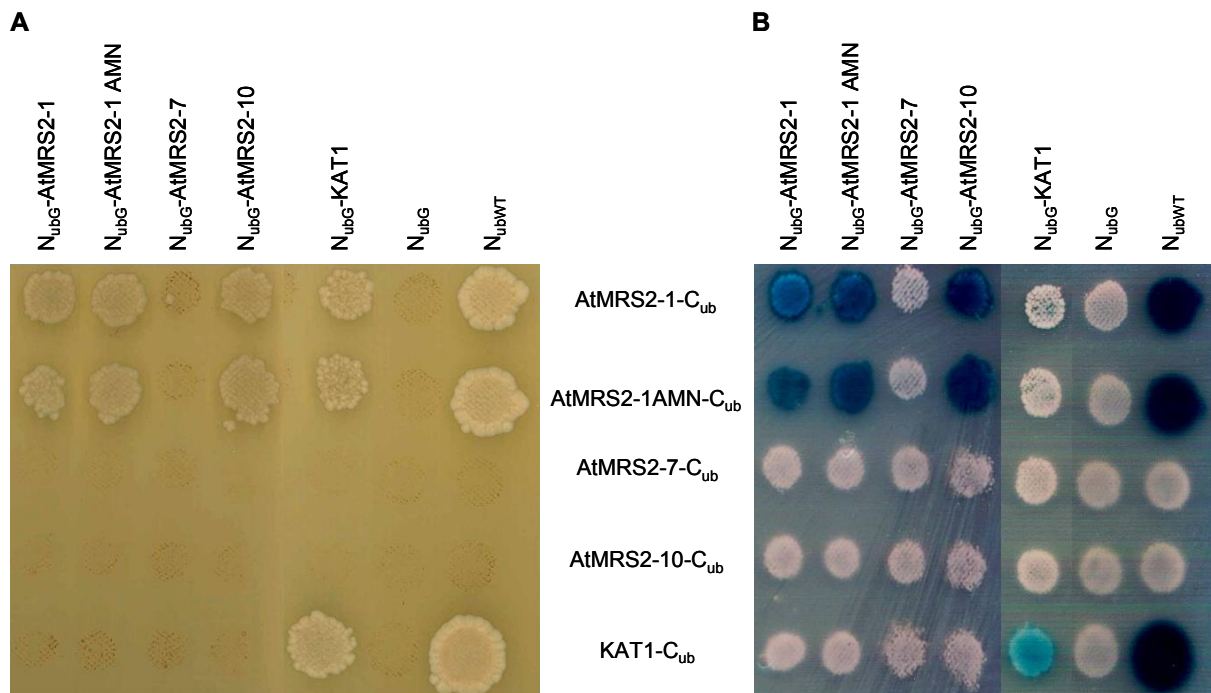


**Figure 3.4.2: Second mbSUS screening with four different AtMRS2 proteins**

AtMRS2-1, the mutated AtMRS2-1 AMN, AtMRS2-7, and AtMRS2-10 were both fused to the N-terminal mutated half of ubiquitin,  $N_{ubG}$ , and to the C-terminal half,  $C_{ub}$ . Multiple control constructs were used:  $N_{ubG}$  and  $C_{ub}$  fusions of the *Arabidopsis* potassium channel KAT1; the mutated  $N_{ubG}$  half solely expressed; and the wild type half  $N_{ubWT}$ . The yeast cells expressing the  $N_{ub}$  constructs were mated with those ones expressing the  $C_{ub}$  constructs in every possible combination. After selection of the diploid cells on medium lacking leucine, tryptophane, and uracil, the diploid cells were screened for interaction either via a growth assay on medium lacking histidine and adenine for six days at 28 °C (A) or via an X-Gal assay on medium containing adenine and histidine by coating with the staining solution (B).

Indispensable for the interpretation of the results is a positive reaction, i.e. an interaction, of every  $C_{ub}$  construct with the  $N_{ubWT}$  construct, and vice versa a negative reaction, i.e. no interaction, of every  $C_{ub}$  construct with the solely expressed mutated  $N_{ubG}$  construct. No interactions were observed for the  $C_{ub}$  constructs coexpressed with the  $N_{ubG}$  protein, but only for three of the five  $C_{ub}$  constructs, an interaction with  $N_{ubWT}$  could be detected (cf. Figure 3.4.2). These three constructs were: AtMRS2-1- $C_{ub}$ , AtMRS2-1 AMN- $C_{ub}$ , and KAT1- $C_{ub}$ . No interactions were detected for AtMRS2-7- $C_{ub}$  and AtMRS2-10- $C_{ub}$ . Likewise, these  $C_{ub}$  constructs showed no interactions with any of the  $N_{ubG}$  constructs tested, either. As expected,

KAT1-C<sub>ub</sub> interacted only with N<sub>ubG</sub>-KAT1 besides the positive control. The other N<sub>ubG</sub> constructs used were: N<sub>ubG</sub>-AtMRS2-1, N<sub>ubG</sub>-AtMRS2-1 AMN, N<sub>ubG</sub>-AtMRS2-7, N<sub>ubG</sub>-AtMRS2-10, and the control constructs mentioned above, N<sub>ubG</sub> and N<sub>ubWT</sub>. AtMRS2-1-C<sub>ub</sub> and AtMRS2-1 AMN-C<sub>ub</sub> showed the same interaction patterns: both interacted with the two AtMRS2-1 constructs (N<sub>ubG</sub>-AtMRS2-1 and N<sub>ubG</sub>-AtMRS2-1 AMN) and with NubG-AtMRS2-10. No interaction was observed for N<sub>ubG</sub>-AtMRS2-7 and N<sub>ubG</sub>-KAT1 (cf. Figure 3.4.2).

This limited number of results from the second mbSUS screening confirms the results obtained in the first screening: AtMRS2-1 and AtMRS2-10 can interact both with themselves and among each other. New results are: mutation of the conserved GMN motif to AMN does not have any influence on the oligomerisation properties as the mutated proteins show the same interaction pattern as AtMRS2-1 “WT”, and, although only seen in one direction, no interaction of AtMRS2-1-C<sub>ub</sub> and AtMRS2-1 AMN-C<sub>ub</sub> takes place with the more distantly related N<sub>ubG</sub>-AtMRS2-7 giving the first hint that interaction between the AtMRS2 proteins does not take place in every possible combination. This result should be confirmed by the cross experiment with AtMRS2-7-C<sub>ub</sub> and the N<sub>ubG</sub> constructs; unfortunately this C<sub>ub</sub> construct and AtMRS2-10-C<sub>ub</sub> gave no results in the second screening.

A new screening approach was subsequently performed in our group together with Karoline Meschenmoser, who will take over the mbSUS experiments. This approach included, besides further constructs, the following C<sub>ub</sub> and N<sub>ubG</sub> constructs originally cloned by myself: AtMRS2-1, AtMRS2-1 AMN, AtMRS2-1 –N (with the N-terminal 93 amino acids missing), AtMRS2-2, AtMRS2-7, and AtMRS2-10. Once again, the positive control with the N<sub>ubWT</sub> protein did not give positive results for all of the C<sub>ub</sub> constructs: AtMRS2-1 AMN-C<sub>ub</sub>, AtMRS2-1 –N-C<sub>ub</sub>, and AtMRS2-7-C<sub>ub</sub> did not show any interaction with N<sub>ubWT</sub> and neither with the further NubG constructs tested. Thus, only the interaction pattern for AtMRS2-1-C<sub>ub</sub>, AtMRS2-2-C<sub>ub</sub>, and AtMRS2-10-C<sub>ub</sub> with an extended number of N<sub>ubG</sub> constructs could be determined (data not shown).

Table 3.4-1 sums up the results achieved overall in the three screening approaches. In none of the combinations, contrary results were obtained in the different screenings, but the same interaction patterns resulted from repetition of the experiments.

**Table 3.4-1: Summary of the results obtained for interaction of the AtMRS2 proteins within the mbSUS**

++: strong interaction; +: weak interaction; +/-: maybe interaction; -: no interaction; nd: not determined

$C_{ub}$	$N_{ub}$	AtMRS	AtMRS2-1	AtMRS2-1	AtMRS	AtMRS	AtMRS	$N_{ubG}$	$N_{ubWT}$
	2-1	AMN	-N	2-2	2-7	2-10			
AtMRS2-1	++	++	+	+	-	++	-	++	
AtMRS2-1AMN	++	++	nd <sup>1</sup>	nd <sup>1</sup>	-	++	-	++	
AtMRS2-1-N	-	-	-	-	-	-	-	-	
AtMRS2-2	++	++	++	++	+	++	-	++	
AtMRS2-7	-	-	-	-	-	-	-	-	
AtMRS2-10	+	+	+/-	+	-	+	-	++	

<sup>1</sup>: these two NubG constructs were not included in the second screening approach

AtMRS2-1 can both with its wild type sequence and with the AMN mutation interact with itself, AtMRS2-10, AtMRS2-2, and an N-terminally shortened version of AtMRS2-1 lacking the first 93 amino acids. No interaction takes place with AtMRS2-7.

AtMRS2-10 shows principally the same, but overall weaker interaction pattern: interactions with all three versions of AtMRS2-1, AtMRS2-2, and itself, but no interaction with AtMRS2-7.

AtMRS2-2, newly included in the third screening, shows the broadest interaction pattern of the examined proteins: it interacts with each of the AtMRS2 proteins tested, including, although weaker than with the rest, AtMRS2-7. This result shows that no interaction with AtMRS2-7 for the further constructs is not due to a non-functional  $N_{ubG}$ -AtMRS2-7 protein but most likely reflects the true interaction possibilities of these proteins.

Altogether, the results so far achieved with the mating-based split ubiquitin system suggest that the AtMRS2 proteins can both form homo- and heterooligomers, however, not in every combination theoretically possible.

The mbSUS experiments are further extended to all members of the gene family by Karoline Meschenmoser in her PhD thesis.



## 4. Discussion

### 4.1 The *Arabidopsis thaliana* MRS2 family of magnesium transport proteins

A new chapter in the investigation of plant ion transport was opened with the description of the MRS2 magnesium transporter family in *Arabidopsis thaliana* by our group (Schock et al., 2000) and the researchers around Richard C. Gardner and Sheng Luan (Li et al., 2001). The AtMRS2 proteins are a second transport system for magnesium described in plants, the first one being the vacuolar  $Mg^{2+}/H^{+}$  exchanger AtMHX which is related to a mammalian plasma membrane  $Na^{+}/Ca^{2+}$  exchanger (Shaul et al., 1999). The AtMRS2 proteins belong to the large superfamily of 2-TM-GxN proteins including the bacterial CorA-like proteins, the fungal ALR- and MRS2-like proteins, and many further proteins from all domains of life sharing the characteristic feature of a long soluble N-terminal domain and two C-terminal transmembrane domains with the conserved GMN motif at the end of TM domain 1 (Knoop et al., 2005). Among known ion transport proteins, this topology is highly unusual, as are the properties of the magnesium ion to be transported (cf. the introduction for further details).

The tendency of plants to extend a single copy gene into a large family (recent database research revealed that there are at least 780 gene families in *Arabidopsis* and at least 824 in rice consisting of more than five members each; Horan et al. (2005)) can also be observed for the AtMRS2 family with eleven “core” members in *Arabidopsis* and nine in rice, not counting the further distantly related proteins recently identified in these two organisms (cf. the introduction for further details, pages 9 ff). Figure 4.1.1 displays the phylogenetic tree of the *Arabidopsis* and rice proteins next to the exon-intron structure of the coding sequences. Although relatively uniform in length of the corresponding protein sequences (ranging from 380 aa (AtMRS2-8) to 484 aa (AtMRS2-3, cf. Table 3.1-5 on page 50) in *Arabidopsis* and from 384 aa (Os03g53110) to 474 aa (Os03g48000) in rice), the numbers and sizes of introns in the coding regions are heterogeneous within the plant gene family. On the other hand, the protein clusters derived from the phylogenetic analysis are also clearly revealed on the genomic level by exon/intron numbers and intron conservation: the AtMRS2-4/2-6, Os03g04480/Os10g39790 cluster e.g. shows the lowest number of introns with two and three, respectively, which are conserved between the four genes. The coding sequences of the gene cluster on chromosome five (AtMRS2-2, 2-7, 2-8) are disrupted into eleven exons with conserved introns in between, as is the corresponding rice gene Os03g53110. The highest number of introns can be found in the most distantly related genes AtMRS2-11 and

Os03g48000 with 12 introns each, having no intron in common with the cluster on chromosome five mentioned above.

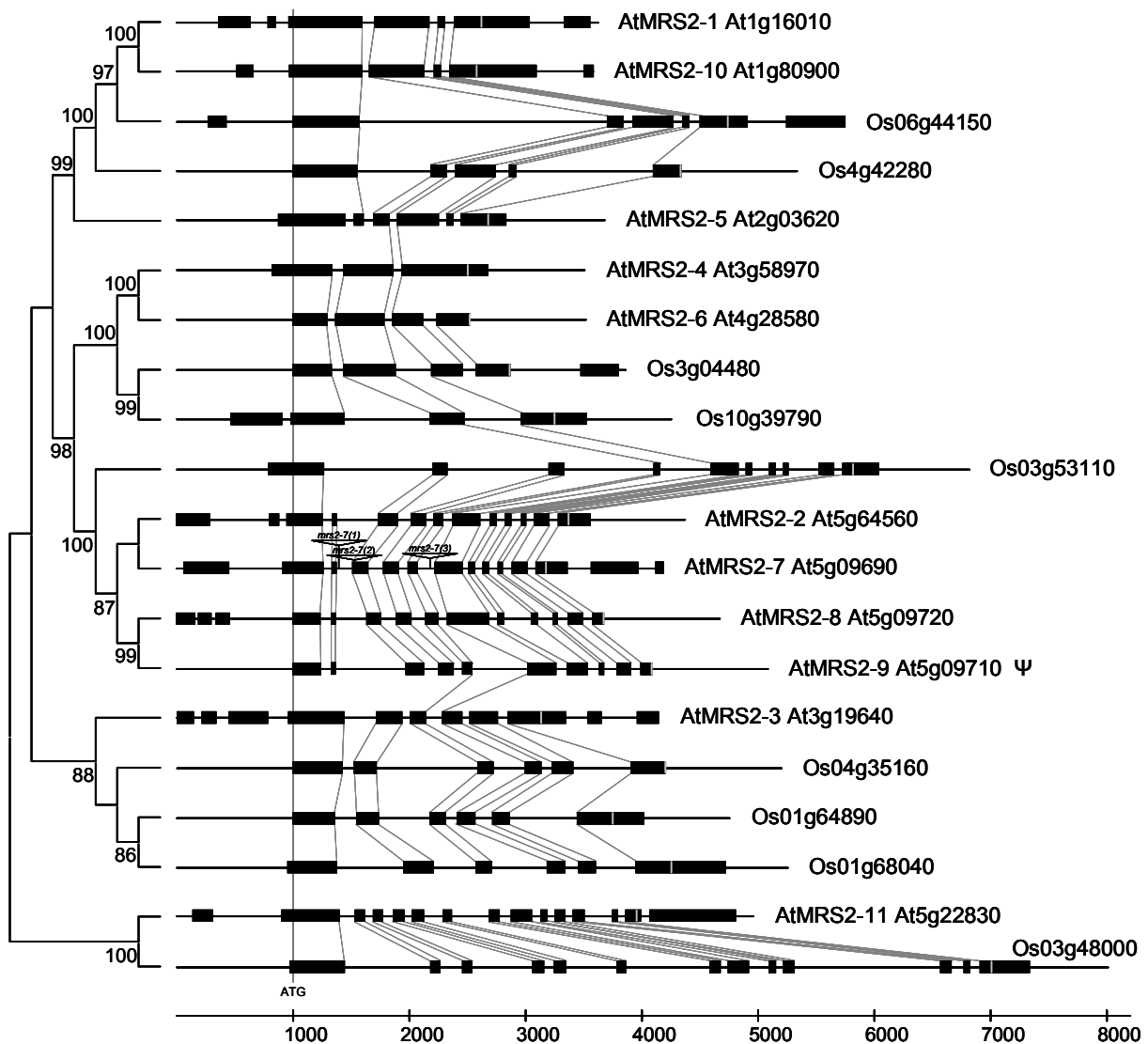


**Figure 4.1.1: Phylogenetic tree and exon-intron structures of the *Arabidopsis* and *Oryza* magnesium transporters**

The left part of the figure displays the phylogenetic relationships of the *Arabidopsis* and rice magnesium transport proteins; numbers indicate significant bootstrap values. The right part of the figure gives an overview of the genomic gene structure starting 1000 bp upstream of the start codon (denoted with the line at position 1000) and ending 1000 bp downstream of the respective stop codon (denoted with a grey line within the last coding exon). Exons are indicated by black boxes, the lines represent the introns. Introns conserved between the genes are connected by thin lines. Exon-intron structures in the UTRs are given if EST data were available. The ruler at the bottom gives the length of the sequences in bp. The insertion sites of the three independent Salk T-DNA lines in AtMRS2-7 displaying a phenotype are shown (named “*mrs2-7(1) – (3)*”).

Calculation of the phylogenetic tree was as in Figure 1.3.1 (cf. page 10). For the exon-intron structures, genomic sequences of the eleven *Arabidopsis* and nine rice genes starting 1000 bp upstream of the start codon and ending 1000 bp downstream of the stop codon were collected and compared with the cDNA and EST data available at NCBI (<http://www.ncbi.nlm.nih.gov/>) to determine the exon-intron boundaries and 5' and 3' UTR structures, if possible.

At least for the MRS2 genes, the overall larger size of the rice genome compared to the *Arabidopsis* genome (an estimated 430 Mb on twelve chromosomes compared to 157 Mb on five chromosomes; <http://btn.genomics.org.cn:8080/rice/> and Bennett et al. (2003)) is not due to an increased number of genes within this family (on the contrary, the gene family is smaller in rice) but to an increased size of the introns within the coding regions of the genes, culminating in a 7 kb coding sequence for Os03g48000 compared to 4 kb for the corresponding AtMRS2-11 gene (cf. Figure 4.1.1).

Before the beginning of this thesis, research on the AtMRS2 gene family in our group had been performed on different levels: the two members of the gene family first identified, AtMRS2-1 and AtMRS2-2, had been functionally analysed in yeast, subcellular localization assays were performed for these two genes and AtMRS2-6 (Schock et al., 2000; Schock, 2000), and first promoter-GUS and RNAi lines had been created (N. Isci, unpublished results). Extending the studies on subcellular localization to all members of the gene family was the main focus of the present thesis.

## 4.2 Subcellular localization: no convincing, positive results, but a multitude of insights

### 4.2.1 Stable transformation approaches

Work on the analysis of the subcellular localization of the AtMRS2 proteins was started by the former PhD student Irene Schock. She used different approaches for the genes AtMRS2-1, AtMRS2-2, and AtMRS2-6, cloning both full length and C-terminally shortened cDNA sequences upstream of the coding sequence of soluble modified GFP (smGFP4; Davis and Vierstra (1998)) and expressing them transiently in tobacco and *Arabidopsis* protoplasts. She could not observe fluorescence for the full length constructs. The shortened constructs for AtMRS2-1 and AtMRS2-2 resulted in green fluorescence which could not be assigned to a distinct plant cell membrane (Schock et al., 2000; Schock, 2000), but the C-terminally shortened AtMRS2-6-GFP construct displayed fluorescence corresponding to the mitochondria as verified via MitoTracker (Molecular Probes) staining of the respective protoplasts (I. Schock, unpublished results). The research group around Sheng Luan in Berkeley working on the AtMRS2 family had published subcellular localization data for a full

length AtMRS2-10-GFP construct stably expressed in *Arabidopsis* plants (Li et al., 2001), showing a plasma membrane localization.

The question of subcellular localization was addressed again via gene-GFP fusions in this thesis, this time by stable transformation of full length constructs for all members of the family into *Arabidopsis thaliana* and subsequent analysis of transgenic plants. The cloning vector of choice was pK7FWG2 from the Karimi series of binary vectors (Karimi et al., 2002) containing the coding sequence for enhanced GFP (Egfp, Clontech), a GFP version which is improved in its fluorescence and optimized for human codon usage, simultaneously removing a cryptic intron splice site formerly recognized by *Arabidopsis* (Cormack et al., 1996; Yang et al., 1996). Plant and human codon usages are very similar, thus Egfp can be and has been used successfully in plants as well (see e.g. Chiu et al. (1996), Cutler et al. (2000)). The vector pK7FWG2 itself has also been applied successfully for subcellular localization questions, both by the vector designers themselves (Van Damme et al., 2004) and by Favery et al. (2004), these being the two examples published so far.

An advantage of this vector is the possibility to use it with the Gateway™ system from Invitrogen Inc. which simplifies cloning of expression constructs concerning both the experimental design (no need to search for appropriate restriction enzyme sites etc.) and the time spent for cloning of the constructs. Sequencing of the expression constructs revealed that the two recombination reactions used in this system worked reliably, producing the desired in-frame sequence between the C-terminus of the AtMRS2 gene and the N-terminus of Egfp.

Hence, the prerequisites for observation of GFP fluorescence *in planta* were given, but no fluorescence could be seen looking at different tissues and protoplasts of the transgenic plant lines received after transformation. Analysis on the level of transcription (for all plant lines) and of translation (for selected lines showing transcription) showed both transcription and translation of the respective transgenes. Translation was checked just for four different plant lines, but the strong signals of the expected protein sizes identified in a western blot suggested that the further plant lines tested positive for transcription would also show expression of the fusion protein. A large amount of fusion proteins could be expected, as the constructs are driven from the strong, constitutive 35S promoter of the cauliflower mosaic virus.

The second approach using promoter and first exon of the respective AtMRS2 gene in fusion to Egfp again using pK7FWG2 was based on the possibility that the transmembrane domains directly preceding the GFP might interfere with the correct folding of the fluorescent protein (see below for further discussion of this possibility). Entry clones were already available from

a promoter-GUS fusion approach and could be utilised directly for recombination into pK7FWG2, explaining why the respective AtMRS2 promoter sequences are found between 35S promoter and first exon-GFP translational fusion in the destination vectors. The action of the native promoters should be masked by the action of the constitutive 35S promoter.

Analysis of the obtained transgenic plants under the fluorescence microscope once again revealed no detectable fluorescence. Transcription was checked for one plant line per construct immediately giving positive results except for AtMRS2-6short-GFP where three plant lines had to be examined, one of which showed transcription of the transgene. Two of these transcripts were further used to control the transcribed GFP gene; sequencing revealed that there were no nucleotide differences from the published sequence of Egfp ruling out the possibility of an aberrant Egfp sequence preventing fluorescence.

The results for the translation control were not as unambiguous as for the full length gene-GFP plant lines: the signals obtained in the western blots were very weak and did not have the correct size for a first exon-GFP fusion protein. A band around 35 kDa in size, which also appeared additionally to the strong bands corresponding to the full length gene-GFP fusion proteins, was the only detectable band in both approaches of translation control for the shortened gene-GFP constructs. This band might be the result of degradation of the fusion protein which might have occurred partly for the full length gene-GFP constructs and to a greater extent, up to complete degradation, with the shortened constructs. This would, of course, also explain the lack of fluorescence.

Within this second western blot of the shortened constructs, two full length gene-GFP plant lines were tested again, this time not displaying the same strong bands of the correct size as in the first approach. The experimental setup was nearly identical, both times total proteins were isolated without further purification; and western blotting and immunodetection were identical in both cases. The difference in the results remains, at least for the time being, unexplainable.

The third approach utilised a different vector (pMDC83; Curtis and Grossniklaus (2003)) which provides both a longer spacer between the AtMRS2 coding sequence and GFP and a slightly different version of GFP, mgfp6 (Schuldt et al., 1998). Unfortunately, within this thesis, transgenic plant lines could not be analysed; the seeds obtained after transformation have been collected and will be used for selection of transformed seedlings. The more than 50 % longer linker (24 amino acids versus eleven amino acids in pK7FWG2) might solve spatial problems in formation of a correctly folded GFP, if those were responsible for the lack

of fluorescence observed (see below). There should be no major difference between the two GFP versions; both are optimized for the application in plants. A final answer whether this vector background leads to fluorescent fusion proteins in stably transformed *Arabidopsis* plants cannot be given at this point.

All constructs described above were subsequently subjected to transient transformation assays, going back to the methodological approach which had been used successfully by Irene Schock for the shortened AtMRS2-6-GFP construct (see above).

#### **4.2.2 Transient transformation approaches**

Two different transient transformation assays were followed, both using tobacco (*Nicotiana benthamiana* and *Nicotiana tabacum*) as the model plant. Infiltration of tobacco leaves or leaf sections with an *Agrobacterium* solution carrying the respective expression construct is a widely used method leading to expression of the transgene in transformed epidermal cells, as e.g. described in Batoko et al. (2000). This group used GFP fusion proteins targeted to the endoplasmatic reticulum (ER), the Golgi apparatus, or the apoplast to study membrane trafficking in wild type and knockout plants; the protocol given in their paper was used in this thesis.

A selection of expression vectors both from the full length and the C-terminally shortened gene-GFP constructs was used for tobacco leaf infiltration. The functionality of the method was checked using a binary plasmid expressing mGFP (which differs in one amino acid from mgfp6 in pMDC83) under the control of the 35S promoter: pPGTkan (kindly provided by Dr. Guillaume Pilot). As stated before, the three different GFP versions used in this thesis all are optimized in fluorescence and codon usage for application in plants, thus, no major differences arising from the GFP versions should be expected. Expression of pPGTkan both in *N. benthamiana* and in *N. tabacum* leaves led to the expected bright GFP fluorescence in cyto- and nucleoplasm of the transformed cells. None of the four full length and three shortened AtMRS2-GFP constructs in pK7FWG2 used in this transient assay led to detection of fluorescence. This negative result fits the results obtained before with the stable transgenic plant lines.

The second transient expression assay used is the PEG-mediated transformation of protoplasts, also an established method applied by numerous research groups. Experiments both with *Arabidopsis thaliana* and with *Nicotiana benthamiana* protoplasts showed that the

more reliable results were obtained with *N. benthamiana* protoplasts, largely due to the advantageous protoplast purification protocol which efficiently separates intact protoplasts from destroyed ones (Koop et al., 1996). In both cases, the pPGTkan plasmid was used as the control for efficient transformation; and congruent with the *Agrobacterium*-infiltration method bright green fluorescence was observed in the transformed protoplasts. This control was applied in each transformation assay, allowing statements on the efficiency of the transformation (although the transformation rate was never exactly quantified) and enabling to correlate it to the state of the plants used for protoplast isolation or of the transformation batch which was not always in an optimal condition. Problems appeared with fission yeast contaminating the transformation approaches, or with protoplasts having lost their turgescence on the day after transformation, the day of microscopical observation. Altogether, the tobacco protoplast transformation could not be applied completely reliably, but at least in those approaches with a brightly shining positive control the results obtained for the AtMRS2-GFP constructs can be regarded as trustworthy.

For this assay, five full length AtMRS2-GFP constructs in pK7FWG2, four C-terminally shortened constructs (in pK7FWG2), and the four cloned full length gene-GFP constructs in the second vector, pMDC83, were used together with the C-terminally shortened AtMRS2-6-GFP construct cloned by Irene Schock (unpublished). After repeatedly seeing no fluorescence for the latter construct, sequencing revealed that the linker between the AtMRS2-6 sequence and the GFP was built of ten base pairs, thus preventing a translational fusion of the two proteins. The positive results Irene Schock achieved with this fusion protein must have been obtained with a different clone; time limitations prohibited further analysis of two more clones in this thesis.

The results obtained with transient expression of the AtMRS2-GFP constructs in tobacco protoplasts differ from those obtained after *Agrobacterium* infiltration as fluorescence was observed in some cases. Both the full length and the shortened AtMRS2-4-GFP construct in pK7FWG2 showed green fluorescence which co-localized with the red autofluorescence of the chloroplasts in two independent transformation approaches each, all contaminated with fission yeast. The results could not be repeated with contamination-free protoplasts; no fluorescence was observed for the further seven constructs in pK7FWG2 used for protoplast transformation. Utilisation of *N. tabacum* protoplasts as originally used by Irene Schock gave the same negative result.

These rare positive results do not exactly fit into the overall non-fluorescence obtained with the pK7FWG2 constructs in stable and transient transformation assays. A final answer why

fluorescence of the chloroplasts could be observed in four transformation approaches (two for each construct) cannot be given, but minor differences in the incubation time after transformation and before observation of the protoplasts might play a role. Furthermore, the site of transgene integration into the transformed protoplast's genome might have been advantageous in these four transformation approaches. Speaking against this explanation is the fact that per transformation approach more than one independently transformed protoplast exhibited fluorescence. The fission yeast contamination itself should have no direct influence on the fluorescence of the tobacco protoplasts.

The four AtMRS2 genes fused to mgfp6 in vector pMDC83 featuring the longer linker sequence were also used for tobacco protoplast transformation assays, and two of the constructs (the ones for AtMRS2-1 and AtMRS2-2) displayed the same fluorescence pattern. No fluorescence was repeatedly observed for the further two constructs. Fluorescence of full length AtMRS2-1- and AtMRS2-2-mgfp6 constructs appeared in patches within the cytosol of the protoplasts, not co-localising with an organelle (mitochondria or chloroplasts) or other defined subcellular structures. The patches might be the result of overexpressed and degraded fusion proteins accumulating in the cytosol. Unfortunately a comparison to the fluorescence of the fusion proteins stably expressed in *Arabidopsis* cannot be made (see above).

Taking together all results obtained with the various methods used, no confirmed new statements concerning the subcellular localization of the AtMRS2 proteins can be made. Possible reasons for the inability to successfully use AtMRS2-GFP fusion proteins as reporters are discussed in the following section.

### **4.2.3 Conclusions**

Leaving aside the non-reproduced fluorescence obtained for the AtMRS2-4-GFP constructs, no fluorescence at all could be observed for all gene-GFP fusions in pK7FWG2, neither stably nor transiently expressed both in the homologous plant *Arabidopsis* and in the heterologous plant tobacco. The clear evidence for the functionality of the vector is missing, as pK7FWG2 was not modified to express Egfp alone from the 35S promoter, but sequencing of transcripts showed no aberrances in the Egfp coding sequence, and the same vector has been used successfully by other research groups, as mentioned above (Van Damme et al., 2004; Favery et al., 2004). The possibility remains that the Egfp protein alone would not fluoresce *in planta*, either, but the probability is not very high, and different explanations should be considered.



Concerning the full length AtMRS2-GFP fusions in pK7FWG2, the most plausible explanation would be sterical preventions of the correct folding of GFP. Since the beginning of 2006, the crystal structure of the *Thermotoga maritima* CorA protein is resolved (Lunin et al., 2006; Eshaghi et al., 2006). As mentioned in the introduction (cf. pages 3 ff), the pentameric structure can most probably be assumed for the further members of the 2-TM-GxN superfamily as well. The crystal structure shows that the C-termini of CorA are located immediately below the membrane, as they are only some amino acids apart from the second transmembrane domain. In very close proximity to the C-termini, the funnel-shaped soluble part of the pentamer occupies a large amount of space (cf. Figure 1.2.1 on page 4). The green fluorescent protein, on the other side, has a comparatively rigid  $\beta$ -barrel structure which encloses the chromophore (Ormö et al., 1996), with C- and N-terminus displayed on one end of the barrel. It is well conceivable that linking the GFP coding sequence to the C-terminus of an AtMRS2 protein does not allow for the folding of the  $\beta$ -barrel as not enough space is provided between the membrane and the funnel-shaped N-terminal domain of the AtMRS2 protein.

Subcellular localization studies via GFP fusions have been performed with the following members of the 2-TM-GxN superfamily: within the AtMRS2 family, besides the already mentioned full length and C-terminally shortened gene-GFP fusions cloned by Irene Schock and the full length AtMRS2-10-GFP construct published in Li et al. (2001), Drummond et al. (2006) have performed full length gene-GFP fusions for all members of the AtMRS2 family except for AtMRS2-7 and expressed them heterologously in yeast; the AtMRS2-11-GFP construct was also stably expressed in *Arabidopsis*. Two further eukaryotic members of the 2-TM-GxN family have been fused to GFP: the yeast ALR1 protein (Graschopf et al., 2001) and the human MRS2 protein (Zsurka et al., 2001) were both fused to the N-terminus of GFP, the constructs were expressed in yeast (ScALR1) or mouse fibroblast cells (HsMRS2). Thus, all GFP fusions performed fused the C-terminus of the respective 2-TM-GxN family member to the N-terminus of GFP.

Besides neglectable differences in the GFP versions used (see above) and the length of the linker sequence, huge differences exist between the lengths of the C-termini of the respective proteins, the portion of the protein following the second transmembrane domain. As mentioned above, this sequence is comparatively short for the members of the AtMRS2 protein family, ranging from six to nine amino acids as predicted by the TMHMM-server at <http://www.cbs.dtu.dk/services/TMHMM/>. The two proteins further used for GFP localization studies each display longer C-termini following the second transmembrane domain: the length of the HsMRS2 C-terminus is 53 amino acids, the one of ScALR1 is 65 amino acids long.

Independent of the linker chosen between ScALR1/HsMRS2 and GFP, the long C-termini of those two proteins should allow for a proper folding of the GFP  $\beta$ -barrel structure, as is shown by the fluorescence patterns published in the two studies (Graschopf et al., 2001; Zsurka et al., 2001): ScALR1 is located to the yeast plasma membrane, and HsMRS2 is found in mouse mitochondria, confirming the localizations expected for both proteins.

Concerning the plant full length gene-GFP fusions, no fluorescence had been observed for the AtMRS2-1 and AtMRS2-2 constructs (Schock et al., 2000; Schock, 2000), whereas the AtMRS2-10-GFP and the AtMRS2-11-GFP constructs designed by the group of R.C. Gardner led to detection of fluorescence; plasma membrane-localized in the case of AtMRS2-10 (Li et al., 2001) and chloroplast-localized for AtMRS2-11 (Drummond et al., 2006), the latter as expected from *in silico* predictions. The linker region between the C-terminus of the respective AtMRS2 gene (of course always omitting the stop codon) and the start codon of GFP is three amino acids for the constructs cloned by Irene Schock. No exact statements are given in the publication by Li et al. (2001), and Drummond et al. (2006) fused the two proteins directly without a linker sequence in between. The linker sequence in the pK7FWG2 constructs is, as mentioned before, eleven amino acids long. These linker sequences are very similar in length and far away from the lengths obtained through the long C-termini of ScALR1 and HsMRS2. Still, no congruent pattern in fluorescence is achieved, thus it cannot be the length of the linker alone deciding about the fluorescence of the fusion protein. Likewise the location of expression of the fusion protein (either stable in *Arabidopsis* or transient in tobacco or *Arabidopsis* protoplasts) cannot be the decisive aspect: although Irene Schock never expressed her full length constructs stably in *Arabidopsis*, all of the constructs in vector pK7FWG2 cloned in this thesis were both stably and transiently expressed, showing no difference between the results. The positive results achieved for AtMRS2-10 and AtMRS2-11 were observed upon stable expression (Drummond et al., 2006; Li et al., 2001), whereas the AtMRS2-6-GFP construct gave a fluorescence signal upon protoplast expression (I. Schock, unpublished results).

There seems to be a difference between expression of the same fusion protein in plants and in yeast, though. Drummond et al. (2006) expressed full length gene-GFP fusions for all members of the AtMRS2 family except for AtMRS2-7 in yeast, resulting in different fluorescence patterns which could often not be assigned to a certain cellular membrane. The AtMRS2-11-GFP construct seemed to co-localize with plasma membrane and ER, whereas exactly the same fusion protein stably expressed in *Arabidopsis* showed the expected chloroplast localization. Thus, even if an AtMRS2-GFP fusion shows fluorescence in yeast

---

cells, it can obviously not be transferred to a corresponding localization *in planta*, making yeast an unsuitable tool for localization studies of the AtMRS2 proteins.

Which further possibilities could be thought of for not observing any fluorescence with the constructs in vector pK7FWG2? The most significant argument speaking against GFP folding problems is the fact that no fluorescence was observed with the C-terminally shortened constructs omitting the transmembrane domains, either. One might think that the first exon might not be long enough to direct the GFP into the cellular compartment to whose membrane the native protein would be localized, but at least for mitochondrial and chloroplast localized proteins it has been shown that the targeting sequence itself is sufficient to direct GFP into the respective organelle. This targeting sequence is always found at the N-terminus and can be as short as 12 amino acids for mitochondrial proteins (Hurt and van Loon, 1986). The first exons cloned in front of GFP comprise at least 76 amino acids, thus the complete targeting sequences for mitochondrial or chloroplast proteins should be included. But also those proteins known or presumed to be localized to one of these organelles (AtMRS2-4, 2-6, and 2-11) gave no fluorescence signals.

For the C-terminally shortened constructs a “double” promoter consisting of first the 35S promoter and then the native AtMRS2 promoter was used (for the reasons mentioned above). The AtMRS2 promoter is thought to be ignored by the polymerase or maximally used additionally to the 35S promoter which might add some copies of the transgene in those tissues where the respective AtMRS2 gene is expressed. But maybe this second promoter does interfere with the expression of the transgene in some way; an idea which is argued against by the abundance of RT-PCR products obtained upon analysis of the transgenic plant lines.

The artificially prolonged 5' UTR region now also consisting of the promoter sequence if transcribed downstream of the 35S promoter might, though, cause problems concerning the translation initiation of the fusion protein. There is an obvious difference in the amount and integrity of fusion protein between the full length and the C-terminally shortened constructs as judged from the western blot results. Whereas a large amount of fusion proteins of the correct size could be observed for the full length gene-GFP constructs, no bands of the expected sizes could be detected for the shortened constructs. The only band observed came from an obviously degraded protein. Thus, the expected first exon-GFP fusion protein seems not to have been translated or rapidly degraded in the transgenic plant lines. An approach omitting the AtMRS2 promoter sequence might be more successful, maybe according to the

fluorescence observed for the shortened AtMRS2-6-GFP construct by Irene Schock. On the other side, the C-terminally shortened constructs accordingly designed for AtMRS2-1 and AtMRS2-2 by Irene Schock did show fluorescence, but not of a distinct cellular compartment. The approach omitting the transmembrane domains bears the risk that those fusion proteins which do not contain an N-terminal targeting sequence as they might be expressed in the plasma membrane or some further cellular compartment will be degraded after translation and maybe lead to the patchy fluorescence observed for the AtMRS2-1- and AtMRS2-2-GFP constructs (Schock et al., 2000).

A further aspect is the efficiency with which GFP fluorescence is observed in transgenic plants. Although the plant lines created and analysed after transformation mostly transcribed the transgene, as checked for all full length gene-GFP plants and assumed for most of the C-terminally shortened plant lines (see above), the fluorescence of the fusion protein might be too weak to be detected. Differences in fluorescence efficiency between plant lines transformed with the same construct are known (de Ruijter et al., 2003); Pang et al. (1996) for example give a rate of 31 out of 118 *Arabidopsis* plants transformed with a certain GFP construct displaying strong fluorescence. It is not exactly clear whether all of the 118 plants were transgenic, but if they were, then the rate of fluorescence of transgenic plant lines would be more than 1 out of 4. For a second GFP construct, Pang et al. (1996) describe a fluorescence efficiency of 20 out of 67 transgenic plants, 1 out of 3.3 plants. If these are approximately the numbers to expect after receiving transgenic plant lines, then at least a fourth of the independent plant lines obtained in this thesis should display visible fluorescence. The rate of bright fluorescence might be even lower, though, but still a certain proportion of the 66 and 57 plant lines obtained for the full length and C-terminally shortened gene-GFP constructs in pK7FWG2, respectively, should display fluorescence, thus ruling out this aspect as the sole explanation for the lack of fluorescence.

The identical full length sequences of AtMRS2-1, AtMRS2-2, AtMRS2-6, and AtMRS2-10 recombined into pK7FWG2 were used for recombination into the second vector employed in this thesis, pMDC83 containing mgfp6 (Curtis and Grossniklaus, 2003). Transient transformation into tobacco protoplasts gave a certain fluorescence pattern for AtMRS2-1-mgfp6 and AtMRS2-2-mgfp6, thus differing from the lack of fluorescence observed for the pK7FWG2 constructs. The fluorescence pattern could be seen repeatedly in contamination-free approaches. Unfortunately, no distinct cellular membrane was coloured by the green fluorescent protein; a rather patchy pattern was observed which might be caused by degraded

fusion proteins. Nevertheless, the different vector background seems to cause a difference in the fusion protein expression, at least when transiently expressed in tobacco protoplasts. The possibility exists that in stably transformed plants distinct fluorescence e.g. of the plasma membrane would be observed. This question cannot be answered now, as the transformed seeds are just being analysed.

No unambiguous answers could be given concerning the question why near-identical AtMRS2-GFP expression constructs cause such a difference in fluorescence, from clear plasma membrane, chloroplast or mitochondrial expression (Drummond et al. (2006); Li et al. (2001); I. Schock, unpublished) across patches within the cytoplasm pointing at degradation (Schock (2000); this thesis) to no fluorescence at all (Schock (2000); this thesis). It may simply be an unidentified feature of the expression construct which allows or permits observation of fluorescence, making pK7FWG2 not a suited vector for localization studies of the AtMRS2 family. Maybe pMDC83 turns out to allow detection of fluorescence in stably transformed *Arabidopsis*.

#### 4.2.4 Perspectives

So, what are the alternatives to solve the question of subcellular localization of the AtMRS2 proteins? There is no doubt that this question needs to be addressed again, as knowledge about the subcellular localization of each member is crucial for an overall understanding of the AtMRS2 family (cf. also the further parts of this discussion).

The easiest solution would be a successful green fluorescence coming from the full length constructs in pMDC83. If the four constructs already transformed into *Arabidopsis* gave positive results, then the further full length entry clones could be recombined comparatively quickly with pMDC83 and used for plant transformation. But, with the results obtained so far, the possibility that no fluorescence will be detected is equally given.

In this case, the only usage of the stably transformed full length gene-GFP plants might be for a classical immunodetection of the fusion protein via cross-sectioning of plant tissue, fixation, and incubation with anti-GFP antibody. To raise the resolution to subcellular levels, the utilisation of an electron microscope would be necessary, using immunogold labelled antibodies. Successful usage of anti-GFP antibodies requires that the AtMRS2-GFP fusion proteins are indeed expressed at the same subcellular localization as the native protein. This cannot be said for sure with the results obtained in this thesis.

Immunogold labelling would of course also be possible in wild type plants with antibodies specific for each AtMRS2 protein, but there are two obstacles concerning this method: first, due to relatively high similarities between certain members of the gene family on protein level (AtMRS2-1 and AtMRS2-10 are e.g. 89 % identical) it will be difficult to find peptide motifs specific for each AtMRS2 protein, and second, if motifs can be found, generation of eleven (or fifteen, if the recently identified, more distinct members of the gene family were included) antibodies will cost a fair amount of money.

The advantages of GFP as a reporter towards immunodetection methods (no necessity for sectioning of the material, fixation, and incubation with the respective antibody; but direct visualisation of the fusion protein) could be exploited by fusion of GFP to a different part of the AtMRS2 proteins. Although every approach within the 2-TM-GxN family used the C-terminus for fusion to GFP, it is obvious from the results obtained in this thesis that at least for the AtMRS2 proteins a different fusion site should be searched. The N-terminus is not suited for an approach spanning the whole gene family, as the mitochondrial and chloroplast targeting signals will be masked by the GFP sequence, thus preventing a correct localization of the constructs. Taking the crystal structure of the *Thermotoga* CorA protein (cf. Figure 1.2.1 on page 4) as a model for the AtMRS2 proteins, a site within the soluble domain should be chosen, maybe a loop between two of the  $\beta$ -sheets found there. This would require modelling of the AtMRS2 proteins upon this prokaryotic crystal structure so that, as clear as possible, the corresponding  $\alpha$ -helices and  $\beta$ -sheets could be identified for each AtMRS2 protein.

A further possibility for immunodetection of the AtMRS2 proteins, without the need for AtMRS2-specific antibodies, would be fusion of the proteins to an epitope tag like HA, His-6, or c-myc. These tags are much smaller than the GFP protein and can be detected by specific antibodies after sectioning and fixation of the plant material. Due to the reduced size, fusion of the tag to the C-terminus of the AtMRS2 protein should be possible, omitting the search for intramolecular fusion sites.

The promoter-GUS analysis performed by Karoline Meschenmoser in our group uses a different vector from the Karimi series (pKGWFS7; Karimi et al. (2002)) which contains, upstream of the GUS coding sequence, the Egfp coding sequence for fluorescence detection of promoter activities. Fusion of not only the promoter sequence but also of the first exon to these two reporter genes was thought to maybe allow detection of subcellular localization via GFP expression, but the AtMRS2 promoters are generally too weak to express GFP in a sufficient amount (K. Meschenmoser and K. Weyand, unpublished observations).

Nevertheless, sectioning of stained plant material for the AtMRS2-11-GUS construct, e.g., shows blue stained chloroplasts within guard cells (K. Meschenmoser, unpublished data), raising the possibility to observe subcellular localization via GUS staining. The disadvantage of this reporter protein is the possible diffusion of the  $\beta$ -glucuronidase out of the original cellular compartment, thus leading to staining of unspecific parts of the cell as well. But at least for organelles like chloroplasts and mitochondria (if these can be visualised by the microscopical devices available), as surrounded by two membranes, GUS expression and detection might be an alternative for determination of the subcellular localization. Thin sections of the GUS expressing transgenic plants are currently made by Karoline Meschenmoser; microscopical observation will reveal whether the subcellular localization of at least a couple of AtMRS2 proteins can be determined or confirmed.

#### 4.3 Studies on the functional properties of the AtMRS2 proteins via heterologous expression and characterisation

Determination of expression site and subcellular localization of a protein of interest is only one part of the characterisation of this protein. Analyses on the function of the protein of interest are equally important for gaining a complete picture. Concerning the AtMRS2 proteins, analysis of magnesium transport *in vivo*, i.e. in the plant, can hardly be performed with the means available in a standard laboratory. Thus, usage of heterologous systems provides an easier way for functional studies.

##### 4.3.1 Usage of the yeast $\Delta mrs2$ system

*Saccharomyces cerevisiae* combines the advantages of a unicellular organism (easy handling in the laboratory, fast reproduction rate, transformation ability and efficient screening of transformed cells, etc.) with the characteristics of a eukaryotic organism, making it a frequently used tool for functional studies of a wide range of genes. Concerning the 2-TM-GxN proteins, *S. cerevisiae* itself harbours the plasma membrane localized ALR1 and ALR2 proteins, and the MRS2 and LPE10 proteins of the inner mitochondrial membrane, each one being functionally characterised as a transporter for magnesium (MacDiarmid and Gardner, 1998; Bui et al., 1999; Gregan et al., 2001a). The yeast  $\Delta mrs2$  mutant, created by Wiesenberger et al. (1992), displays a well-identifiable phenotype: growth is restricted on non-fermentable carbon sources (a so-called  $pet^-$  phenotype) due to a defect in the respiratory

system. Growth can be restored by expression of a magnesium transporter in the inner mitochondrial membrane, making the mutant strain an efficient tool for the screening of functional magnesium transporters.

First hints, besides the structural homology to the prokaryotic CorA and the yeast ALR1 and MRS2 proteins, on the AtMRS2 proteins being functional magnesium transporters came from analysis of AtMRS2-1 and AtMRS2-2 in the  $\Delta mrs2$  yeast strain. AtMRS2-1 is able to complement the yeast mutant when targeted to the yeast mitochondria via the ScMRS2 targeting sequence; when expressed with its native N-terminus, no complementation is observed (Schock et al., 2000; Schock, 2000). The negative results achieved for both approaches with AtMRS2-2 are explained by usage of a wrong coding sequence prediction leading to a non-functional expression construct.

In this thesis, further members of the AtMRS2 family were heterologously expressed in the yeast  $\Delta mrs2$  strain. Besides phenotypical complementation of the mutant via growth restoration, direct measurement of magnesium uptake into isolated yeast mitochondria could be performed as well, due to a method recently developed in the laboratory of our cooperation partner, Prof. R. J. Schweyen (Kolisek et al., 2003).

The organellarly targeted proteins AtMRS2-4 and AtMRS2-6 (as predicted by *in silico* analysis and preliminarily confirmed by gene-GFP fusions (see above), respectively) should be cloned both with their native and with the mitochondrial targeting sequence of the yeast MRS2 protein to allow for a comparison of the plant and yeast targeting mechanisms. Unfortunately, this double approach could only be followed for AtMRS2-4, as amplification of the full length cDNA sequence of AtMRS2-6 proved impossible. This protein, as known from promoter-GUS studies, is solely expressed in the pollen of the flowers (K. Meschenmoser, unpublished results), a plant tissue which can rather not be isolated in quantitative amounts for an RNA extraction and subsequent RT-PCR. RNA extraction from complete flowers, however, and synthesis of cDNA using only AtMRS2-6 specific oligonucleotides, did not lead to amplification of the full length AtMRS2-6 coding sequence; an approach using two overlapping halves of AtMRS2-6 did not yield the desired product, either. A new kit for RNA extraction from plant material promising to isolate a greater portion of mRNA and a subsequent mRNA purification matched with this kit (both Macherey & Nagel) might allow for the amplification of this cDNA, which is currently under investigation.



Thus, results were obtained for AtMRS2-4, AtMRS2-6, and the third protein used, AtMRS2-3, expressed with the yeast MRS2 targeting sequence and solely for AtMRS2-4 with its native targeting sequence. The exact length of the mitochondrial presequence of ScMRS2 containing the targeting signal is not known, thus, the first amino acid sequence conserved between plant and yeast MRS2 proteins was chosen as the carboxyterminal end for the exchange of the N-terminal sequences. This sequence, A/PRDLR (with minor deviations in some plant proteins), is located at position 95 in the yeast MRS2 protein, hence the first 94 amino acids were chosen as the presequence, including the mitochondrial targeting signal. Likewise, amplification of the N-terminally shortened AtMRS2 genes was started at the first codon of the conserved amino acid sequence. This strategy was already used successfully for AtMRS2-1 (Schock et al., 2000), and the results obtained in this thesis confirm its functionality. All constructs using the yeast MRS2 targeting sequence are driven from the yeast MRS2 promoter, mimicking the native protein expression as closely as possible.

Both the trickle tests on a medium containing the non-fermentable glycerol as the sole carbon source and the mag-fura 2 measurements of isolated yeast mitochondria gave the same results: AtMRS2-3 and AtMRS2-6, when targeted to the yeast mitochondria, can complement the  $\Delta mrs2$  strain, restoring magnesium uptake into the mitochondria to nearly wild type levels. AtMRS2-4 shows complementation of the phenotype only when expressed with its native N-terminus from the constitutive ADH (alcohol dehydrogenase) promoter; the approach using the ScMRS2 targeting sequence did not significantly complement the mutant strain. This is the only unexpected part of the result: AtMRS2-4, as it is able to complement the  $\Delta mrs2$  strain when no yeast targeting signal is used, should be able to show the same result when fused to the yeast N-terminus. Sequencing of the construct revealed no aberrances, the design is the same as for the further two constructs. A final answer why this construct showed no complementation ability cannot be given.

AtMRS2-4 is predicted to be localized either to chloroplasts or to mitochondria (different prediction servers give different probabilities for both organelles, as can be seen by the summary given at <http://aramemnon.botanik.uni-koeln.de/>; Schwacke et al. (2003)) in *Arabidopsis*. The possibility exists that this member of the gene family is indeed targeted to both organelles. Dual targeting has been observed for a wide range of organellar proteins, e.g. for 17 aminoacyl-tRNA synthetases (Duchene et al. (2005); see also the recent review by Millar et al. (2006)). A role for AtMRS2-4 in magnesium transport both in mitochondria and in chloroplasts might be underlined by the fact that no T-DNA inactivation lines are available

for this gene, showing that AtMRS2-4 is most likely indispensable for the development of the plant.

Plant mitochondrial proteins can be efficiently transported into yeast mitochondria, as shown e.g. by Chaumont et al. (1990), whereas only those plant chloroplast proteins containing an amphipathic  $\alpha$ -helix within their transit sequence seem to be transported into yeast mitochondria (Brink et al., 1994). The amphipathic  $\alpha$ -helix is a mutual feature of mitochondrial presequences and some chloroplast transit sequences and seems to be required for the efficient transport of chloroplast proteins into yeast mitochondria. Generally, those chloroplast proteins targeted to the inner envelope contain this  $\alpha$ -helix (Brink et al., 1994). If AtMRS2-4 is located to the chloroplast (one example where successful protein localization studies are needed; see above), then it will most likely be found in the inner envelope membrane, the major metabolite limiting boundary of the chloroplast where a large number of transport proteins have already been identified (Douce and Joyard, 1990). The outer envelope membrane is permeable to macromolecules up to sizes of about 10 kDa (Flügge and Benz, 1984); most likely, magnesium can pass it without the need for a specific transporter. Furthermore, AtMRS2-11, as shown by gene-GFP fusions, is probably located in the inner chloroplast membrane as well (Drummond et al., 2006). Thus, the AtMRS2-4 N-terminus will most likely harbour an amphipathic  $\alpha$ -helix which allows for its import into yeast mitochondria and functional expression in the inner mitochondrial membrane, as shown by the ability to complement the yeast  $\Delta$ mrs2 mutant strain.

Similar results would have been expected when expressing the AtMRS-6 gene with its native targeting sequence in the  $\Delta$ mrs2 strain: this protein is localized to the mitochondria *in planta* and should thus be likewise imported into yeast mitochondria.

Although the trickle tests on glycerol medium performed with the yeast cells expressing the different constructs allow for qualitative statements on the complementation ability, a quantification of the efficiency of each different transporter is rather difficult. The measurement of magnesium uptake into isolated yeast mitochondria expressing exactly those constructs thus provides a simple and convenient way to quantify the different transporter capacities. The method, as described in Kolisek et al. (2003), is based on the different excitation wavelengths of the fluorescent dye mag-fura 2 (Molecular Probes) depending on whether magnesium is bound to it or not which are recorded simultaneously. After each measurement, maximum and minimum ratios of  $\text{Mg}^{2+}$ -bound to free mag-fura 2 are determined and the magnesium concentration inside the mitochondria is calculated. As a ratio

of two values is used for further calculations, the method functions independent of the starting amount of mitochondria, allowing a direct comparison of the results achieved with mitochondria expressing different constructs.

The endogenous yeast MRS2 protein, when expressed in the  $\Delta mrs2$  strain, quickly elevates the innermitochondrial magnesium concentration to approximately 5 mM at an extramitochondrial concentration of 9 mM, the same value as described in Kolisek et al. (2003). Expression of AtMRS2-3 and AtMRS2-6 leads to approximately 4 and 3.5 mM magnesium inside the mitochondria; these two proteins do not show the same capacity as ScMRS2, but still import a reasonable amount of magnesium.

Mag-fura 2 measurements have not yet been performed with the native AtMRS2-4 construct expressed in the mutant strain; uptake capacities similar to those of AtMRS2-3 and AtMRS2-6 would be expected.

This thesis provides data on three more AtMRS2 proteins showing that they are indeed functional magnesium transporters. The  $\Delta mrs2$  strain seems to be advantageous over a second mutant yeast strain also used for complementation tests of AtMRS2 proteins, CM66, deleted for the two plasma membrane proteins ALR1 and ALR2 (MacDiarmid and Gardner, 1998). This strain has been transformed with the full length coding sequences for nine of the eleven AtMRS2 proteins, excluding AtMRS2-7 and the pseudogene AtMRS2-9 (Drummond et al., 2006; Li et al., 2001). Complementation of the mutant phenotype, i.e. growth restoration on medium containing 4 mM magnesium, was observed only for three proteins: AtMRS2-1, AtMRS2-10, and AtMRS2-11. These three proteins seem to be targeted to the yeast plasma membrane, the site of expression of the ALR proteins. AtMRS2-10 is shown to be localized to the plasma membrane in *Arabidopsis* (Li et al., 2001), its close homologue AtMRS2-1 might be expressed at the same site, which might be the reason why these two proteins are targeted to the plasma membrane when expressed in yeast. AtMRS2-11, on the contrary, is expressed in chloroplasts in *Arabidopsis*, as shown by Drummond et al. (2006), but complements the yeast  $\Delta alr1 \Delta alr2$  strain best. Localization studies in yeast showed that this protein is indeed targeted to plasma membrane and ER, as already mentioned in the GFP section of the discussion (see chapter 4.2). The differences of protein localization in yeast and *Arabidopsis* show that making use of the ScMRS2 targeting sequence for complementation assays ensures the expression of the heterologous protein at the correct location, the prerequisite for functional analyses. Furthermore, the  $\Delta mrs2$  strain offers the possibility of quantification of the magnesium uptake capacities. No further statements on the

complementation abilities of the remaining AtMRS2 proteins can be made by usage of the CM66 yeast strain (Drummond et al., 2006).

A diploma thesis building on this work completed the cloning of expression constructs for the remaining AtMRS2 proteins (Eifler, 2006). Subsequent trickle tests and mag-fura 2 measurements now provide us with a pattern of transport capacities for the whole AtMRS2 family, showing differences in the uptake capacity between the members of the family. AtMRS2-11 and AtMRS2-7 show magnesium uptake nearly equal to the yeast MRS2 protein, whereas AtMRS2-10, similarly to AtMRS2-4, seems not to be able to complement the phenotype. The further AtMRS2 proteins display medium uptake capacities similar to those of AtMRS2-3 and AtMRS2-6 (Eifler, 2006). The functionality of AtMRS2-10 as a magnesium transporter has been shown by complementation of the  $\Delta$ alr1  $\Delta$ alr2 mutant (Drummond et al. (2006); see above), thus, similarly to AtMRS2-4, some further reason for its non-ability to complement the  $\Delta$ mrs2 mutant must be considered.

In summary, nine of the eleven AtMRS2 proteins could be characterised as functional magnesium transporters in this thesis, the diploma thesis of Karolin Eifler (2006), and the PhD thesis by Irene Schock (2000).

#### **4.3.2 Usage of the *Xenopus* oocyte expression system**

A widely used tool for the functional characterisation of transport proteins is the heterologous expression in *Xenopus* oocytes and subsequent application of electrophysiological methods to measure the electrogenic properties of the transport protein. In cooperation with the group of Prof. Hedrich in Würzburg, a group very experienced in the use of *Xenopus* oocytes for characterisation of transport proteins (see e.g. Marten et al. (1999); Geiger et al. (2002); Becker et al. (2004)), three AtMRS2 proteins were subjected to these analyses.

The coding sequences of the AtMRS2 proteins were cloned into three different *Xenopus* expression vectors, and double electrode voltage clamping (DEVCl) techniques were applied to the oocytes injected with cRNAs of the respective constructs. A multitude of different solutions were applied, including magnesium concentrations ranging from 0 to 50 mM  $\text{Mg}^{2+}$ , in the presence and absence of  $\text{Na}^+$ , using different  $\text{Mg}^{2+}$  sources and two different pH values, 7.5 and 5.6. For none of the different AtMRS2 constructs, a magnesium-dependent current could be measured; the oocytes did not react to the solutions different from non-injected oocytes.

---

There was one exception from these results: oocytes expressing AtMRS2-5 in vector backgrounds pcDNA3.1D/V5-His and pGEMHE showed some obviously magnesium-dependent reactions: a positive current was recorded when raising the extracellular magnesium concentration, which means that either cations are effluxed from the oocyte or anions are influxed into the oocyte. This result is not in line with the expected  $Mg^{2+}$  uptake into the oocyte upon increase of the extracellular magnesium concentration. Furthermore, it could not be repeated with oocytes expressing AtMRS2-5 in the stronger expression vector pDK148. The oocytes expressing AtMRS2-5 in pcDNA3.1D/V5-His, which showed stronger reactions with larger amplitudes than those expressing AtMRS2-5 in pGEMHE, also showed a feature not seen for any other oocyte: the outer membranes were thinner than usual, became patchy, and a large proportion of the oocytes died a few days after injection. The remaining oocytes still had thinner membranes and often displayed a little leak upon injection of the electrodes. Obviously, the injection and expression of the AtMRS2-5 cRNA had some detrimental effects on the *Xenopus* oocytes, something not observed before for any of the transport proteins measured via this technique (D. Geiger, personal communication).

The currents measured in these oocytes might not necessarily be caused by the action of the AtMRS2-5 protein, but might have been evoked by the poor physiological state of the oocytes. As mentioned before, if a sole magnesium transport through the AtMRS2 proteins without co- or antiport with further ions is assumed, then the direction of the transport measured is opposite to what is to be expected: magnesium would be transported out of the oocyte upon raising of the extracellular magnesium concentration. This enhances the assumption that not an AtMRS2-5-dependent magnesium transport has been measured with these oocytes.

Oocytes expressing AtMRS2-5 in pGEMHE reacted in the same way, but with overall lower amplitudes; the transport was weaker than for the construct in pcDNA3.1D7V5-His. The pGEMHE oocytes looked phenotypically normal, but might also have had the same problems like the other oocytes, only weaker and thus not noticeable. The expression level of AtMRS2-5 in the pGEMHE constructs might simply be lower and thus not lead to detectable disturbances of the outer membrane.

The magnesium-dependent currents had also not been measured in previous experiments with the same constructs, confirming the assumption that whatever has been measured was not caused by the action of AtMRS2-5.

Thus, none of the constructs for AtMRS2-1, AtMRS2-3, and AtMRS2-5 led to detection of magnesium-dependent currents when expressed and measured in *Xenopus* oocytes. Immunoblot analysis using the V5-His6 tag added to the AtMRS2 proteins in vector pcDNA3.1D/V5-His showed that the AtMRS2 proteins are most probably expressed in the oocyte plasma membrane, a prerequisite for the DEVC measurements. The results are not completely convincing, as the size obtained on the gel does not fit perfectly to the size expected for the AtMRS2-1 protein, which appears to be 5 kDa smaller on the blot membrane than expected. For AtMRS2-5, the size of the band corresponds well to the predicted molecular mass. Maybe some post-translational modification leads to a reduction in size for AtMRS2-1, which might be a phenomenon only observed upon expression in *Xenopus* oocytes and therefore might yield an explanation for the inability to measure any currents. On the other side, AtMRS2-5 seems unchanged, but still no magnesium-dependent currents could be measured for this protein, either.

*Xenopus* oocytes, in summary, seem not to be a suitable system for the electrogenic characterisation of the AtMRS2 proteins. So far, none of the further 2-TM-GxN proteins have been subjected to exactly this kind of analysis. The yeast ALR1 protein has been measured successfully with the DEVC technique by clamping protoplasts of different yeast strains (Liu et al., 2002). In this approach, the ALR1 protein was expressed in its native membrane, which might explain why this approach yielded the desired results. The possibility exists that plant protoplasts overexpressing a plasma membrane localized AtMRS2 protein could be used successfully for DEVC measurements of the transporter properties.

Principally, *Xenopus* oocytes are suited for the characterisation of magnesium transporters, as was shown by Goytain and Quamme for a series of mammalian magnesium transporters different from HsMRS2 (Goytain and Quamme, 2005d; Goytain and Quamme, 2005a; Goytain and Quamme, 2005c; Goytain and Quamme, 2005b). They could characterise both the SLC41A1 and SLC41A2 proteins, the MagT1 protein, and an ancient, conserved domain protein, ACDP2, as functional magnesium transporters and determine their transport capacities for further divalent cations. A recent report by Gabriel and Günzel (2006) who studied the ability of *Xenopus* oocytes to buffer cytosolic magnesium came to the conclusion that *Xenopus* oocytes are not suited for measurement of magnesium transport if the transport is electroneutral. Electroneutral transport cannot be measured by e.g. the DEVC technique, as this technique requires the transport of ions across the oocyte membrane, but would require usage of electrodes sensitive for the respective ion. As magnesium changes within the oocyte

are immediately buffered, no changes could be determined (Gabriel and Günzel, 2006). All results obtained so far for the different 2-TM-GxN proteins point to the sole transport of magnesium (or of one of the cations further transported by the respective protein) and not at an electroneutral transport together with a further ion. Thus, electroneutrality is not a likely reason why no currents could be measured in *Xenopus* oocytes.

### 4.3.3 Conclusions

Two different heterologous expression systems have been used in this thesis for the functional characterisation of the AtMRS2 proteins, and two different results have been obtained: whereas the yeast  $\Delta mrs2$  strain is a very suitable tool for proof of function of the AtMRS2 proteins as true magnesium transporters, performing better than the yeast  $\Delta alr1 \Delta alr2$  strain, expression in *Xenopus* oocytes and electrophysiological measurements showed not to be suited for the AtMRS2 proteins.

During this thesis, approaches were conducted to establish a third heterologous expression system for complementation analysis: an *Escherichia coli* strain deficient for its two endogenous magnesium transporters, CorA and MgtA (Park et al., 1976). In contrast to the existing pathogenic *Salmonella enterica*  $\Delta corA \Delta mgtA \Delta mgtB$  strain (MM281; Snavely et al. (1989)) which was used successfully for complementation assays with AtMRS2-10 (Li et al., 2001), an *E. coli* mutant strain could be used in biosafety level 1 laboratories. Besides growth assays on medium containing low magnesium concentrations (*S. enterica* MM281 does not grow on magnesium concentrations up to 10 mM, whereas the *Salmonella* wild type strain grows well on this concentration) to observe the functional complementation of the mutant, disk sensitivity assays could be performed with the *E. coli* mutant strain to allow statements about the transportation spectrum and possible inhibitors of each AtMRS2 protein. For the transportation spectrum, *E. coli* wild type, mutant and complemented mutant strain would be grown on magnesium-depleted medium, and a filter containing different magnesium or other divalent cation concentrations would be placed in the middle of the petri dish. The zones of growth around the filter would be measured and compared between the different strains. The effect of toxic concentrations of further divalent cations could be monitored by measuring the zone of growth inhibition around the filter for the mutant strain complemented with the AtMRS2 protein of interest. Similar experiments are e.g. described for the *Salmonella* ZntB protein (Worlock and Smith, 2002).

For the generation of the *E. coli* mutant strain, the “one-step inactivation of chromosomal genes” protocol developed by Datsenko and Wanner (2000) was chosen. This protocol is

based on the ability of *Escherichia coli* to perform homologous recombination if the necessary enzyme, a recombinase, is provided. In this case, the phage  $\lambda$  Red recombinase is epigenetically expressed in an *E. coli* wild type strain which is used for transformation with a PCR product consisting of an antibiotic resistance gene flanked by 36 to 60 nucleotides homologous to the gene to be disrupted (here *CorA* and *MgtA*, respectively). After transformation, the antibiotic resistance gene is recombined into the genome replacing the gene to be disrupted, monitored by expression of the antibiotic resistance and verified by PCR approaches. This strain is then transformed with the second PCR product consisting of a different antibiotic resistance gene and flanking sequences of the remaining gene of interest. After successful recombination and verification, an *E. coli* strain disrupted for the *CorA* and *MgtA* genes exists.

During this thesis, the respective *Escherichia coli* strains were ordered from the *E. coli* Genetic Stock Center (CGSC; <http://cgsc.biology.yale.edu>), grown, and used for plasmid isolation. Oligonucleotides for the two recombination reactions were designed and PCR products amplified, and the  $\lambda$  Red recombinase expressing strain was transformed with the PCR products. Unfortunately, PCR testing of the *E. coli* colonies obtained on the respective selective media proved that none of the colonies tested contained a disrupted *CorA* or *MgtA* gene, respectively. Usage of a new aliquot of the  $\lambda$  Red recombinase expressing *E. coli* strain gave the same negative result; further approaches to obtain the mutant strain could not be performed so far. The negative results obtained so far might be traced back to the *E. coli* strain used for transformation: if the  $\lambda$  Red recombinase is not expressed in this strain, transformation with the linear PCR products will not lead to a recombination of the resistance gene into the gene to be disrupted. A further possibility might be insufficient concentrations of the respective antibiotics used for selection of transformants, although a wide range of concentrations was applied. The magnesium concentration in the medium was set to 100 mM, a concentration which should be sufficient to allow growth of *E. coli* cells even if both magnesium transport systems were disrupted; thus, it should not account for the negative result.

The *E. coli* mutant strain would nicely add up to the analyses in the other heterologous systems: the magnesium uptake capacities of the AtMRS2 proteins have been determined with the mag-fura 2 system in the  $\Delta mrs2$  yeast strain, and expression in the *E. coli*  $\Delta corA$   $\Delta mgtA$  strain would allow for the determination of the cation spectrum transported by each AtMRS2 protein or inhibiting transport. Thus, approaches to get hold of the mutant strain will be continued in our group.



## 4.4 First indications of (hetero-) oligomerisation properties

### 4.4.1 The mating-based split ubiquitin system for interaction studies

The resolution of the crystal structure of the *Thermotoga maritima* CorA protein (Lunin et al., 2006; Eshaghi et al., 2006) confirmed what was already suspected and verified by biochemical experiments (Kolisek et al., 2003): the functional CorA transporter is composed of five subunits, so a pentamer. As mentioned before, this structure can most likely be modelled on the other 2-TM-GxN proteins as well, as all members display the same amount of transmembrane domains at approximately the same position within the protein (Knoop et al., 2005). Whereas the prokaryotic CorA transporters are necessarily homopentamers, the diversification into a gene family within the plants offers the possibility of heteropentamerisation.

Promoter-GUS studies show that a range of the AtMRS2 proteins are indeed expressed in the same tissues (K. Meschenmoser, unpublished results), but statements whether these proteins are also localized to the same cellular membrane cannot be made, due to the lack of data on the subcellular localization (see chapter 4.2). Nevertheless, the general ability of some of the AtMRS2 proteins to form homo- and heteromers was tested in this thesis, making use of the mating-based split ubiquitin system (mbSUS; Obrdlik et al. (2004)).

The functionality of this yeast system, adapted by Petr Obrdlik for the interaction screening of plant membrane proteins, was shown by determining the interaction pattern of different plant potassium channels (Obrdlik et al., 2004) and since then applied to a broad screening approach of plant membrane proteins as well as to more specific questions (see e.g. Ludewig et al. (2003) and Reinders et al. (2002)).

The first two proteins to be analysed with the mbSUS were AtMRS2-1 and AtMRS2-10, the two most closely related members of the gene family. Interaction screening showed that both proteins interact with themselves and with each other when expressed in a diploid yeast strain. No interactions were observed between the AtMRS2 proteins and the potassium channels serving as positive controls in each mbSUS assay.

A relatively high number of base pair exchanges was determined by sequencing of the *in vivo* recombined plasmids harbouring AtMRS2-1 and AtMRS2-10, respectively. This might be due to mistakes of the DNA polymerase used, which did not have a proofreading function, but might, at least partly, also result from the recombination reaction of vector and PCR product performed in the respective yeast strain (P. Obrdlik, personal communication). For the further

experiments, a proofreading DNA polymerase was used, which reduced, but not completely eliminated the number of base pair exchanges in the PCR products. No functional changes within the respective protein are expected from the amino acid changes resulting from some of the base pair mutations.

The mbSUS screening was extended to further members of the AtMRS2 family and mutated versions of AtMRS2-1, an N-terminally shortened protein lacking the first 93 amino acids and a protein with an AMN motif instead of the conserved GMN motif. In these screening approaches, a difference between the fusions to the N-terminal and the C-terminal half of ubiquitin became obvious: whereas the  $N_{ubG}$ -AtMRS2 constructs could be gained without problems after transformation of the respective yeast strain, transformation efficiencies for the AtMRS2- $C_{ub}$  fusions were lower. Subsequent usage of the transformed yeast strains in the mating approach and the interaction screening showed that often the positive interaction of these  $C_{ub}$  constructs with the  $N_{ub}$  wild type protein was not observed. This problem might be solved by using a larger amount of yeast cells expressing the AtMRS2- $C_{ub}$  constructs for the mating approach.

Nevertheless, some more results could be obtained from the new screening approaches: the interactions of AtMRS2-1 and AtMRS2-10 with themselves and with each other were confirmed; both proteins also interacted with AtMRS2-2, but not with AtMRS2-7. No difference in the interaction pattern was observed for both mutated versions of AtMRS2-1 compared to the wild type AtMRS2-1. AtMRS2-2 showed interaction with itself and all further proteins, including AtMRS2-7.

Several aspects should be highlighted: first, each AtMRS2 protein shows interaction with itself, thus, should be able to build homotetramers. Second, interaction between the different AtMRS2 proteins takes place, but not in every possible combination. Interaction with AtMRS2-7 was e.g. only shown for AtMRS2-2. Hence, heteropentamerisation might be restricted to some protein pairs. Third, mutation of the conserved GMN motif to AMN, which was shown to abolish magnesium transport in *S. enterica* (Szegedy and Maguire, 1999) and in *S. cerevisiae* (Lee and Gardner, 2006), does not have an influence on the interaction ability. Thus, this motif is not required for pentamerisation, which also becomes obvious when regarding the crystal structure of CorA: the soluble N-termini seem to be responsible for the interaction of the five subunits (Lunin et al., 2006; Eshaghi et al., 2006). Concerning this, the first 93 amino acids of AtMRS2-1 seem to be dispensable as well, as no difference in the interaction pattern compared to the wild type protein was observed.

Often, dimerisation between proteins involves so-called coiled-coil regions,  $\alpha$ -helices of both proteins which coil into each other, thereby mediating interaction of the proteins (see e.g. Obrdlik et al. (2000)). These coiled-coil regions can be identified by computer algorithms and were found both in the ScMRS2 protein (Weghuber et al., 2006) and in the AtMRS2 proteins. They are located in the middle part of the ScMRS2 and AtMRS2 proteins, upstream of the first TM domain. They can also be identified in the CorA crystal structure (cf. Figure 1.2.1 on page 4), lying within the long  $\alpha$ -helix called stalk helix, which in some parts interacts with the neighbouring stalk helix. The first 93 amino acids deleted in the AtMRS2-1 mutant construct are not involved in the coiled-coil formation, which may conclusively explain why no differences in the interaction patterns are observed.

The transferability of the results obtained in the yeast-based mbSUS to the plant system was shown for the tomato ammonium transporter-1, LeAMT1: homooligomerisation was observed both in the mbSUS and *in planta* (Ludewig et al., 2003). The AtMRS2 proteins themselves were shown to be functional upon expression in the  $\Delta$ mrs2 yeast strain (see chapter 4.3.1). The probability is very high that the interaction pattern observed in the mbSUS screening can be transferred to the situation found in *Arabidopsis*. As mentioned before, it is crucial to know about the localization of each AtMRS2 protein both on the tissue and on the subcellular level, so that detected interaction patterns can be combined with *in planta* practicable protein interaction.

Analysis of the interaction patterns for all members of the AtMRS2 family is continued by Karoline Meschenmoser in her PhD thesis.

#### 4.4.2 Conclusions

The second system in this thesis using yeast as the heterologous expression organism for the *Arabidopsis* AtMRS2 proteins, the mating-based split ubiquitin system (mbSUS), proved to be a powerful tool as well. Different patterns of interaction could be detected for four members of the gene family, allowing first insights into what seems to be a complex interaction scheme. Not every protein can interact with every other one, whereas homooligomerisation seems to be possible in all cases. Although not tested for each AtMRS2 protein in the mbSUS, the results obtained in the  $\Delta$ mrs2 yeast complementation assays also point at this possibility, as all members of the gene family (except for AtMRS2-10) show complementation ability. To complement the yeast mutant, the single AtMRS2 protein expressed in the cell has to build a functional transporter within the inner mitochondrial

membrane, and no further AtMRS2 protein is present for building a heteropentamer. Thus, the AtMRS2 proteins showing magnesium uptake in the  $\Delta mrs2$  yeast are necessarily homopentamers. One could speculate now that the poor complementation ability of some proteins might be connected with their physiological state *in planta*: some proteins might only exist as heteropentamers in *Arabidopsis*, and thus not perform well when expressed alone in yeast, or even show no magnesium transport capacity at all, as observed for AtMRS2-10 (see chapter 4.3.1). Interestingly, the interaction pattern of AtMRS2-10 in the mbSUS screening is reminiscent of that in the  $\Delta mrs2$  strain: interaction with itself and with the further AtMRS2 proteins is observed, but only very weakly, although the expression level as judged from the positive control is as high as that of the further AtMRS2 proteins. AtMRS2-10 might require one of the AtMRS2 proteins not included in these first screens to show a strong interaction; and maybe co-expression of these two proteins in the  $\Delta mrs2$  strain would lead to an uptake of magnesium as high as for the best performing plant proteins, AtMRS2-7 and AtMRS2-11. Concerning AtMRS2-7, interaction was not observed with two of the further three AtMRS2 proteins. Although the results for all members of the gene family are not yet known, one might speculate that this protein is found as a homopentamer in *Arabidopsis*, as it can take up magnesium nearly as well as the ScMRS2 protein in the mag-fura 2 system. A further indication for this idea comes from the analysis of gene knockout plants: *Arabidopsis* plants not expressing the AtMRS2-7 gene anymore are restricted in growth on medium containing minimal concentrations of magnesium, whereas plants deleted for further AtMRS2 proteins show normal growth on this medium (M. Gebert, unpublished results). AtMRS2-7 might be a member of the gene family which builds homopentameric channels and thus cannot be replaced easily by action of a second AtMRS2 protein.

With more and more results accumulating from the studies on the AtMRS2 proteins, the picture of magnesium uptake into and distribution within the plant gets clearer, but still much more data need to be obtained before we will be able to view the complete picture.

## 5. Outlook

This PhD thesis covers some aspects of the studies on the MRS2 gene family of magnesium transporters in *Arabidopsis thaliana*. On the plant side, the expression pattern for each member of the gene family was resolved via promoter-GUS studies (K. Meschenmoser, unpublished results), whereas the subcellular localization still needs to be determined for most AtMRS2 proteins. This thesis has shown that gene-GFP fusions might not be the method of choice to approach this question; immunodetection either via GFP-specific antibodies or using a c-myc-, His-6-, or HA-specific antibody on plants expressing likewise tagged AtMRS2 proteins should yield the desired information about the subcellular localization.

The yeast-based approaches used in this thesis (complementation and magnesium uptake measurements in the  $\Delta mrs2$  mutant strain and protein interaction screening via the mating-based split ubiquitin system) have led to functional data on some AtMRS2 proteins; both approaches have been and are further followed in a diploma and a PhD thesis, respectively. We already know that each member of the AtMRS2 family alone is a functional magnesium transporter, and with the full interaction pattern and the localization data we will be able to determine which AtMRS2 protein(s) is (are) located at which site in the plant. The generation and usage of an *E. coli* strain disrupted for its endogenous magnesium transporters, a project started in this thesis, will offer an easily amenable experimental system to evaluate the cation spectrum transported by each AtMRS2 protein or inhibiting transport, thus completing the functional data on the properties of the AtMRS2 proteins.

Gene inactivation studies complete the picture: although not for every gene a single gene knockout is available, it is already obvious that the AtMRS2 proteins have different importance for the plant: a knockout of AtMRS2-7 leads to a strong morphological phenotype on minimal magnesium concentrations, whereas no phenotype is observed for the further gene knockouts available so far (M. Gebert, unpublished results). Completion of the knockout set via T-DNA insertions or RNAi lines and generation of multiple gene knockouts for those genes showing no detectable phenotype will allow us to correlate the interaction and localization patterns to the true magnesium transporter abilities *in planta*.



## 6. Summary

Magnesium is unique in its chemical properties compared to the other biologically relevant cations. It plays an important role in many biological functions, e.g. as a cofactor for numerous enzymes, as the central atom of the chlorophyll, and as a regulator of key photosynthetic enzymes. The magnesium transport proteins described so far correlate with the unique physicochemical properties of the  $Mg^{2+}$  cation: they form new classes of transport proteins, mostly with no homology to known ion transporters. One class of magnesium transport proteins found in every domain of life are the 2-TM-GxN proteins belonging to the metal ion transporter superfamily. Members of this superfamily are the well-characterised CorA protein of prokaryotes and the yeast ALR1/2 and MRS2/LPE10 proteins. Our group has described the extended MRS2 gene family in the model plant *Arabidopsis thaliana*, comprised of eleven core members and four distantly related members.

Analysis of the members of the AtMRS2 gene family in this thesis was focused both on localization and functional studies. The question of subcellular localization was addressed via cotranslational fusions of the AtMRS2 proteins to the N-terminus of the green fluorescent protein, GFP. Multiple approaches with full length and C-terminally shortened AtMRS2-GFP constructs were conducted, both stably expressed in *Arabidopsis* and transiently expressed in tobacco leaf sections and protoplasts, using two different vector backbones. No positive, convincing results could be obtained, though. Obviously, gene-GFP fusions seem not to be the best suited tool for determination of the subcellular localization of the AtMRS2 proteins; different approaches should be considered in the future.

Characterisation of three members of the AtMRS2 family in the  $\Delta mrs2$  mutant yeast strain could prove their functionality as magnesium transporters; the transport capacities were measured using the mag-fura 2 system in combination with isolated yeast mitochondria. A second approach to determine the properties of three further magnesium transporters through expression in *Xenopus* oocytes and electrophysiological measurements gave no results; *Xenopus* oocytes seem not to be suited for the functional characterisation of the AtMRS2 proteins.

First hints on the oligomerisation properties of the AtMRS2 proteins, which form a pentamer as the functional transporter, could be gained from protein interaction studies in the mating-based split ubiquitin system in yeast. The results obtained so far for a limited number of AtMRS2 proteins indicate that the AtMRS2 proteins can form both homo- and heterooligomers; heterooligomerisation, though, seems to be restricted to certain protein pairings.





## 7. Zusammenfassung

Im Vergleich zu den anderen biologisch relevanten Kationen ist Magnesium einzigartig in seinen chemischen Eigenschaften. Es spielt bei vielen biologischen Funktionen eine wichtige Rolle, z.B. als Cofaktor für zahlreiche Enzyme, als das Zentralatom des Chlorophylls und als ein Regulator von photosynthetischen Schlüsselenzymen. Die bisher beschriebenen  $Mg^{2+}$ -Transportproteine korrelieren mit den einzigartigen physikochemischen Eigenschaften des  $Mg^{2+}$ -Ions: Sie bilden neue Proteinklassen, meist ohne Homologie zu bekannten Ionen-transportern. Eine Klasse von ubiquitären  $Mg^{2+}$ -Transportproteinen sind die 2-TM-GxN-Proteine. Mitglieder dieser Familie sind das gut charakterisierte CorA-Protein der Prokaryoten und die Hefe-ALR1/2- und -MRS2/LPE10-Proteine. Unsere Gruppe hat die erweiterte MRS2-Genfamilie in der Modellpflanze *Arabidopsis thaliana* beschrieben, die aus elf Kern- und vier entfernter verwandten Mitgliedern besteht.

Die Analyse der Mitglieder der AtMRS2-Genfamilie in dieser Arbeit konzentrierte sich auf Lokalisations- und Funktionsstudien. Die Frage der subzellulären Lokalisation wurde durch co-translationale Fusionen der AtMRS2-Proteine an den N-Terminus des grün fluoreszierenden Proteins, GFP, behandelt. Zahlreiche Ansätze mit Vollängen- und C-terminal verkürzten Gen-GFP-Konstrukten wurden durchgeführt, welche sowohl stabil in *Arabidopsis* als auch transient in Tabak-Blättern und -Protoplasten exprimiert wurden; zwei verschiedene Vektoren wurden verwendet. Dennoch konnten keine positiven, überzeugenden Resultate erzielt werden. Offensichtlich sind Gen-GFP-Fusionen nicht das am besten geeignete Mittel zur Bestimmung der subzellulären Lokalisation der AtMRS2-Proteine; für die Zukunft sollten andere Ansätze erwogen werden.

Charakterisierung von drei Mitgliedern der Genfamilie im  $\Delta mrs2$ -Hefestamm konnte deren Funktionalität als Magnesiumtransporter bestätigen; mittels des mag-fura2-Systems konnten die Transportkapazitäten gemessen werden. Ein zweiter Ansatz zur Bestimmung der Eigenschaften von drei weiteren Magnesiumtransportern durch Expression in *Xenopus*-Oocyten und elektrophysiologische Messungen blieb ohne Ergebnis; *Xenopus*-Oocyten scheinen für die funktionale Charakterisierung der AtMRS2-Proteine nicht geeignet zu sein.

Erste Hinweise auf die Oligomerisierungseigenschaften der AtMRS2-Proteine, deren funktionale Form ein Pentamer ist, konnten durch Protein-Interaktionsstudien im „mating-based split ubiquitin system“ in der Hefe gewonnen werden. Die bisher für eine begrenzte Anzahl der AtMRS2-Proteine erhaltenen Resultate deuten an, dass sowohl Homo- als auch Heterooligomere gebildet werden können; Heterooligomerisierung scheint allerdings auf einige Proteinpaarungen beschränkt zu sein.



## 8. Appendix

### 8.1 Oligonucleotide sequences

#### 8.1.1 Full length GFP constructs

#	name	sequence (5' → 3')	amplification of
1	gate2-1up	attB1 + GAATTTT <b>T</b> GCAACA <b>A</b> ATGTCTGAG	coding sequence of
2	gate2-1down	attB2 + ATAGAGGCATGAGTCTTCTGTA	AtMRS2-1
33	gate2-2up	attB1 + AGTTTTT <b>T</b> GAAAGAC <b>A</b> TGGCGCAA	coding sequence of
34	gate2-2down	attB2 + AAGATCCCA <b>A</b> AGTCCTTGTGA	AtMRS2-2
3	gate2-3up	attB1 + AACAATCATATGCG <b>A</b> TGAGAGGA	coding sequence of
4	gate2-3down	attB2 + ATTCAAGAAGGCGCTTGTACTT	AtMRS2-3
75	gate2-4up	attB1 + TTGTTTCGTGGCTGGAATCC <b>A</b> T <b>G</b>	coding sequence of
6	gate2-4down	attB2 + AGCCTAGCAGCTTCTTCCACCT	AtMRS2-4
7	gate2-5up	attB1 + ATTGTGCAAAC <b>A</b> TGGGAGAACAA	coding sequence of
8	gate2-5down	attB2 + AGAGAGGGGAATACTTTCTTGTG	AtMRS2-5
15	gate2-6up	attB1 + CTGCAGGTAAGTCA <b>A</b> TGGGATCA	coding sequence of
10	gate2-6down	attB2 + CAAGTAGCTTCTTCCACTTGGC	AtMRS2-6
35	gate2-7up	attB1 + GTGAAGAATCGGAG <b>A</b> TGTCACCT	coding sequence of
36	gate2-7down	attB2 + AGGTAAAGGTGTTCCATTCTGG	AtMRS2-7
76	gate2-8up	attB1 + AAGAGTCGAAG <b>A</b> TGTTGCCTAAC	coding sequence of
77	gate2-8down	attB2 + CCCATTTGAACATATGTTTTTTGAt	AtMRS2-8
78	gate2-9up	attB1 + ATCAGACGGAG <b>A</b> TGTCGATTGAT	coding sequence of
79	gate2-9down	attB2 + CCCATTTGAACATATGTTCTTTGGT	AtMRS2-9
11	gate2-10up	attB1 + GGAGATTGGCAACA <b>A</b> TGTCTGAA	coding sequence of
12	gate2-10down	attB2 + ACAGAGGCATGAGTCTTCTACG	AtMRS2-10
13	gate2-11up	attB1 + TAATTTT <b>T</b> GCCAACA <b>A</b> TGGCGTTA	coding sequence of
14	gate2-11down	attB2 + AAAAGATTTT <b>T</b> GCGTCTACTGAG	AtMRS2-11
	attB1	GGGGACAAGTTTGTACAAAAAAGCAGGCT	Gateway™
	attB2	GGGGACCACTTTGTACAAGAAAGCTGGGT	attachment sites

The start codons of the respective genes are printed in **bold**.

**8.1.2 C-terminally shortened GFP constructs**

#	name	sequence (5' → 3')	amplification of
53	2-1gfp-gus up	attB1 + AAGGAAGAGGAGCAGGTGGACAG	promoter + 1 <sup>st</sup> exon
54	2-1gfp-gus down	attB2 + GGGAATCGAGAAACGTACAAGCAGC	of AtMRS2-1
55	2-2gfp-gus up	attB1 + GCTTAAGCTTTTGCAAGTTGGA	promoter + 1 <sup>st</sup> exon
56	2-2gfp-gus down	attB2 + CCAAATTGAGAACAATGGCTCT	of AtMRS2-2
57	2-3gfp-gus up	attB1 + CGACTCTTCCTTGGGAATTCTCC	promoter + 1 <sup>st</sup> exon
58	2-3gfp-gus down	attB2 + GAGGTTTAGTGCCGTGATGGTG	of AtMRS2-3
59	2-4gfp-gus up	attB1 + CAAAACCTTGCTCAAAGTTTTGCC	promoter + 1 <sup>st</sup> exon
60	2-4gfp-gus down	attB2 + GAATGTTAGAGGAGTGAGAGAA	of AtMRS2-4
61	2-5gfp-gus up	attB1 + GCAATCATCAATGCATCATTTTA	promoter + 1 <sup>st</sup> exon
62	2-5gfp-gus down	attB2 + TAACATTTAGGTTGTGGTTTGA	of AtMRS2-5
63	2-6gfp-gus up	attB1 + ATATATGCACCAAGATTCAAGAA	promoter + 1 <sup>st</sup> exon
64	2-6gfp-gus down	attB2 + CTAGAATTTTAGAAGAGTGCGA	of AtMRS2-6
65	2-7gfp-gus up	attB1 + TAGGGACTTATTCGGTGAATTTA	promoter + 1 <sup>st</sup> exon
66	2-7gfp-gus down	attB2 + CTAAGTTAAGAACAATGGCTCT	of AtMRS2-7
67	2-8gfp-gus up	attB1 + AAAAAAATGGTGGTTCAAGCGG	promoter + 1 <sup>st</sup> exon
68	2-8gfp-gus down	attB2 + CCTCTAAGTTAAGAACAATGGC	of AtMRS2-8
69	2-9gfp-gus up	attB1 + CGATGGAAGGAATTGATACTCGT	promoter + 1 <sup>st</sup> exon
70	2-9gfp-gus down	attB2 + CTAAGTTCAGCACAATGGCTCC	of AtMRS2-9
71	2-10gfp-gus up	attB1 + GCTTCTAAGAGCTCATTAACACC	promoter + 1 <sup>st</sup> exon
72	2-10gfp-gus down	attB2 + GGGAATCAAGGAAGGTACAAGC	of AtMRS2-10
73	2-11gfp-gus up	attB1 + TCCTTTGCCCTTATTTCTCTTCT	promoter + 1 <sup>st</sup> exon
209	2-11gfp-gus down	attB2 + CATAAACCGGTTACGAATTC	of AtMRS2-11
	attB1	GGGGACAAGTTTGTACAAAAAAGCAGGCT	Gateway™
	attB2	GGGGACCACTTTGTACAAGAAAGCTGGGT	attachment sites

### 8.1.3 Yeast complementation and mbSUS constructs

#	name	sequence (5' → 3')	amplification of
170	heproup	GATCGACCAGG <u>GAGCTCG</u> TATACCTAC	yeast MRS2
171	heprodo	GGGAAAAGGGAAATGTTCA	promoter + aa 1-94
267	YEP 2-3 up	GGCGCGTGATCTTAGGATTCTCGAT	AtMRS2-3
268	YEP 2-3 down	GACTCTAG <u>AGACTC</u> ATTCAAGAAGGCG	aa 74 - stop
172	YEP 2-4 up	TAGGGATTTGAGGATACTTGGCC	AtMRS2-4
173	YEP 2-4 down	GTAATCTAG <u>AGGGAGATT</u> TATGAGC	aa 92 - stop
176	pVT 2-4 up	GTGTCTAG <u>AAATCCAT</u> GGGGAA	coding sequence of
177	pVT 2-4 down	GTAAGAGAGCTCGAGATTATGAG	AtMRS2-4
174	YEP 2-6 up	TAAGGATTTAAGAACTGCCTTCTC	AtMRS2-6
175	YEP 2-6 down	ATGTGTCTAG <u>ACTCTTAT</u> CAGTCA	aa 82 - stop
226	pVT 2-6 up	GGTCTAG <u>AAATGGGATCA</u> CTTCGCCGTAGTA	coding sequence of
227	pVT 2-6 down	GTGAGCTCTCAGTCAAGTAGCTTCTCCAC	AtMRS2-6
254	2-6 cDNA miup	TCGGAAGGATGGTCTGAAAATAT	cDNA product in
255	2-6 cDNA mido	AGAAGACCTCGAATGCAATCTCT	two halves
186	2-1 SplitU up	B1 + <b>ATGTCTGAGCTAAAAGAGCGC</b>	coding sequence of
187	2-1 SplitU down	B2 + TAGAGGCATGAGTCTTCTGTA	AtMRS2-1
188	2-10 SplitU up	B1 + <b>ATGTCTGAACTCAAAGAGCGT</b>	coding sequence of
189	2-10 SplitU down	B2 + CAGAGGCATGAGTCTTCTA	AtMRS2-10
240	2-1AMNmiup	TTGCTGGGATCTTTGCGATGA	mutagenesis of
241	2-1AMNmido	GTCTATCTCAAAGTTCATCGCAA	GMN motif
246	2-1 SplitU up -N	B1 + ACTATCCTAGGCCGAGAGAA	deletion of aa 1-93
247	2-2 SplitU up	B1 + <b>ATGGCGCAAAACGGGTA</b> CTTG	coding sequence of
248	2-2 SplitU down	B2 + AGATCCCACAAGTCCTTTGTACC	AtMRS2-2
249	2-7 SplitU up	B1 + <b>ATGTCACCTGACGGAGA</b> ACTT	coding sequence of
281	2-7 SplitU down	B2 + AGATCCGATGAGTCCTCTAAAC	AtMRS2-7
	B1	ACAAGTTTGTACAAAAAAGCAGGCTCTCCAACCACC	att sites for yeast
	B2	TCCGCCACCACCAACCACTTTGTACAAGAAAGCTGGGTA	recombination

The start and stop codons of the respective coding sequences are printed in **bold**.

Restriction enzyme recognition sequences are underlined.

### 8.1.4 *Xenopus* constructs and sequencing primers

#	name	sequence (5' → 3')	amplification of
80	Xenopus2-1up	TATCTGGATCCTTGCAACAAT <b>GT</b> CTGAGCTAA	coding sequence of
81	Xenopus2-1down	ATTCTAGATCTTATAGAGGCATGAGTCTTCTG	AtMRS2-1
88	Xenopus2-2up	TTTTTCCCGGGTTTGAAAGACAT <b>GG</b> CGCAAAA	coding sequence of
83	Xenopus2-2down	ATGAATTCCCATCAAGATCCCAAGTCCTTT	AtMRS2-2
84	Xenopus2-3up	AATCCCGGGTCACAACAATCATAAGCAAT <b>GAG</b>	coding sequence of
85	Xenopus2-3down	ATTCTAGAGACTCATTCAAGAAGGCGCTTGTA	AtMRS2-3
86	Xenopus2-5up	AAAGGATCCAGCAAACAT <b>GGG</b> GAGAACAATA	coding sequence of
89	Xenopus2-5down	CAGAATTCTTCAGAGAGGGAATACTTTCTTGTG	AtMRS2-5
180	2-1 V5 up	CGCCGGGTACCAACAAT <b>GT</b> CTGAGCTAAAA	coding sequence of
181	2-1 V5 down	TAGCGGCCGCTAATTAGAGGCATGAGTCTT	AtMRS2-1
182	2-3 V5 up	TACAAGGTACCAGCGAT <b>GAG</b> AGGAGCTAGA	coding sequence of
183	2-3 V5 down	TAGCGGCCGCTAATTTCAAGAAGGCGCTTG	AtMRS2-3
184	2-5 V5 up	CGCACGGTACCAAACAT <b>GGG</b> GAGAACAATA	coding sequence of
185	2-5 V5 down	TAGCGGCCGCTAATGAGAGGGAATACTTTC	AtMRS2-5
224	2-6 V5 up	GCTGCAGGTACCTCAAT <b>GGG</b> ATCACTTCGC	coding sequence of
225	2-6 V5 down	GAGCGGCCGCCACTGTCAAGTAGCTTCTT	AtMRS2-6
242	2-5AMNmiup	TGTAACCGCTGTCTTCGCGAT	mutagenesis of
243	2-5AMNmido	GAGTCTTGCAAATTCATCGCGAA	GMN motif
244	2-1 pDK148 down	TAGCGGCCGCTAATTTATAGAGGCATGAGT	for usage with
245	2-5 pDK148 down	TAGCGGCCGCTAATTCAGAGAGGGAATA	“Xenopus” primers
52	gfp-pK7FWG2	CGGTGGTGCAGATGAACTTC	
130	35S-Prom. pK7FWG2	TACGCGGCAGGTCTCATCAA	
131	35S-Ter. pK7FWG2	GAGACTGGTGATTTTTGCGG	
132	KanR-pK7FWG2	GCTGATAGTGACCTTAGGCG	primers used for
133	LB-pK7FWG2	CAGCAACGCTCTGTCATCGT	sequencing,
134	RB-pK7FWG2	CTCTTAGGTTTACCCGCCAA	binding in vector
	PBJS	CACTGACGTAAGGGATGACG	backbones
358	3' GFP pK7FWG2	GACTCTAGCATGGCCGCG	
406	pMDC202 3' GFP	CGGCAACAGGATTCAATCTTAA	
407	pMDC202 GFP	TTCCCTTAAGCTCGATCCTGTT	
190	Oligo (dT)23 VN	TTTTTTTTTTTTTTTTTTTTTTTTTVN	for RT-PCR

The start and stop codons of the respective coding sequences are printed in **bold**.

Restriction enzyme recognition sequences are underlined.

## 8.2 Sequences of exemplary constructs

### 8.2.1 A destination clone of the full length gene-GFP constructs: AtMRS2-10c-GFP

in vitro AtMRS2-10c-GFP (1) 1 10 20 30 40 50 60 70 80 90  
 in silico AtMRS2-10c-GFP (1) GACTAGAGCCAAGTCTGATCTCCTTTGCCCCGGAGATCACCATGGACGACTTCTCTATCTCTACGATCTAGGAAGAAAGTTCGACGGAGA  
 Promoter Prokaryotic(1..1028): 35S promoter

in vitro AtMRS2-10c-GFP (91) 91 100 110 120 130 140 150 160 170 180  
 in silico AtMRS2-10c-GFP (91) AGGTGACGATACCATGTTCAACCACCGATAATGAGAAGATTAGCCCTTCAATTCAGAAAGAAATGCTGACCCACAGATGGTTAGAGAGGC  
 Promoter Prokaryotic(1..1028): 35S promoter

in vitro AtMRS2-10c-GFP (181) 181 190 200 210 220 230 240 250 260 270  
 in silico AtMRS2-10c-GFP (181) CTACGCGGCGAGTCTCATCAAGACGATCTACCCGAGTAATAATCTCCAGGAGATCAAATACCTTCCCAAGAAGGTTAAAGATGCAGTCAA  
 Promoter Prokaryotic(1..1028): 35S promoter

in vitro AtMRS2-10c-GFP (271) 271 280 290 300 310 320 330 340 350 360  
 in silico AtMRS2-10c-GFP (271) AAGATTGAGGACTAAGTGCATCAAGAACACAGAGAAGATATATTTCTCAAGATCAGAAGTACTATCCAGTATGGACGATCAAGGCTT  
 Promoter Prokaryotic(1..1028): 35S promoter

in vitro AtMRS2-10c-GFP (361) 361 370 380 390 400 410 420 430 440 450  
 in silico AtMRS2-10c-GFP (361) GCTTCATAAACCAAGGCAAGTAATAGAGATTGGAGTCTCTAAGAAAGTAGTTCCTACTGAATCAAAGGCCATGGAGTCAAAAATTCAGAT  
 Promoter Prokaryotic(1..1028): 35S promoter

in vitro AtMRS2-10c-GFP (451) 451 460 470 480 490 500 510 520 530 540  
 in silico AtMRS2-10c-GFP (451) CGAGGATCTAACAAGACTGCGGTGAAGACTGGCGAAGCAGTTCATACAGAGTCTTTACGACTCAATGACAAGAAGAAATCTTCGTCAA  
 Promoter Prokaryotic(1..1028): 35S promoter

in vitro AtMRS2-10c-GFP (541) 541 550 560 570 580 590 600 610 620 630  
 in silico AtMRS2-10c-GFP (541) CATGGTGGAGCAGACACTCTCGTCTACTCCAAGAATATCAAAGATACAGTCTCAGAAGACCAAAGGCTATTGAGACTTTTCAACAAAG  
 Promoter Prokaryotic(1..1028): 35S promoter

in vitro AtMRS2-10c-GFP (631) 631 640 650 660 670 680 690 700 710 720  
 in silico AtMRS2-10c-GFP (631) GGTAAATATCGGGAACCTCCTCGGATTCCATTGCCAGCTATCTGTCACTTCATCAAAGGACAGTAGAAAAGGAAGGTGGCACCTACAA  
 Promoter Prokaryotic(1..1028): 35S promoter

in vitro AtMRS2-10c-GFP (721) 721 730 740 750 760 770 780 790 800 810  
 in silico AtMRS2-10c-GFP (721) ATGCCATCATTCGATAAAGGAAAGGCTATCGTTCAAGATGCCTCTGCCGACAGTGGTCCCAAGATGGACCCCAACCCACGAGGAGCAT  
 Promoter Prokaryotic(1..1028): 35S promoter

in vitro AtMRS2-10c-GFP (811) 811 820 830 840 850 860 870 880 890 900  
 in silico AtMRS2-10c-GFP (811) CGTGGAAAAGAAGCGTCCCAACCACGCTCTCAAAGCAAGTGGATTGATGTGATATCTCCACTGACGTAAGGGATGACGCACAATCCCA  
 Promoter Prokaryotic(1..1028): 35S promoter

in vitro AtMRS2-10c-GFP (901) 901 910 920 930 940 950 960 970 980 990  
 in silico AtMRS2-10c-GFP (901) CTATCCTTCGCAAGACCTTCCCTCTATAAAGGAAGTTCATTTCATTTGGAGAGGACTCCGGTATTTTACAACAATACCACAACAAAAC  
 Promoter Prokaryotic(1..1028): 35S promoter

in vitro AtMRS2-10c-GFP (991) 991 1000 1010 1020 1030 1040 1050 1060 1070 1080  
 in silico AtMRS2-10c-GFP (991) AAACAACAACAACATTACAATTTACTATTCTAGTCGACCTGCAGGGCGGCCACTAGTGATATC-----ACAAGTTTGTACAAAAAAG  
 Promoter Prokaryotic(1..1028): 35S promoter Misc. Recombination(1063..1083): attB1

in vitro AtMRS2-10c-GFP (1081) 1081 1090 1100 1110 1120 1130 1140 1150 1160 1170  
 in silico AtMRS2-10c-GFP (1081) CAGGCTGGAGATTGGCAACAATGTCTGAACCTCAAAGAGCGTTTGCTTCCTCCAAGACCTGCTTCGGCTATTAACCTTAGAGGTGATGCAG  
 Misc. Recombination(1063..1083): attB1 CDS(1087..2430): AtMRS2-10 cDNA  
 Primer Binding Site(1087..1109): gate2-10up

in vitro AtMRS2-10c-GFP (1171) 1171 1180 1190 1200 1210 1220 1230 1240 1250 1260  
 in silico AtMRS2-10c-GFP (1171) GCTCTCGTCCCTTCTCCCTCAGGGAGACAACCACTCCTTGGAGTTGATGTTTTGGGICTCAAGAAGCGTGGACAAGGCCCTTAAGTCGTGGGA  
 CDS(1087..2430): AtMRS2-10 cDNA

in vitro AtMRS2-10c-GFP (1261) 1261 1270 1280 1290 1300 1310 1320 1330 1340 1350  
 in silico AtMRS2-10c-GFP (1261) TTCGGTTGATACTTCTGCCAATCTCAGGTCATTGAGGTTGATAAGTTCACTATGATGCGTAGATGTGATTTACCAGCACGGGATTTCA  
 CDS(1087..2430): AtMRS2-10 cDNA

(1351) 1351 1360 1370 1380 1390 1400 1410 1420 1430 1440  
 in vitro AtMRS2-10c-GFP (429) GGCTGCTTGATCCCTTTGTTTGTGTATCCGTCACACTATTCCTTGGTAGAGAGAAGGCTATTGTTGTTAACTTAGAGCAGATCCGTTGTATTA  
 in silico AtMRS2-10c-GFP (1351) GGCTGCTTGATCCCTTTGTTTGTGTATCCGTCACACTATTCCTTGGTAGAGAGAAGGCTATTGTTGTTAACTTAGAGCAGATCCGTTGTATTA

CDS(1087..2430): AtMRS2-10 cDNA

(1441) 1441 1450 1460 1470 1480 1490 1500 1510 1520 1530  
 in vitro AtMRS2-10c-GFP (519) TTACTGCGGATGAGGTTTTGCTCTTGAATCCCTTGACAACATATGTCCTTCGCTATGTTGTTGAGCTGCAGCAGAGACTAAAGGCAAGTT  
 in silico AtMRS2-10c-GFP (1441) TTACTGCGGATGAGGTTTTGCTCTTGAATCCCTTGACAACATATGTCCTTCGCTATGTTGTTGAGCTGCAGCAGAGACTAAAGGCAAGTT

CDS(1087..2430): AtMRS2-10 cDNA

(1531) 1531 1540 1550 1560 1570 1580 1590 1600 1610 1620  
 in vitro AtMRS2-10c-GFP (609) CTGTTACTGAGGTTTGAATCAGGACAGTCTCGAATTGAGCAGGAGGAGTAGGAGTTTAGACAATGTGCTTCAGAACTCATCCCCTG  
 in silico AtMRS2-10c-GFP (1531) CTGTTACTGAGGTTTGAATCAGGACAGTCTCGAATTGAGCAGGAGGAGTAGGAGTTTAGACAATGTGCTTCAGAACTCATCCCCTG

CDS(1087..2430): AtMRS2-10 cDNA

(1621) 1621 1630 1640 1650 1660 1670 1680 1690 1700 1710  
 in vitro AtMRS2-10c-GFP (699) ATTATTTACCTTTCGAGTTCAGGGCTCTTGAAGTTGCACTTGAAGCTGCTTGTACCTTCCTTGATCCCAGGCTTCAGAGTTAGAGATTG  
 in silico AtMRS2-10c-GFP (1621) ATTATTTACCTTTCGAGTTCAGGGCTCTTGAAGTTGCACTTGAAGCTGCTTGTACCTTCCTTGATCCCAGGCTTCAGAGTTAGAGATTG

CDS(1087..2430): AtMRS2-10 cDNA

(1711) 1711 1720 1730 1740 1750 1760 1770 1780 1790 1800  
 in vitro AtMRS2-10c-GFP (789) AGGCATACCCATTATTGGATGAGCTTACCTCAAAGATCAGTACTCTAAACTTGGAGCGTGCTCGTAGACTAAAGAGCAGACTTTGATGAT  
 in silico AtMRS2-10c-GFP (1711) AGGCATACCCATTATTGGATGAGCTTACCTCAAAGATCAGTACTCTAAACTTGGAGCGTGCTCGTAGACTAAAGAGCAGACTTTGATGAT

CDS(1087..2430): AtMRS2-10 cDNA

(1801) 1801 1810 1820 1830 1840 1850 1860 1870 1880 1890  
 in vitro AtMRS2-10c-GFP (879) TGACGAGACGAGTTTCAAGGTTTCGGGATGAGATTGAACAGCTAATGGACGATGATGGGGATATGGCAGAAATGTATCTAACAGAGAAGA  
 in silico AtMRS2-10c-GFP (1801) TGACGAGACGAGTTTCAAGGTTTCGGGATGAGATTGAACAGCTAATGGACGATGATGGGGATATGGCAGAAATGTATCTAACAGAGAAGA

CDS(1087..2430): AtMRS2-10 cDNA

(1891) 1891 1900 1910 1920 1930 1940 1950 1960 1970 1980  
 in vitro AtMRS2-10c-GFP (969) AGAAGAGAATGGAAGGATCTTTATATGGTGATCAATCTTACCTGTTTATCGAACAAATGATTTTCTCTGCTGGCCAGTTTCTC  
 in silico AtMRS2-10c-GFP (1891) AGAAGAGAATGGAAGGATCTTTATATGGTGATCAATCTTACCTGTTTATCGAACAAATGATTTTCTCTGCTGGCCAGTTTCTC

CDS(1087..2430): AtMRS2-10 cDNA

(1981) 1981 1990 2000 2010 2020 2030 2040 2050 2060 2070  
 in vitro AtMRS2-10c-GFP (1059) CTGTTTCTTCTCCTCCTGAGTCCCGTAGACTTGAAGAAAGCTTGGACATTGTAAGGAGCCGGCATGACAGTGTAGGAGCTCAGAAGACG  
 in silico AtMRS2-10c-GFP (1981) CTGTTTCTTCTCCTCCTGAGTCCCGTAGACTTGAAGAAAGCTTGGACATTGTAAGGAGCCGGCATGACAGTGTAGGAGCTCAGAAGACG

CDS(1087..2430): AtMRS2-10 cDNA

(2071) 2071 2080 2090 2100 2110 2120 2130 2140 2150 2160  
 in vitro AtMRS2-10c-GFP (1149) CAACCGAGAATATAGAGGAGCTAGAGATGTTGCTGGAAGCATACTTGTGTCATTGACAGCACTCTCAACAAGCTAACCTCGTTAAAGG  
 in silico AtMRS2-10c-GFP (2071) CAACCGAGAATATAGAGGAGCTAGAGATGTTGCTGGAAGCATACTTGTGTCATTGACAGCACTCTCAACAAGCTAACCTCGTTAAAGG

CDS(1087..2430): AtMRS2-10 cDNA

(2161) 2161 2170 2180 2190 2200 2210 2220 2230 2240 2250  
 in vitro AtMRS2-10c-GFP (1239) AGTACATCGATGATACCGAAGATTTCAATCAACATTCAAATGGATAACGTCAGGAATCAGCTGATCCAAATCGAGCTGCTGCTAACTACTG  
 in silico AtMRS2-10c-GFP (2161) AGTACATCGATGATACCGAAGATTTCAATCAACATTCAAATGGATAACGTCAGGAATCAGCTGATCCAAATCGAGCTGCTGCTAACTACTG

CDS(1087..2430): AtMRS2-10 cDNA

(2251) 2251 2260 2270 2280 2290 2300 2310 2320 2330 2340  
 in vitro AtMRS2-10c-GFP (1329) CCACATTCGTTGTAGCCATCTTCGGGGTTGTAGCCGGGATCTTTGGGATGAAATTTGAGATAGACTTCTTTGAAAAGCCTGGTGTCTTCA  
 in silico AtMRS2-10c-GFP (2251) CCACATTCGTTGTAGCCATCTTCGGGGTTGTAGCCGGGATCTTTGGGATGAAATTTGAGATAGACTTCTTTGAAAAGCCTGGTGTCTTCA

CDS(1087..2430): AtMRS2-10 cDNA

(2341) 2341 2350 2360 2370 2380 2390 2400 2410 2420 2430  
 in vitro AtMRS2-10c-GFP (1419) AATGGGTTTTAGCCATTACTGGAGTGTGTGGCCCTTGTGATTTTGGCATTCCCTGGTACACAAAACCTAGAAGACTCATGCCCTCTGT  
 in silico AtMRS2-10c-GFP (2341) AATGGGTTTTAGCCATTACTGGAGTGTGTGGCCCTTGTGATTTTGGCATTCCCTGGTACACAAAACCTAGAAGACTCATGCCCTCTGT

CDS(1087..2430): AtMRS2-10 cDNA

Primer Binding Site(2409..2430): gate2-10down

(2431) 2431 2440 2450 2460 2470 2480 2490 2500 2510 2520  
 in vitro AtMRS2-10c-GFP (1509) ACCCAGCTTTCCTGTACAAAGTGGTGATATCAATGGTGAGCAAGGGCGAGGAGCTGTTCCACCGGGGTTGGTCCCCATCCTGGTCGAGCTGG  
 in silico AtMRS2-10c-GFP (2431) ACCCAGCTTTCCTGTGTACAAAGTGGTGATATCAATGGTGAGCAAGGGCGAGGAGCTGTTCCACCGGGGTTGGTCCCCATCCTGGTCGAGCTGG

Misc. Recombination(2434..2454): attB2  
 Misc. Feature(2463..3182): Eglp  
 Primer Binding Site(2409..2430): gate2-10down

(2521) 2521 2530 2540 2550 2560 2570 2580 2590 2600 2610  
 in vitro AtMRS2-10c-GFP (1599) ACGGCGACGTAACGGCCACAAAGTTTCAGCGTGTCCGGCGAGGGCGAGGGCGATGCCACCTACGGCAAGCT-----  
 in silico AtMRS2-10c-GFP (2521) ACGGCGACGTAACGGCCACAAAGTTTCAGCGTGTCCGGCGAGGGCGAGGGCGATGCCACCTACGGCAAGCTGACCCCTGAAGTTCATCTGCA

Misc. Feature(2463..3182): Eglp

(2611) 2611 2620 2630 2640 2650 2660 2670 2680 2690 2700  
 in vitro AtMRS2-10c-GFP (1669) -----  
 in silico AtMRS2-10c-GFP (2611) CCACCGGCAAGCTGCCCTGGCCCTGGCCCAACCTCGTGACCACCTGACCTACGGGTGCAGTGCTTACGGCGTACCCCGACCCACATGA

Misc. Feature(2463..3182): Eglp



```

(2701) 2701      2710      2720      2730      2740      2750      2760      2770      2780      2790
in vitro AtMRS2-10c-GFP (1669) -----
in silico AtMRS2-10c-GFP (2701) AGCAGCACGACTTCTTCAAGTCCGCCATGCCCGAAGGCTACGTCAGGAGCGCACCATCTTCTTCAAGGACGACGGCAACTACAAGACCC
Misc. Feature(2463..3182): Eglp

(2791) 2791      2800      2810      2820      2830      2840      2850      2860      2870      2880
in vitro AtMRS2-10c-GFP (1669) -----
in silico AtMRS2-10c-GFP (2791) GCGCCGAGGTGAAGTTCGAGGGCGACACCCTGGTGAACCGCATCGAGCTGAAGGCATCGACTTCAAGGAGGACGGCAACATCCTGGGGC
Misc. Feature(2463..3182): Eglp

(2881) 2881      2890      2900      2910      2920      2930      2940      2950      2960      2970
in vitro AtMRS2-10c-GFP (1669) -----
in silico AtMRS2-10c-GFP (2881) ACAAGCTGGAGTACAACCTACAACAGCCCAACCGTCTATATCATGGCCGACAAGCAGAAAGACGGCATCAAGGTGAACCTCAAGATCCGGC
Misc. Feature(2463..3182): Eglp

(2971) 2971      2980      2990      3000      3010      3020      3030      3040      3050      3060
in vitro AtMRS2-10c-GFP (1669) -----
in silico AtMRS2-10c-GFP (2971) ACAACATCGAGGACGGCAGCGTGCAGCTCGCCGACCACTACCGAGCAACACCCCATCGGCGACGGCCCGTGTCTGCTGCCGACAACC
Misc. Feature(2463..3182): Eglp

(3061) 3061      3070      3080      3090      3100      3110      3120      3130      3140      3150
in vitro AtMRS2-10c-GFP (1669) -----
in silico AtMRS2-10c-GFP (3061) ACTACCTGAGCACCAGTCCGCCCTGAGCAAAGACCCCAACGAGAAAGCGCGATCACATGGTCTGCTGGAGTTCGTGACCGCCCGGGGA
Misc. Feature(2463..3182): Eglp

(3151) 3151      3160      3170      3182
in vitro AtMRS2-10c-GFP (1669) -----
in silico AtMRS2-10c-GFP (3151) TCACTCTCGGCATGGACGAGCTGTACAAGTAA
Misc. Feature(2463..3182): Eglp

```

The sequence of the *in vitro* full length AtMRS2-10c-GFP destination clone received after sequencing with the oligonucleotides PBJs and gfp-pK7FWG2 (cf. Figure 3.1.1 on page 44 for primer binding sites) was aligned with the sequence of the destination clone generated *in silico* via Vector NTI (Invitrogen Inc.). This *in silico* sequence was annotated to identify the major elements of the sequence: the 35S promoter, attachment site B1, AtMRS2-10c coding sequence, attachment site B2, and the GFP coding sequence. The primer binding sites used to amplify the original PCR product are also given. The AtMRS2-10c coding sequence starts at position 1101; the GFP coding sequence starts 1362 bp or 454 amino acids downstream at position 2463 in frame with the AtMRS2-10c coding sequence. 443 of the 454 amino acids are comprised by the AtMRS2-10 protein, the further eleven amino acids constitute the linker region between the two coding sequences (cf. section 3.1.1 on page 40 for a description of the linker region).

There are some deviations of the *in vitro* sequence from the *in silico* sequence. The two codons missing upstream of the recombination region *in vitro* are most likely due to incorrect vector sequences given by the constructors (Karimi et al. (2002); see <http://www.psb.rug.ac.be/gateway/> for their homepage). The vectors are constantly getting re-sequenced and the correct sequences published.

Within the coding region of AtMRS2-10 cDNA there are three sites with base pair exchanges between the database entry NM\_106738 and the *in vitro* sequence changing the amino acid sequence in the following way:

- position 1349: Leu to Phe (TTC instead of TTA)
- position 2403: Tyr to His (CAC instead of TAC)
- position 2410: Arg to Pro (CCT instead of CGT).

These exchanges can be explained either by incorrect integration of nucleotides by the DNA polymerase or by differences in the DNA sequence existing between ecotypes Col-0 (the sequenced one) and Col-5 used here for amplification of the PCR products.

## 8.2.2 A destination clone of the C-terminally shortened GFP constructs: AtMRS2-3short-GFP

	(1)	1	10	20	30	40	50	60	70	89	
in vitro AtMRS2-3short-GFP	(1)	-----									
in silico AtMRS2-3short-GFP	(1)	GACTAGAGCC AAGCTGATCTCCITTTGCCCCGGAGATCACCATGGACGACTTTCTCTATCTCTACGATCTAGGAAGAAGTTTCGACGGAG									
		Promoter Prokaryotic(1..1028): 35S promoter									
	(90)	90	100	110	120	130	140	150	160	178	
in vitro AtMRS2-3short-GFP	(1)	-----									
in silico AtMRS2-3short-GFP	(90)	AAGGTGACGATACCATGTTCCACCACCGATAATGAGAAGATTAGCCCTTTC AATTTTCAGAAAAGATGCTGACCCACAGATGGTTAGAGAG									
		Promoter Prokaryotic(1..1028): 35S promoter									
	(179)	179	190	200	210	220	230	240	250	267	
in vitro AtMRS2-3short-GFP	(1)	-----									
in silico AtMRS2-3short-GFP	(179)	GCCTACGCGG CAGGCTCATCAAGACGATCTACCCGAGTAAATATCTCCAGGAGATCAAAATACCTTCCCAAGAAGGTTAAAGATGCAGT									
		Promoter Prokaryotic(1..1028): 35S promoter									
	(268)	268	280	290	300	310	320	330	340	356	
in vitro AtMRS2-3short-GFP	(32)	-----									
in silico AtMRS2-3short-GFP	(268)	CAAAAGATTTCAGGACTAATGTCATCAAGAACACAGAGAAAAGATATATTTCTCAAGATCAGAACTACTATTCAGTATGGACGATTC AAG									
		Promoter Prokaryotic(1..1028): 35S promoter									
	(357)	357	370	380	390	400	410	420	430	445	
in vitro AtMRS2-3short-GFP	(121)	-----									
in silico AtMRS2-3short-GFP	(357)	GCTTGCTTCATAAACC AAGGCCAAGTAATAGAGATTGGAGTCTCTAAGAAAAGTAGTTCCTACTGAATCAAAGGCCATGGAGTCAAAAAT									
		Promoter Prokaryotic(1..1028): 35S promoter									
	(446)	446	460	470	480	490	500	510	520	534	
in vitro AtMRS2-3short-GFP	(210)	-----									
in silico AtMRS2-3short-GFP	(446)	CAGATCGAGGATCTAACAGAACTCGCCGTGAAGACTGGCGAACAGTTCATACAGAGTCTTTACGACTCAATGACAAAGAAAGAAAATCTT									
		Promoter Prokaryotic(1..1028): 35S promoter									
	(535)	535	540	550	560	570	580	590	600	610	623
in vitro AtMRS2-3short-GFP	(299)	-----									
in silico AtMRS2-3short-GFP	(535)	CGTCAACATGGTGGAGCAGCAGACTCTCGTCTACTCCAAGAATATCAAAGATACAGTCTCAGAAAGCCAAAGGGCTATTGAGACTTTTC									
		Promoter Prokaryotic(1..1028): 35S promoter									
	(624)	624	630	640	650	660	670	680	690	700	712
in vitro AtMRS2-3short-GFP	(388)	-----									
in silico AtMRS2-3short-GFP	(624)	AACAAAGGGTAATATCGGGAAACCTCCTCGGATTCCATTCGCCAGCTATCTGTACCTCATCAAAGGACAGTAGAAAAGGAAGGTGGC									
		Promoter Prokaryotic(1..1028): 35S promoter									
	(713)	713	720	730	740	750	760	770	780	790	801
in vitro AtMRS2-3short-GFP	(477)	-----									
in silico AtMRS2-3short-GFP	(713)	ACCTACAAATGCCATCATTCGGATAAAGGAAAGGCTATCGTTCAAAGATGCCCTGCGGACAGTGGTCCAAAGATGGACCCCAACCCAC									
		Promoter Prokaryotic(1..1028): 35S promoter									
	(802)	802	810	820	830	840	850	860	870	880	890
in vitro AtMRS2-3short-GFP	(566)	-----									
in silico AtMRS2-3short-GFP	(802)	GAGGAGCATCGTGGAAAAAGAGACGTTCCAAACCAGCTTCAAAGCAAGTGGATTGATGTGATATCCCACTGACGTAAGGGATGAGC									
		Promoter Prokaryotic(1..1028): 35S promoter									
	(891)	891	900	910	920	930	940	950	960	979	
in vitro AtMRS2-3short-GFP	(655)	-----									
in silico AtMRS2-3short-GFP	(891)	CACAAATCCCCTATCCTTCGCAAGACCCCTCCTCTATATAAGGAAGTTCATTTCAATTTGGAGAGGACTCCGGTATTTTACAACAATA									
		Promoter Prokaryotic(1..1028): 35S promoter									
	(980)	980	990	1000	1010	1020	1030	1040	1050	1068	
in vitro AtMRS2-3short-GFP	(744)	-----									
in silico AtMRS2-3short-GFP	(979)	CCACAACAAAACAAAACAAAACAAACATTAACAATTTACTATTCTAGTCGACCTGCAGGCGGCCGACATAGTGATAT-----CACAAAGT									
		Promoter Prokaryotic(1..1028): 35S promoter									
		Misc. Recombination(1063..1083): attB1									
	(1069)	1069	1080	1090	1100	1110	1120	1130	1140	1157	
in vitro AtMRS2-3short-GFP	(827)	-----									
in silico AtMRS2-3short-GFP	(1068)	TTGTACAAAAAGCAGGCTCGACTCTTCTTTGGGAATTCCTCCGCTCGCCGTGCGCGATTTTAAAAGCCCTAAACTTTTAAAGCAAATCC									
		Promoter Eukaryotic(1087..1380): AtMRS2-3 promoter									
		Primer Binding Site(1087..1109): 2-3 gfp-gus up									
	(1158)	1158	1170	1180	1190	1200	1210	1220	1230	1246	
in vitro AtMRS2-3short-GFP	(916)	-----									
in silico AtMRS2-3short-GFP	(1157)	CTCCGTCACAACAAAATTCAAAAGAAGCTAAAACCGGTTTGGTTTTGGTGGAAAATCAAACCGGTTTGAATTTGATATTTGG									
		Promoter Eukaryotic(1087..1380): AtMRS2-3 promoter									
	(1247)	1247	1260	1270	1280	1290	1300	1310	1320	1335	
in vitro AtMRS2-3short-GFP	(1005)	-----									
in silico AtMRS2-3short-GFP	(1246)	GGGAAAAGTAAAACCGGTTTGTCTTAAACCGTTTTTGTCTTTTGGTGGAGCGAGCCGGAATATAAATTCACCAATTTTCACTTCCAC									
		Promoter Eukaryotic(1087..1380): AtMRS2-3 promoter									

	(1336)	1336	1350	1360	1370	1380	1390	1400	1410	1424	
in vitro AtMRS2-3short-GFP (1094)		ATTCTCAGCTGCTCGATCTCTCTGATCACAACAATCATAAGCGATGAGAGGAGCTAGACCCGATGAATTC AATTTT AGTACGAATC									
in silico AtMRS2-3short-GFP (1335)		ATTCTCAGCTGCTCGATCTCTCTGATCACAACAATCATAAGCGATGAGAGGAGCTAGACCCGATGAATTC AATTTT AGTACGAATC									
		Promoter Eukaryotic(1087..1380): AtMRS2-3 promoter					CDS(1381..1810): AtMRS2-3 1st exon				
	(1425)	1425	1430	1440	1450	1460	1470	1480	1490	1500	1513
in vitro AtMRS2-3short-GFP (1183)		CATCAACGCCAACAACTGGTCAGCCGACACCGAAGCTACCCCGCCGGTGTGGCGGCGCGCGGTGGAAGGAAAAAAGGCGTTGGCGTG									
in silico AtMRS2-3short-GFP (1424)		CATCAACGCCAACAACTGGTCAGCCGACACCGAAGCTACCCCGCCGGTGTGGCGGCGCGCGGTGGAAGGAAAAAAGGCGTTGGCGTG									
		CDS(1381..1810): AtMRS2-3 1st exon									
	(1514)	1514	1520	1530	1540	1550	1560	1570	1580	1590	1602
in vitro AtMRS2-3short-GFP (1272)		AGGACGTGGTGGTACTTAACTCGTCAGGGCAATCGGAGCCGAGGAAGAAGGGAAACACTCCATCATGCGGGCAACGGGATTACCGGC									
in silico AtMRS2-3short-GFP (1513)		AGGACGTGGTGGTACTTAACTCGTCAGGGCAATCGGAGCCGAGGAAGAAGGGAAACACTCCATCATGCGGGCAACGGGATTACCGGC									
		CDS(1381..1810): AtMRS2-3 1st exon									
	(1603)	1603	1610	1620	1630	1640	1650	1660	1670	1680	1691
in vitro AtMRS2-3short-GFP (1361)		CGGTGATCTTAGGATTCGATCCACTGTTGTCGATCCATTTACTGTTTTAGGTAGAGAGAGGCGGATTGTCATCAATTTGGAGCATA									
in silico AtMRS2-3short-GFP (1602)		CGGTGATCTTAGGATTCGATCCACTGTTGTCGATCCATTTACTGTTTTAGGTAGAGAGAGGCGGATTGTCATCAATTTGGAGCATA									
		CDS(1381..1810): AtMRS2-3 1st exon									
	(1692)	1692	1700	1710	1720	1730	1740	1750	1760	1770	1780
in vitro AtMRS2-3short-GFP (1450)		TCAAGGCAATCATCACTGCTCAAGAAGTTTTGTTGCTTAATCCAAGGATCCTTCGGTCTCACCCCTTATTGATGAGTTGCAGAGGCGG									
in silico AtMRS2-3short-GFP (1691)		TCAAGGCAATCATCACTGCTCAAGAAGTTTTGTTGCTTAATCCAAGGATCCTTCGGTCTCACCCCTTATTGATGAGTTGCAGAGGCGG									
	(1781)	1781	1790	1800	1810	1820	1830	1840	1850	1869	
in vitro AtMRS2-3short-GFP (1539)		ATTCTCTGTACCATCAGCCACTAAACCTCACCCAGCTTCTTGTACAAAGTGGTGATATCAATGGTGAGCAAGGGCGAGGAGCTGTT									
in silico AtMRS2-3short-GFP (1780)		ATTCTCTGTACCATCAGCCACTAAACCTCACCCAGCTTCTTGTACAAAGTGGTGATATCAATGGTGAGCAAGGGCGAGGAGCTGTT									
		Primer Binding Site(1789..1810): 2.3 gfp-gus down Misc. Recombination(1814..1834): attB2					Misc. Feature(1843..2562): Eglp				
		CDS(1381..1810): AtMRS2-3 1st exon									
	(1870)	1870	1880	1890	1900	1910	1920	1930	1940	1958	
in vitro AtMRS2-3short-GFP (1628)		CACCGGGTGGTGCCCATCCTGGTCGAGCTGGACGGCGACGTAACCGGCCACAAGTTCAGCGTGTCCGGCGAGGGCGAGGGCGATGCCA									
in silico AtMRS2-3short-GFP (1869)		CACCGGGTGGTGCCCATCCTGGTCGAGCTGGACGGCGACGTAACCGGCCACAAGTTCAGCGTGTCCGGCGAGGGCGAGGGCGATGCCA									
		Misc. Feature(1843..2562): Eglp									
	(1959)	1959	1970	1980	1990	2000	2010	2020	2030	2047	
in vitro AtMRS2-3short-GFP (1717)		-----									
in silico AtMRS2-3short-GFP (1958)		CTACGGCAAGCTGACCCCTGAAGTTTCACTGACCAACCGGCAAGCTGCCCGTGCCTGGCCACCCCTGTCGACACCCCTGACCTACGGC									
		Misc. Feature(1843..2562): Eglp									
	(2048)	2048	2060	2070	2080	2090	2100	2110	2120	2136	
in vitro AtMRS2-3short-GFP (1718)		GTGCAGTGCTTCAGCCGCTACCCCGACACATGAAGCAGCAGCACTTCTTCAAGTCCGCCATGCCGAAGGCTACGTCCAGGAGCGCAC									
in silico AtMRS2-3short-GFP (2047)		GTGCAGTGCTTCAGCCGCTACCCCGACACATGAAGCAGCAGCACTTCTTCAAGTCCGCCATGCCGAAGGCTACGTCCAGGAGCGCAC									
		Misc. Feature(1843..2562): Eglp									
	(2137)	2137	2150	2160	2170	2180	2190	2200	2210	2225	
in vitro AtMRS2-3short-GFP (1718)		-----									
in silico AtMRS2-3short-GFP (2136)		CATCTTCTTCAAGGACGACGGCAACTACAAGACCCGCGCGAGGTGAAGTTCGAGGGCGACACCCCTGGTGAACCCGATCGAGCTGAAGG									
		Misc. Feature(1843..2562): Eglp									
	(2226)	2226	2240	2250	2260	2270	2280	2290	2300	2314	
in vitro AtMRS2-3short-GFP (1718)		-----									
in silico AtMRS2-3short-GFP (2225)		GCATCGACTTCAAGGAGGACGGCAACATCCTGGGACACAAGCTGGAGTACAACATACAACAGCCACAACGCTTATATCATGGCCGACAC									
		Misc. Feature(1843..2562): Eglp									
	(2315)	2315	2320	2330	2340	2350	2360	2370	2380	2403	
in vitro AtMRS2-3short-GFP (1718)		-----									
in silico AtMRS2-3short-GFP (2314)		CAGAAGAACGGCATCAAGGTGAAGTTCAAGATCCGCCACAACATCGAGGACGGCAGCGTGCAGCTCGCCGACCACTACCAGCAGAACAC									
		Misc. Feature(1843..2562): Eglp									
	(2404)	2404	2410	2420	2430	2440	2450	2460	2470	2492	
in vitro AtMRS2-3short-GFP (1718)		-----									
in silico AtMRS2-3short-GFP (2403)		CCCCATCGGCGACGGCCCGTGTGCTGCCGACAACCACTACCTGAGCACCCAGTCCGCCCTGAGCAAAGACCCCAACGAGAAGCGCG									
		Misc. Feature(1843..2562): Eglp									
	(2493)	2493	2500	2510	2520	2530	2540	2550	2563		
in vitro AtMRS2-3short-GFP (1718)		-----									
in silico AtMRS2-3short-GFP (2492)		ATCACATGGTCTGCTGAGTTCGTGACCGCCCGGGATCACCTCGGCATGGACGAGCTGTACAAGTAA									
		Misc. Feature(1843..2562): Eglp									

The sequence of the *in vitro* AtMRS2-3short-GFP destination clone received after sequencing with the oligonucleotides 35S-Prom. pK7FWG2 and gfp-pK7FWG2 (cf. Figure 3.1.4 on page 52 for primer binding sites) was aligned with the sequence of the destination clone generated *in silico* via Vector NTI (Invitrogen Inc.). This *in silico* sequence was annotated to identify the major elements of the sequence: the 35S promoter, attachment site B1, AtMRS2-3 promoter and first exon, attachment site B2, and the GFP coding sequence. The primer

---

binding sites used to amplify the original PCR product are also given. The AtMRS2-3 coding sequence starts at position 1381; the GFP coding sequence starts 462 bp or 154 amino acids downstream at position 1843 in frame with the AtMRS2-3 first exon. This exon comprises 143 of the 154 amino acids, the further eleven amino acids constitute the linker region between the two coding sequences (cf. section 3.1.1 on page 40 for a description of the linker region).

Within the *in vitro* sequence there are some deviations from the *in silico* sequence: the differences in the promoter region and directly upstream of the attB1 region are most probably due to incorrect vector sequences given by the constructors (Karimi et al. (2002); see <http://www.psb.rug.ac.be/gateway/> for their homepage). The vectors are constantly getting re-sequenced and the correct sequences published.

There are two deviations from the genomic AtMRS2-3 entry (GenBank accession AP000417) within the first exon of AtMRS2-3: the first one changes the amino acid sequence from Ser to Phe (codon TCT is changed into TTT), whereas the second exchange is a silent one (AGA to AGG, both coding for Arg). These exchanges can be explained either by incorrect integration of nucleotides by the DNA polymerase or by differences in the DNA sequence existing between ecotypes Col-0 (the sequenced one) and Col-5 used here for amplification of the PCR products.

## 8.3 Abbreviations

<b>abbreviation</b>	<b>term written out</b>
<i>A. thaliana</i>	<i>Arabidopsis thaliana</i>
<i>A. tumefaciens</i>	<i>Agrobacterium tumefaciens</i>
aa	amino acid
ADH	alcohol dehydrogenase
ALR1/2	Al <sup>3+</sup> resistance 1/2
AM	acetoxymethyl
AtMHX	<i>Arabidopsis thaliana</i> Mg <sup>2+</sup> -proton exchanger
BAP	benzylaminopurine
BCIP	5-Bromo-4-chloro-3'-indolyphosphate p-toluidine salt
ccd	coupled cell division
CDS	coding sequence
cf.	compare
Col	Columbia
CorA	Co <sup>2+</sup> resistance A
cRNA	copy-RNA
C <sub>ub</sub>	C-terminal half of ubiquitin
DEVC	double electrode voltage clamping
<i>E. coli</i>	<i>Escherichia coli</i>
e.g.	for example
EDTA	ethylenediamine tetraacetic acid
EGTA	ethylene glycol tetraacetic acid
ER	endoplasmatic reticulum
GFP	green fluorescent protein
GUS	β-glucuronidase
HEPES	[4-(2-hydroxyethyl)-1-piperazine] ethanesulfonic acid
i.e.	that is
kDa	kilo Dalton
Ler	Landsberg
MagT1	magnesium transporter 1
Mas	mannopine synthase
MES	morpholineethanesulfonic acid
Mg <sup>2+</sup>	magnesium ion
MgtA, B, C, E	Mg <sup>2+</sup> transport A, B, C, E
mOsm	milli osmolar

<b>abbreviation</b>	<b>term written out</b>
MRS2	mitochondrial RNA splicing 2
MS	Murashige and Skoog
<i>N. benthamiana</i>	<i>Nicotiana benthamiana</i>
<i>N. tabacum</i>	<i>Nicotiana tabacum</i>
nA	nano ampere
NBT	Nitro-blue tetrazolium chloride
NCX1	Na <sup>+</sup> /Ca <sup>2+</sup> exchanger 1
nd	not determined
ng	nano gramme
nos	nopaline synthase
N <sub>ubG</sub>	mutated N-terminal half of ubiquitin
N <sub>ubWT</sub>	wild type N-terminal half of ubiquitin
ONPG	o-nitrophenylgalactopyranoside
PAGE	polyacrylamid gel electrophoresis
PCR	polymerase chain reaction
PEG	polyethylene glycol
PLV	proteinA-LexA-VP16
Rbcs	RuBisCO small subunit
RuBisCO	Ribulose-1,5-bisphosphate carboxylase/oxygenase
<i>S. enterica</i>	<i>Salmonella enterica</i> serovar Typhimurium
SPI-3	<i>Salmonella</i> pathogenicity island 3
T-DNA	transfer DNA
Ti plasmid	tumour inducing plasmid
TM	transmembrane domain; trade mark
Tris	Tris(hydroxymethyl)aminomethane
TRPM	transient receptor potential, melastatin-related
UBP	ubiquitin-specific protease
USP	ubiquitin-specific protease
UTR	untranslated region
w/o	without

## 8.4 Figure index

Figure 1.2.1: The crystal structure of the CorA Mg <sup>2+</sup> transporter from <i>Thermotoga maritima</i> .	4
Figure 1.2.2: The MgtA/MgtB and MgtE Mg <sup>2+</sup> transporters of <i>Salmonella enterica</i> serovar Typhimurium.....	5
Figure 1.3.1: Phylogeny of the plant 2-TM-GxN homologues .....	10
Figure 2.2.1: BP reaction.....	17
Figure 2.2.2: LR reaction .....	18
Figure 2.2.3: Maps of the Gateway™ vectors for gene-GFP fusion construct expression .....	19
Figure 2.2.4: Maps of the yeast expression vectors used for complementation assays .....	27
Figure 2.2.5: Cloning strategies for yeast complementation constructs .....	28
Figure 2.2.6: Principle of the split ubiquitin system .....	31
Figure 2.2.7: Maps of the vectors used in the mating-based split ubiquitin system .....	32
Figure 2.2.8: Flow chart of the mbSUS approach.....	33
Figure 2.2.9: Maps of the vectors used for heterologous expression in <i>Xenopus</i> oocytes.....	35
Figure 3.1.1: Description of the expression clone of the full length AtMRS2-1-GFP construct .....	44
Figure 3.1.2: Exemplary transcriptional analysis of full length gene-GFP plant lines .....	45
Figure 3.1.3: Test for translation of the transgene in four selected full length gene-GFP plant lines .....	48
Figure 3.1.4: Description of the expression clone of the C-terminally shortened AtMRS2-1-GFP construct.....	52
Figure 3.1.5: Test for transcription within the AtMRS2short-GFP plant lines.....	53
Figure 3.1.6: Test for translation of the transgene in five selected shortened gene-GFP plant lines .....	54
Figure 3.1.7: Description of the expression clone of full length AtMRS2-1 coding sequence in pMDC83.....	57
Figure 3.1.8: Map of the vector pPGTkan used for expression of soluble GFP .....	58
Figure 3.1.9: Fluorescence of tobacco epidermal cells transformed with the 35S-GFP construct .....	59
Figure 3.1.10: Fluorescence of an <i>N. benthamiana</i> protoplast transformed with pPGTkan....	62
Figure 3.1.11: Fluorescence of an <i>N. benthamiana</i> protoplast transformed with full length AtMRS2-4g-GFP .....	63



Figure 3.1.12: Fluorescence of an <i>N. benthamiana</i> protoplast transformed with the full length AtMRS2-1c-GFP construct in pMDC83.....	64
Figure 3.2.1: Complementation of the $\Delta$ mrs2 mutant with AtMRS2 proteins targeted to the mitochondria.....	70
Figure 3.2.2: Complementation of the $\Delta$ mrs2 mutant with the native AtMRS2-4 protein.....	71
Figure 3.2.3: Measurement of $Mg^{2+}$ uptake into isolated yeast mitochondria via mag-fura 2	72
Figure 3.3.1: Western Blot analysis of V5-His6-tagged AtMRS2-1 and AtMRS2-5 proteins	77
Figure 3.3.2: DEVC recording of an AtMRS2-5 injected <i>Xenopus</i> oocyte.....	79
Figure 3.4.1: mbSUS interaction screening with AtMRS2-1 and AtMRS2-10.....	84
Figure 3.4.2: Second mbSUS screening with four different AtMRS2 proteins.....	88
Figure 4.1.1: Phylogenetic tree and exon-intron structures of the <i>Arabidopsis</i> and <i>Oryza</i> magnesium transporters.....	92

## 8.5 Table index

Table 2.2-1: Composition of the solutions used for <i>Xenopus</i> oocyte storage and DEVC measurements.....	37
Table 3.1-1: Templates and sizes of the full length PCR products for the gene-GFP fusions.	41
Table 3.1-2: Number of transgenic plants received after transformation of <i>A. thaliana</i> with the full length gene-GFP constructs.....	42
Table 3.1-3: Number of transgenic full length gene-GFP plants showing transcription of the construct.....	47
Table 3.1-4: Expected sizes of the AtMRS2, GFP, and fusion proteins.....	48
Table 3.1-5: Key data for the C-terminally shortened GFP constructs.....	50
Table 3.1-6: Number of transgenic plant lines obtained for the C-terminally shortened GFP constructs.....	51
Table 3.1-7: Transient transformation of tobacco leaves via <i>Agrobacterium</i> infiltration.....	59
Table 3.1-8: Gene-GFP constructs used for transient transformation of tobacco protoplasts .	61
Table 3.1-9: Summary of the results obtained with the entire gene-GFP fusions in different expression systems.....	65
Table 3.4-1: Summary of the results obtained for interaction of the AtMRS2 proteins within the mbSUS.....	90



## 9. Bibliography

- Abel, S. and Theologis, A. (1994). Transient transformation of *Arabidopsis* leaf protoplasts - a versatile experimental system to study gene expression. *Plant J.* 5, 421-427.
- Batoko, H., Zheng, H.Q., Hawes, C., and Moore, I. (2000). A Rab1 GTPase is required for transport between the endoplasmic reticulum and golgi apparatus and for normal golgi movement in plants. *Plant Cell* 12, 2201-2218.
- Becker, D., Geiger, D., Dunkel, M., Roller, A., Bertl, A., Latz, A., Carpaneto, A., Dietrich, P., Roelfsema, M.R.G., Voelker, C., Schmidt, D., Mueller-Roeber, B., Czempinski, K., and Hedrich, R. (2004). AtTPK4, an *Arabidopsis* tandem-pore K<sup>+</sup> channel, poised to control the pollen membrane voltage in a pH- and Ca<sup>2+</sup>-dependent manner. *PNAS* 101, 15621-15626.
- Becker, D., Dreyer, I., Hoth, S., Reid, J.D., Busch, H., Lehnen, M., Palme, K., and Hedrich, R. (1996). Changes in voltage activation, Cs<sup>+</sup> sensitivity, and ion permeability in H5 mutants of the plant K<sup>+</sup> channel KAT1. *PNAS* 93, 8123-8128.
- Bennett, M.D., Leitch, I.J., Price, H.J., and Johnston, J.S. (2003). Comparisons with *Caenorhabditis* (~100 Mb) and *Drosophila* (~175 Mb) using flow cytometry show genome size in *Arabidopsis* to be ~157 Mb and thus ~25 % larger than the *Arabidopsis* Genome Initiative estimate of ~125 Mb. *Ann. Bot.* 91, 547-557.
- Bernard, P. and Couturier, M. (1992). Cell killing by the F plasmid CcdB protein involves poisoning of DNA-topoisomerase II complexes. *J. Mol. Biol.* 226, 735-745.
- BlancPotard, A.B. and Groisman, E.A. (1997). The *Salmonella* selC locus contains a pathogenicity island mediating intramacrophage survival. *EMBO J.* 16, 5376-5385.
- Blattner, F.R., Plunkett, G., Bloch, C.A., Perna, N.T., Burland, V., Riley, M., ColladoVides, J., Glasner, J.D., Rode, C.K., Mayhew, G.F., Gregor, J., Davis, N.W., Kirkpatrick, H.A., Goeden, M.A., Rose, D.J., Mau, B., and Shao, Y. (1997). The complete genome sequence of *Escherichia coli* K-12. *Science* 277, 1453-1474.
- Brink, S., Flügge, U.I., Chaumont, F., Boutry, M., Emmermann, M., Schmitz, U., Becker, K., and Pfanner, N. (1994). Preproteins of chloroplast envelope inner membrane contain targeting information for receptor-dependent import into fungal mitochondria. *J. Biol. Chem.* 269, 16478-16485.
- Bui, D.M., Gregan, J., Jarosch, E., Ragnini, A., and Schweyen, R.J. (1999). The bacterial magnesium transporter CorA can functionally substitute for its putative homologue Mrs2p in the yeast inner mitochondrial membrane. *J. Biol. Chem.* 274, 20438-20443.
- Chaumont, F., O'Riordan, V., and Boutry, M. (1990). Protein transport into mitochondria is conserved between plant and yeast species. *J. Biol. Chem.* 265, 16856-16862.
- Chiu, W.I., Niwa, Y., Zeng, W., Hirano, T., Kobayashi, H., and Sheen, J. (1996). Engineered GFP as a vital reporter in plants. *Curr. Biol.* 6, 325-330.
- Chubanov, V., Waldegger, S., Schnitzler, M.M., Vitzthum, H., Sassen, M.C., Seyberth, H.W., Konrad, M., and Gudermann, T. (2004). Disruption of TRPM6/TRPM7 complex formation by

- a mutation in the TRPM6 gene causes hypomagnesemia with secondary hypocalcemia. *PNAS* *101*, 2894-2899.
- Clough,S.J. and Bent,A.F. (1998). Floral dip: a simplified method for *Agrobacterium*-mediated transformation of *Arabidopsis thaliana*. *Plant J.* *16*, 735-743.
- Cody,C.W., Prasher,D.C., Westler,W.M., Prendergast,F.G., and Ward,W.W. (1993). Chemical structure of the hexapeptide chromophore of the *Aequorea* green-fluorescent protein. *Biochemistry* *32*, 1212-1218.
- Cormack,B.P., Valdivia,R.H., and Falkow,S. (1996). FACS-optimized mutants of the green fluorescent protein (GFP). *Gene* *173*, 33-38.
- Cromie,M.J., Shi,Y., Latifi,T., and Groisman,E.A. (2006). An RNA Sensor for Intracellular  $Mg^{2+}$ . *Cell* *125*, 71-84.
- Curtis,M.D. and Grossniklaus,U. (2003). A gateway cloning vector set for high-throughput functional analysis of genes *in planta*. *Plant Physiol.* *133*, 462-469.
- Cutler,S.R., Ehrhardt,D.W., Griffiths,J.S., and Somerville,C.R. (2000). Random GFP::cDNA fusions enable visualization of subcellular structures in cells of *Arabidopsis* at a high frequency. *PNAS* *97*, 3718-3723.
- Datsenko,K.A. and Wanner,B.L. (2000). One-step inactivation of chromosomal genes in *Escherichia coli* K-12 using PCR products. *PNAS* *97*, 6640-6645.
- David-Assael,O., Saul,H., Saul,V., Mizrachy-Dagri,T., Berezin,I., Brook,E., and Shaul,O. (2005). Expression of AtMHX, an *Arabidopsis* vacuolar metal transporter, is repressed by the 5' untranslated region of its gene. *J. Exp. Bot.* *56*, 1039-1047.
- Davis,S.J. and Vierstra,R.D. (1998). Soluble, highly fluorescent variants of green fluorescent protein (GFP) for use in higher plants. *Plant Mol. Biol.* *36*, 521-528.
- de Ruijter,N.C.A., Verhees,J., van Leeuwen,W., and van der Krol,A.R. (2003). Evaluation and comparison of the GUS, LUC and GFP reporter system for gene expression studies in plants. *Plant Biol.* *5*, 103-115.
- Douce,R. and Joyard,J. (1990). Biochemistry and function of the plastid envelope. *Annu. Rev. Cell Biol.* *6*, 173-216.
- Drummond,R.S.M., Tutone,A., Li,Y.C., and Gardner,R.C. (2006). A putative magnesium transporter AtMRS2-11 is localized to the plant chloroplast envelope membrane system. *Plant Sci.* *170*, 78-89.
- Duchene,A.M., Giritch,A., Hoffmann,B., Cognat,V., Lancelin,D., Peeters,N.M., Zaepfel,M., Marechal-Drouard,L., and Small,I.D. (2005). Dual targeting is the rule for organellar aminoacyl-tRNA synthetases in *Arabidopsis thaliana*. *PNAS* 0504682102.
- Eifler,K. (2006). Molecular and functional analyses of *Arabidopsis thaliana* cation transport: *in planta* studies and heterologous expression of membrane transport proteins in yeast. (Diploma thesis: University of Bonn).

- Eshaghi,S., Niegowski,D., Kohl,A., Molina,D.M., Lesley,S.A., and Nordlund,P. (2006). Crystal structure of a divalent metal ion transporter CorA at 2.9 Angstrom resolution. *Science* *313*, 354-357.
- Favery,B., Chelysheva,L.A., Lebris,M., Jammes,F., Marmagne,A., Almeida-Engler,J., Lecomte,P., Vaury,C., Arkowitz,R.A., and Abad,P. (2004). *Arabidopsis* formin AtFH6 is a plasma membrane-associated protein upregulated in giant cells induced by parasitic nematodes. *Plant Cell* *16*, 2529-2540.
- Flügge,U.I. and Benz,R. (1984). Pore-forming activity in the outer membrane of the chloroplast envelope. *FEBS Lett.* *169*, 85-89.
- Gabriel,T.E. and Günzel,D. (2006). Quantification of Mg<sup>2+</sup> extrusion and cytosolic Mg<sup>2+</sup>-buffering in *Xenopus* oocytes. *Arch. Biochem. Biophys.* *In Press, Corrected Proof*.
- Gardemann,A., Schimkat,D., and Heldt,H.W. (1986). Control of CO<sub>2</sub> fixation. Regulation of stromal fructose-1,6-bisphosphatase in spinach by pH and Mg<sup>2+</sup> concentration. *Planta* *168*, 536-545.
- Geiger,D., Becker,D., Lacombe,B., and Hedrich,R. (2002). Outer pore residues control the H<sup>+</sup> and K<sup>+</sup> sensitivity of the *Arabidopsis* potassium channel AKT3. *Plant Cell* *14*, 1859-1868.
- Gietz,R.D. and Woods,R.A. (2002). Transformation of yeast by lithium acetate/single-stranded carrier DNA/polyethylene glycol method. *Guide to Yeast Genetics and Molecular and Cell Biology, Part B* *350*, 87-96.
- Goytain,A. and Quamme,G. (2005a). Identification and characterization of a novel mammalian Mg<sup>2+</sup> transporter with channel-like properties. *BMC Genomics* *6*, 48.
- Goytain,A. and Quamme,G.A. (2005b). Functional characterization of ACDP2 (ancient conserved domain protein), a divalent metal transporter. *Physiol. Genomics* *22*, 382-389.
- Goytain,A. and Quamme,G.A. (2005c). Functional characterization of human SLC41A1, a Mg<sup>2+</sup> transporter with similarity to prokaryotic MgtE Mg<sup>2+</sup> transporters. *Physiol. Genomics* *21*, 337-342.
- Goytain,A. and Quamme,G.A. (2005d). Functional characterization of the human solute carrier, SLC41A2. *Biochem. Biophys. Res. Commun.* *330*, 701-705.
- Graschopf,A., Stadler,J.A., Hoellerer,M.K., Eder,S., Sieghardt,M., Kohlwein,S.D., and Schweyen,R.J. (2001). The yeast plasma membrane protein Alr1 controls Mg<sup>2+</sup> homeostasis and is subject to Mg<sup>2+</sup>-dependent control of its synthesis and degradation. *J. Biol. Chem.* *276*, 16216-16222.
- Gregan,J., Bui,D.M., Pillich,R., Fink,M., Zsurka,G., and Schweyen,R.J. (2001a). The mitochondrial inner membrane protein Lpe10p, a homologue of Mrs2p, is essential for magnesium homeostasis and group II intron splicing in yeast. *Mol. Gen. Genet.* *264*, 773-781.
- Gregan,J., Kolisek,M., and Schweyen,R.J. (2001b). Mitochondrial Mg<sup>2+</sup> homeostasis is critical for group II intron splicing in vivo. *Genes Dev.* *15*, 2229-2237.
- Groisman,E.A. (1998). The ins and outs of virulence gene expression: Mg<sup>2+</sup> as a regulatory signal. *Bioessays* *20*, 96-101.

- Grynkiewicz,G., Poenie,M., and Tsien,R.Y. (1985). A new generation of Ca<sup>2+</sup> indicators with greatly improved fluorescence properties. *J. Biol. Chem.* *260*, 3440-3450.
- Hall,T.A. (1999). BioEdit: a user-friendly biological sequence alignment editor and analysis program for Windows 95/98/NT. *Nucl. Acids. Symp. Ser.* *41*, 95-98.
- Harris,D.J., Lambell,R.G., and Oliver,C.J. (1983). Factors predisposing dairy and beef cows to grass tetany. *Aust. Vet. J.* *60*, 230-234.
- Heineke,D. and Heldt,H.W. (1988). Measurement of light-dependent changes of the stromal pH in wheat leaf protoplasts. *Bot. Acta* *101*, 45-47.
- Hill,J.E., Myers,A.M., Koerner,T.J., and Tzagoloff,A. (1986). Yeast/*Escherichia coli* shuttle vectors with multiple unique restriction sites. *Yeast* *2*, 163-167.
- Hmiel,S.P., Snavely,M.D., Florer,J.B., Maguire,M.E., and Miller,C.G. (1989). Magnesium transport in *Salmonella typhimurium*: genetic characterization and cloning of three magnesium transport loci. *J. Bacteriol.* *171*, 4742-4751.
- Hmiel,S.P., Snavely,M.D., Miller,C.G., and Maguire,M.E. (1986). Magnesium transport in *Salmonella typhimurium*: characterization of magnesium influx and cloning of a transport gene. *J. Bacteriol.* *168*, 1444-1450.
- Höfgen,R. and Willmitzer,L. (1988). Storage of competent cells for *Agrobacterium* transformation. *Nucl. Acids Res.* *16*, 9877.
- Horan,K., Lauricha,J., Bailey-Serres,J., Raikhel,N., and Girke,T. (2005). Genome cluster database. A sequence family analysis platform for *Arabidopsis* and rice. *Plant Physiol.* *138*, 47-54.
- Hoth,S., Dreyer,I., Dietrich,P., Becker,D., Muller-Rober,B., and Hedrich,R. (1997). Molecular basis of plant-specific acid activation of K<sup>+</sup> uptake channels. *PNAS* *94*, 4806-4810.
- Hurt,E.C. and van Loon,A.P.G.M. (1986). How proteins find mitochondria and intramitochondrial compartments. *Trends Biochem. Sci.* *11*, 204-207.
- Johnsson,N. and Varshavsky,A. (1994). Split ubiquitin as a sensor of protein interactions *in vivo*. *PNAS* *91*, 10340-10344.
- Karimi,M., Inzé,D., and Depicker,A. (2002). GATEWAY(TM) vectors for *Agrobacterium*-mediated plant transformation. *Trends Plant Sci.* *7*, 193-195.
- Kehres,D.G. and Maguire,M.E. (2002). Structure, properties and regulation of magnesium transport proteins. *Biometals* *15*, 261-270.
- Kier,L.D., Weppelman,R.M., and Ames,B.N. (1979). Regulation of nonspecific acid phosphatase in *Salmonella*: *phoN* and *phoP* genes. *J. Bacteriol.* *138*, 155-161.
- Knoop,V., Groth-Malonek,M., Gebert,M., Eifler,K., and Weyand,K. (2005). Transport of magnesium and other divalent cations: evolution of the 2-TM-GxN proteins in the MIT superfamily. *Mol. Gen. Genomics* *274*, 205-216.

- Kolisek, M., Zsurka, G., Samaj, J., Weghuber, J., Schweyen, R.J., and Schweigel, M. (2003). Mrs2p is an essential component of the major electrophoretic Mg<sup>2+</sup> influx system in mitochondria. *EMBO J.* *22*, 1235-1244.
- Koncz, C. and Schell, J. (1986). The promoter of TL-DNA gene 5 controls the tissue-specific expression of chimeric genes carried by a novel type of *Agrobacterium* binary vector. *Mol. Gen. Genet.* *204*, 383-396.
- Koop, H.U., Steinmuller, K., Wagner, H., Rossler, C., Eibl, C., and Sacher, L. (1996). Integration of foreign sequences into the tobacco plastome via polyethylene glycol-mediated protoplast transformation. *Planta* *199*, 193-201.
- Kucharski, L.M., Lubbe, W.J., and Maguire, M.E. (2000). Cation hexaamines are selective and potent inhibitors of the CorA magnesium transport system. *J. Biol. Chem.* *275*, 16767-16773.
- Kumar, S., Tamura, K., and Nei, M. (2004). MEGA3: integrated software for molecular evolutionary genetics analysis and sequence alignment. *Brief. Bioinformatics* *5*, 150-163.
- Langmeier, M., Ginsburg, S., and Matile, P. (1993). Chlorophyll breakdown in senescent leaves - demonstration of Mg-dechelataase activity. *Physiol. Plantarum* *89*, 347-353.
- Lee, J. and Gardner, R. (2006). Residues of the yeast ALR1 protein that are critical for magnesium uptake. *Curr. Genet.* *49*, 7-20.
- Li, L., Tutone, A.F., Drummond, R.S.M., Gardner, R.C., and Luan, S. (2001). A novel family of magnesium transport genes in *Arabidopsis*. *Plant Cell* *13*, 2761-2775.
- Liman, E.R., Tytgat, J., and Hess, P. (1992). Subunit stoichiometry of a mammalian K<sup>+</sup> channel determined by construction of multimeric cDNAs. *Neuron* *9*, 861-871.
- Liu, G.J., Martin, D.K., Gardner, R.C., and Ryan, P.R. (2002). Large Mg<sup>2+</sup>-dependent currents are associated with the increased expression of ALR1 in *Saccharomyces cerevisiae*. *FEMS Microbiol. Lett.* *213*, 231-237.
- Ludewig, U., Wilken, S., Wu, B., Jost, W., Obrdlik, P., El Bakkoury, M., Marini, A.M., Andre, B., Hamacher, T., Boles, E., von Wiren, N., and Frommer, W.B. (2003). Homo- and hetero-oligomerization of ammonium transporter-1 NH<sub>4</sub><sup>+</sup> uniporters. *J. Biol. Chem.* *278*, 45603-45610.
- Lunin, V.V., Dobrovetsky, E., Khutoreskaya, G., Zhang, R., Joachimiak, A., Doyle, D.A., Bochkarev, A., Maguire, M.E., Edwards, A.M., and Koth, C.M. (2006). Crystal structure of the CorA Mg<sup>2+</sup> transporter. *Nature* *440*, 833-837.
- Lusk, J.E. and Kennedy, E.P. (1969). Magnesium transport in *Escherichia coli*. *J. Biol. Chem.* *244*, 1653-1655.
- MacDiarmid, C.W. and Gardner, R.C. (1998). Overexpression of the *Saccharomyces cerevisiae* magnesium transport system confers resistance to aluminium ion. *J. Biol. Chem.* *273*, 1727-1732.
- Maguire, M.E. and Cowan, J.A. (2002). Magnesium chemistry and biochemistry. *Biometals* *15*, 203-210.

- Maguire, M.E., Snavely, M.D., Leizman, J.B., Gura, S., Bagga, D., Tao, T., and Smith, D.L. (1992). Mg<sup>2+</sup> transporting P-type ATPases of *Salmonella typhimurium*. Wrong way, wrong place enzymes. *Ann. N. Y. Acad. Sci.* *671*, 244-255.
- Marschner, H. (1995). Mineral nutrition of higher plants. (London: Elsevier Academic Press).
- Marten, I., Hoth, S., Deeken, R., Ache, P., Ketchum, K.A., Hoshi, T., and Hedrich, R. (1999). AKT3, a phloem-localized K<sup>+</sup> channel, is blocked by protons. *PNAS* *96*, 7581-7586.
- Millar, A.H., Whelan, J., and Small, I. (2006). Recent surprises in protein targeting to mitochondria and plastids. *Curr. Opin. Plant Biol.* *9*, 610-615.
- Moncrief, M.B. and Maguire, M.E. (1999). Magnesium transport in prokaryotes. *J. Biol. Inorg. Chem.* *4*, 523-527.
- Monteilh-Zoller, M.K., Hermosura, M.C., Nadler, M.J.S., Scharenberg, A.M., Penner, R., and Fleig, A. (2002). TRPM7 provides an ion channel mechanism for cellular entry of trace metal ions. *J. Gen. Physiol.* *121*, 49-60.
- Nadler, M.J.S., Hermosura, M.C., Inabe, K., Perraud, A.L., Zhu, Q., Stokes, A.J., Kurosaki, T., Kinet, J.P., Penner, R., Scharenberg, A.M., and Fleig, A. (2001). LTRPC7 is a Mg-ATP-regulated divalent cation channel required for cell viability. *Nature* *411*, 590-595.
- Nelson, D.L. and Kennedy, E.P. (1971). Magnesium transport in *Escherichia coli*. Inhibition by cobaltous ion. *J. Biol. Chem.* *246*, 3042-3049.
- Nelson, D.L. and Kennedy, E.P. (1972). Transport of magnesium by a repressible and a nonrepressible system in *Escherichia coli*. *PNAS* *69*, 1091-1093.
- Newton, C.R. and Graham, A. (1994). PCR. (Heidelberg: Spektrum Akademischer Verlag).
- Obrdlik, P., El Bakkoury, M., Hamacher, T., Cappellaro, C., Vilarino, C., Fleischer, C., Ellerbrok, H., Kamuzinzi, R., Ledent, V., Blaudez, D., Sanders, D., Revuelta, J.L., Boles, E., Andre, B., and Frommer, W.B. (2004). K<sup>+</sup> channel interactions detected by a genetic system optimized for systematic studies of membrane protein interactions. *PNAS* *101*, 12242-12247.
- Obrdlik, P., Neuhaus, G., and Merkle, T. (2000). Plant heterotrimeric G protein  $\beta$  subunit is associated with membranes via protein interactions involving coiled-coil formation. *FEBS Lett.* *476*, 208-212.
- Oja, V., Laisk, A., and Heber, U. (1986). Light-induced alkalization of the chloroplast stroma in vivo as estimated from the CO<sub>2</sub> capacity of intact sunflower leaves. *Biochim. Biophys. Acta-Bioenerg.* *849*, 355-365.
- Ormö, M., Cubitt, A.B., Kallio, K., Gross, L.A., Tsien, R.Y., and Remington, S.J. (1996). Crystal structure of the *Aequorea victoria* green fluorescent protein. *Science* *273*, 1392-1395.
- Pang, S.Z., DeBoer, D.L., Wan, Y., Ye, G., Layton, J.G., Neher, M.K., Armstrong, C.L., Fry, J.E., Hinchee, M.A., and Fromm, M.E. (1996). An improved green fluorescent protein gene as a vital marker in plants. *Plant Physiol.* *112*, 893-900.



- Papenbrock, J., Mock, H.P., Tanaka, R., Kruse, E., and Grimm, B. (2000). Role of magnesium chelatase activity in the early steps of the tetrapyrrole biosynthetic pathway. *Plant Physiol.* *122*, 1161-1169.
- Park, M.H., Wong, B.B., and Lusk, J.E. (1976). Mutants in 3 genes affecting transport of magnesium in *Escherichia coli* - genetics and physiology. *J. Bacteriol.* *126*, 1096-1103.
- Portis, A.R. (1981). Evidence of a low stromal Mg concentration in intact chloroplasts in the dark: I. Studies with the ionophore A23187. *Plant Physiol.* *67*, 985-989.
- Portis, A.R., Jr. and Heldt, H.W. (1976). Light-dependent changes of the Mg<sup>2+</sup> concentration in the stroma in relation to the Mg<sup>2+</sup> dependency of CO<sub>2</sub> fixation in intact chloroplasts. *Biochim. Biophys. Acta* *449*, 434-436.
- Rao, I.M., Sharp, R.E., and Boyer, J.S. (1987). Leaf magnesium alters photosynthetic response to low water potentials in sunflower. *Plant Physiol.* *84*, 1214-1219.
- Reinders, A., Schulze, W., Kuhn, C., Barker, L., Schulz, A., Ward, J.M., and Frommer, W.B. (2002). Protein-protein interactions between sucrose transporters of different affinities colocalized in the same enucleate sieve element. *Plant Cell* *14*, 1567-1577.
- Sambrook, J., Fritsch, E.F., and Maniatis, T. (1989). *Molecular cloning: a laboratory manual*. (New York: Cold Spring Harbour Laboratory Press).
- Schmitz, C., Perraud, A.L., Johnson, C.O., Inabe, K., Smith, M.K., Penner, R., Kurosaki, T., Fleig, A., and Scharenberg, A.M. (2003). Regulation of vertebrate cellular Mg<sup>2+</sup> homeostasis by TRPM7. *Cell* *114*, 191-200.
- Schock, I. (2000). Spleißen mitochondrialer Gruppe II Introns: Molekulare Analysen und Identifikation einer Genfamilie von putativen Magnesiumtransportern in Pflanzen. (PhD thesis: University of Ulm).
- Schock, I., Gregan, J., Steinhauser, S., Schweyen, R., Brennicke, A., and Knoop, V. (2000). A member of a novel *Arabidopsis thaliana* gene family of candidate Mg<sup>2+</sup> ion transporters complements a yeast mitochondrial group II intron-splicing mutant. *Plant J.* *24*, 489-501.
- Schuldt, A.J., Adams, J.H.J., Davidson, C.M., Micklem, D.R., Haseloff, J., Johnston, D.S., and Brand, A.H. (1998). Miranda mediates asymmetric protein and RNA localization in the developing nervous system. *Genes Dev.* *12*, 1847-1857.
- Schwacke, R., Schneider, A., van der Graaff, E., Fischer, K., Catoni, E., Desimone, M., Frommer, W.B., Flugge, U.I., and Kunze, R. (2003). ARAMEMNON, a novel database for *Arabidopsis* integral membrane proteins. *Plant Physiol.* *131*, 16-26.
- Shaul, O. (2002). Magnesium transport and function in plants: the tip of the iceberg. *Biometals* *15*, 309-323.
- Shaul, O., Hilgemann, D.W., Almeida-Engler, J., Van Montagu, M., Inzé, D., and Galili, G. (1999). Cloning and characterization of a novel Mg<sup>2+</sup>/H<sup>+</sup> exchanger. *EMBO J.* *18*, 3973-3980.
- Silver, S. (1969). Active transport of magnesium in *Escherichia coli*. *PNAS* *62*, 764-771.

- Silver, S. and Clark, D. (1971). Magnesium transport in *Escherichia coli*. Interference by manganese with magnesium metabolism. *J. Biol. Chem.* *246*, 569-576.
- Smith, D.L., Tao, T., and Maguire, M.E. (1993a). Membrane topology of a P-type ATPase: the MgtB magnesium transport protein of *Salmonella typhimurium*. *J. Biol. Chem.* *268*, 22469-22479.
- Smith, R.L., Banks, J.L., Snavely, M.D., and Maguire, M.E. (1993b). Sequence and topology of the CorA magnesium transport systems of *Salmonella typhimurium* and *Escherichia coli*. Identification of a new class of transport protein. *J. Biol. Chem.* *268*, 14071-14080.
- Smith, R.L., Thompson, L.J., and Maguire, M.E. (1995). Cloning and characterization of MgtE, a putative new class of Mg<sup>2+</sup> transporter from *Bacillus firmus* OF4. *J. Bacteriol.* *177*, 1233-1238.
- Smith, R.L. and Maguire, M.E. (1998). Microbial magnesium transport: unusual transporters searching for identity. *Mol. Microbiol.* *28*, 217-226.
- Smith, R.L., Szegedy, M.A., Kucharski, L.M., Walker, C., Wiet, R.M., Redpath, A., Kaczmarek, M.T., and Maguire, M.E. (1998). The CorA Mg<sup>2+</sup> transport protein of *Salmonella typhimurium*. Mutagenesis of conserved residues in the third membrane domain identifies a Mg<sup>2+</sup> pore. *J. Biol. Chem.* *273*, 28663-28669.
- Snavely, M.D., Florer, J.B., Miller, C.G., and Maguire, M.E. (1989). Magnesium transport in *Salmonella typhimurium*: <sup>28</sup>Mg<sup>2+</sup> transport by the CorA, MgtA, and MgtB systems. *J. Bacteriol.* *171*, 4761-4766.
- Sperrazza, J.M. and Spremulli, L.L. (1983). Quantitation of cation binding to wheat-germ ribosomes - influences on subunit association equilibria and ribosome activity. *Nucl. Acids Res.* *11*, 2665-2679.
- Stagljar, I., Korostensky, C., Johnsson, N., and te Heesen, S. (1998). A genetic system based on split-ubiquitin for the analysis of interactions between membrane proteins *in vivo*. *PNAS* *95*, 5187-5192.
- Steinhauser, S. (1999). Prozessierung von pre-mRNA in pflanzlichen Mitochondrien: RNA-Editing und Splicing von Gruppe II Introns. (PhD thesis: University of Ulm).
- Szegedy, M.A. and Maguire, M.E. (1999). The CorA Mg<sup>2+</sup> transport protein of *Salmonella typhimurium*. Mutagenesis of conserved residues in the second membrane domain. *J. Biol. Chem.* *274*, 36973-36979.
- Townsend, D.E., Esenwine, A.J., George, J., Bross, D., Maguire, M.E., and Smith, R.L. (1995). Cloning of the MgtE Mg<sup>2+</sup> transporter from *Providencia stuartii* and the distribution of MgtE in Gram-negative and Gram-positive Bacteria. *J. Bacteriol.* *177*, 5350-5354.
- Van Damme, D., Bouget, F.Y., Van Poucke, K., Inze, D., and Geelen, D. (2004). Molecular dissection of plant cytokinesis and phragmoplast structure: a survey of GFP-tagged proteins. *Plant J.* *40*, 386-398.
- Vernet, T., Dignard, D., and Thomas, D.Y. (1987). A family of yeast expression vectors containing the phage F1 intergenic region. *Gene* *52*, 225-233.

- Vescovi, E.G., Ayala, Y.M., DiCera, E., and Groisman, E.A. (1997). Characterization of the bacterial sensor protein PhoQ - Evidence for distinct binding sites for  $Mg^{2+}$  and  $Ca^{2+}$ . *J. Biol. Chem.* *272*, 1440-1443.
- Wabakken, T., Rian, E., Kveine, M., and Aasheim, H.C. (2003). The human solute carrier SLC41A1 belongs to a novel eukaryotic subfamily with homology to prokaryotic MgtE  $Mg^{2+}$  transporters. *Biochem. Biophys. Res. Commun.* *306*, 718-724.
- Wagner, C.A., Friedrich, B., Setiawan, I., Lang, F., and Broer, S. (2000). The use of *Xenopus laevis* oocytes for the functional characterization of heterologously expressed membrane proteins. *Cell. Physiol. Biochem.* *10*, 1-12.
- Walker, C.J. and Weinstein, J.D. (1991). Further characterization of the magnesium chelatase in isolated developing cucumber chloroplasts - substrate-specificity, regulation, intactness, and ATP requirements. *Plant Physiol.* *95*, 1189-1196.
- Warren, M.A., Kucharski, L.M., Veenstra, A., Shi, L., Grulich, P.F., and Maguire, M.E. (2004). The CorA  $Mg^{2+}$  transporter is a homotetramer. *J. Bacteriol.* *186*, 4605-4612.
- Webb, M. (1966). The utilization of magnesium by certain Gram-positive and Gram-negative bacteria. *J. Gen. Microbiol.* *43*, 401-409.
- Weghuber, J., Dieterich, F., Froschauer, E.M., Svidova, S., and Schweyen, R.J. (2006). Mutational analysis of functional domains in Mrs2p, the mitochondrial  $Mg^{2+}$  channel protein of *Saccharomyces cerevisiae*. *FEBS J.* *273*, 1198-1209.
- Wiesenberger, G., Waldherr, M., and Schweyen, R.J. (1992). The nuclear gene MRS2 is essential for the excision of group II introns from yeast mitochondrial transcripts *in vivo*. *J. Biol. Chem.* *267*, 6963-6969.
- Worlock, A.J. and Smith, R.L. (2002). ZntB is a novel  $Zn^{2+}$  transporter in *Salmonella enterica* serovar *typhimurium*. *J. Bacteriol.* *184*, 4369-4373.
- Yang, T.T., Cheng, L., and Kain, S.R. (1996). Optimized codon usage and chromophore mutations provide enhanced sensitivity with the green fluorescent protein. *Nucl. Acids Res.* *24*, 4592-4593.
- Zimmermann, P., Hirsch-Hoffmann, M., Hennig, L., and Gruissem, W. (2004). GENEVESTIGATOR. *Arabidopsis* microarray database and analysis toolbox. *Plant Physiol.* *136*, 2621-2632.
- Zsurka, G., Gregan, J., and Schweyen, R.J. (2001). The human mitochondrial Mrs2 protein functionally substitutes for its yeast homologue, a candidate magnesium transporter. *Genomics* *72*, 158-168.



## Acknowledgements

First of all I'd like to thank Prof. Dr. Volker Knoop for giving me the opportunity to work on my PhD thesis in his laboratory. He was always open for scientific questions and propagated a good working atmosphere. During the last years, I learnt a lot from his broad knowledge and his way to teach students. It was always inspiring to work in his group.

Many thanks go to Prof. Dr. Bartels for accepting to be the second reviser of this thesis, and also to PD Dr. van Echten-Deckert and Prof. Dr. Höhfeld for their participation in the committee.

Tanks to Monika Polsakiewicz and Milena Groth-Malonek who worked together with me from the beginning, and to my former diploma students Karolin Eifler and Michael Gebert. We were a good team. Of course also thanks to the further and former members of the "Molecular Evolution" group, Karoline, Ute, Felix, Mareike, Henning, Jan, Katja, Julia, Theresia, and Asher. It was always a pleasure to work (and celebrate) with you.

Some members of the neighbouring group "Transport in the mycorrhiza" need to be mentioned here: Guillaume Pilot and Réjane Pratelli always helped me with their broad knowledge about *Arabidopsis* and related techniques. Daniel Wipf and his people always were all ears if I needed something.

I want to thank Prof. Schreiber and Prof. Menzel and their groups for letting me use their fluorescence microscopes and sharing their knowledge about GFP fusions with me. The cooperation especially with the members of the Schreiber group on our floor was always excellent.

My thanks also go to our cooperation partners at different universities in Germany and Austria: Dirk Becker, Dietmar Geiger, and Andreas Latz from the group of Prof. Hedrich in Würzburg; Julian Weghuber and Soňa Svidová from the group of Prof. Schweyen in Vienna, and Petr Obrdlik and Wolfgang Koch from the ZMBP in Tübingen.

I feel lucky to have met so many kind, generous people during my PhD time who broadened my horizon in one way or the other.



## **Erklärung**

Ich versichere hiermit, dass ich die vorliegende Arbeit in allen Teilen selbständig angefertigt habe. Ich habe keine anderen als die angegebenen Quellen und Hilfsmittel verwendet. Diese Dissertation wurde in gleicher oder ähnlicher Form in keinem anderen Prüfungsverfahren vorgelegt.

Bonn, 01. November 2006